UNIVERSITY OF CAPE TOWN
IYUNIVESITHI YASEKAPA • UNIVERSITEIT VAN KAAPSTAD

The Use Of Operational Harmful Algal Bloom Monitoring Systems In South Africa To Assess Long Term Changes To Bloom Occurrence & Impacts For Aquaculture.

Thesis Submitted In Fulfilment of MSc Degree in Ocean & Atmosphere Science

Author

Aphiwe Mtetandaba

Supervisor

Ass/Prof Marcello Vichi

Dr Stewart Bernard

Dr Marie Smith

UNIVERSITY OF CAPE TOWN

Department of Oceanography

28 October 2020

“What has been will be again,
what has been done will be done again;
there is nothing new under the sun”

Ecclesiastes 1:9 (NIV)

DECLARATION

I hereby declare that this thesis is my own original work. I acknowledge full support and guidance from my supervisors,

No part of this research has been submitted in the past or is being submitted for a degree at any other University.

ACKNOWLEDGEMENTS

I would like to thank the following individuals, who all had a significant role to play in the completion of this study:

To my supervisor Ass/Prof Marcelo Vichi thank you for your invaluable input, guidance, patience, useful discussions and your understanding on my despairing acts in the department. My co-supervisor and mentor, Dr Stewart Bernard, I acknowledge your patience, guidance, encouragement, advice and critical comments on my work that helped me gain confidence, for believing in me in difficult times during the progress of my dissertation. To my co-supervisor Dr Marie Smith, I have been extremely lucky to have a supervisor who cared so much about my work, and who responded to my questions and queries so promptly, your assisted with improving my writing skills is the major highlight, you showed understanding of my background and gave me encouraging comments that made me trust myself in all the work I did for this dissertation. I would also like to thank Marjolaine Krug for the late-night talks and encouraging words, to Nicolette Chang the sweet treat and snack you provided on our night shift kept me going, your help in cluster connection on CHPC and shortcuts in python programming played a significant role.

For funding this research, I would like to acknowledge CSIR for the scholarship.

I would also like to acknowledge the Department of Agriculture, Forest and Fisheries for providing phytoplankton cell count data.

I would also like to mention the CHPC Rosebank group. I have found friends, mentors and financial advisors (Rakate Edward), and Counsellor (Recardo).

I would like to express my gratitude to my parents Nosandise Mthethanda(uMamxesibe) and Thembela Mthethandaba (uRhadie), and my siblings Khayakhazi, Nakhane, Lisikelelwe, Buntu, Lubabalo, Nathi and Live, your continued support, encouragement and prayers have kept me safe and strong. And lastly my newly found family in Cape Town Megan, Holly, Huwi, and their dog Nate thank you for opening your home for me.

The Use Of Operational Harmful Algal Bloom Monitoring Systems In South Africa To Assess Long Term Changes To Bloom Occurrence & Impacts For Aquaculture.

ABSTRACT

The south coast of South Africa is a very dynamic, productive, high energy environment and is considered to be a generally challenging setting for in-water aquaculture. One of the largest environmental threats to aquaculture are harmful algal blooms (HABs), a natural ecological phenomenon often accompanied by severe impacts on coastal resources and local economies. There is a wide variety of potentially harmful blooming species in the region, with impacts resulting from both toxicity and the negative effects associated with high biomass. While HABs are fairly well documented around the southern Benguela area, the primary concern is the lack of long-term data showing if blooms are becoming more frequent, persistent or are having greater impact over the last decades, consistent with environmental change experienced in the region. For this study, high-resolution satellite remote sensing observations from 16 years of MODIS-Aqua (1 km) and one month of Sentinel-3 OLCI (300 m), using regionally optimised blended algorithms, were used to investigate the spatial distribution and temporal variability of chlorophyll-a (*Chl-a*) along the south coast of South Africa. A *Chl-a* threshold of 27 mg m−3 was used as an analytic to identify the occurrence of high biomass blooms in the remote sensing data. Phytoplankton count data from aquaculture farms are used to provide information corresponding to changes in phytoplankton community structure, and to investigate the distribution and seasonal trends of HABs along the south coast. To further explore the spatial and temporal distribution, phytoplankton species considered harmful for this study were identified and classified to their seasonal occurrence: some species were consistently present throughout the years, however each region showed contrasting seasonality. A second interest of this study is linked to assessing the capacity of the aquaculture industry to make profitable use of existing observational and early warning tools. The impact of HABs on the environment or in aquaculture facilities can be potentially mitigated by increasing the industry awareness and early warnings of HAB development. In this regard, the Fisheries and Aquaculture Decision Support Tool (DeST) was used in order to develop short term alerts on HAB development. The EO analyses conducted here specifically use the same methods used by this DeST to demonstrate the use of this tool for historical analysis in addition to real time alerting. In order to evaluate the effectiveness of

the tool and how the aquaculture farmers use the information provided on the DeST, an online user feedback was generated, and distributed to all stakeholders via email.

TABLE OF CONTENTS

LIST OF FIGURES

LIST OF TABLES

ABBREVIATIONS AND ACRONYMS

BCLME	Benguela Current Large Marine Ecosystem
DAFF	Department of Agriculture, Forestry, and Fisheries
DEA	Department of Environmental Affairs
MLRA	Marine Living Resources Act (No 18 of 1998)
UCT	University of Cape Town
GDP	Gross Domestic Product
nFLH	Normalised Fluorescence Line Height
CI	Color Index
Chl-a	Chlorophyll-a
mg m^{-3}	Milligram per cubic metre
MERIS	Medium Resolution Imaging Spectrometer
MODIS	Moderate Resolution Imaging Spectroradiometer
SeaWiFS	Sea-Viewing Wide Field-of-View Sensor
mltns	Million tons
HABs	Harmful Algal Blooms

1. INTRODUCTION

1.1. Background

Oceanic and coastal marine environments are amongst the most integral, rich and diverse natural assets in the world, providing many valuable services and uses for an ever-increasing population, such as fishing, shipping, oil and gas production, tourism, mining, recreation and aquaculture development (Atkinson and Clark, 2005). More than 60% of the world's population lives within 100 km of the coast (FAO, 2016; GlobalHAB, 2017; World Bank & DESA, 2020). Coastal and marine environments across the world are under a serious threat from Harmful Algal Blooms (HABs) (Al-Azri *et al.,* 2015; Anderson *et al.,* 2015), these HABs are natural processes that occur in all aquatic systems (Carder *et al.,* 2004; Gilbert *et al.,* 2005; Fawcett *et al.,* 2006; Anderson *et al.,* 2014). HABs appear to be occurring globally more frequently (Wells *et al.,* 2015; Glibert and Burford, 2017) and are of great concern to the public since they are associated with mass mortalities of marine organisms (Moradi and Kabiri, 2012) and human illness due to contaminated seafood (Pitcher and Calder 2000; Davidson *et al.,* 2016). HABs consequently have a negative effect on the economy (such as fisheries, tourism and aquaculture) and are of great concern to seafood industries (Anderson *et al.,* 2015; Bernard *et al.,* 2006).

Over the past decades HABs have become the increased subject of research, especially for marine and aquaculture management based on their frequent, extensive and severe occurrence on the coastline environment across the world (Stephen and Hockey, 2007; Trainer et al., 2010; Anderson et al., 2012; Anderson, 2015). HABs are a serious threat to the marine and aquaculture environment and present a global challenge to marine environmental management. It is challenging to predict their phenology and dynamics (McPartlin et al., 2017). Previous studies and some of the current monitoring systems focus on water sampling (Anderson, 2009; Al Gheilani et al., 2011; Marić et al., 2011; Bernard et al., 2014; Cusack et al., 2016a; Maguire et al., 2016) (identifying and discriminating the type of HAB species from other classes that bloom in certain areas) by measuring the concentration of chlorophyll and the amount of toxic cells in the water and toxic levels in shellfish tissue. However, efforts to predict the occurrence, movement and spatial distribution and impacts on the environment have been fragmented and confined to areas where data have been readily accessible or ecosystem-specific predictive models have been developed (Anderson et al., 2014; McGillicuddy et al., 2014).

Although these in-situ based approaches have provided useful insights, they do not provide enough information on the blooms spatial distribution and continue to be constrained by the fact that they are time-consuming, spatially confined to small areas and expensive (McPartlin et al., 2017), while algal blooms shift and change composition within a short period of time covering a large area being driven by current and other factors (El-Alem et al., 2012). HABs are difficult to monitor due to our limited ability to measure them routinely, understanding of their geographic extent. Again there is a great deal known of the factors responsible for the growth and proliferation of HABs. Earth observation based near-real time online monitoring systems can provide valuable solutions (NOAA, NCCOS, EuroHAB) and the OCIMS HAB Decision Support Tool has been developed successfully to provide continuous monitoring on the water quality along the coastline and marine protected areas of South Africa. The OCIMS system will help to guide the formulation of objectively informed mitigation strategies and will provide an informed basis for the government and the aquaculture industry to make decisions.

This study will attempt to contribute to this effort by using remote sensing-based techniques to detect and map the locations and extent of HABs over a period approximating 17 years from 2002 until 2018. Remote sensing is potentially capable of providing numerous advantages not only because of its ability to provide real-time information but also because of its capabilities to offer affordable and repeatable monitoring (Trescott and Park, 2012; Smith, 2016) at the spatial and temporal coverage needed, and to date back in time. Monitoring of HAB frequency, composition and intensity provides crucial indicators of degraded water quality (Richardson, 1996) and understanding the intensity, nature and movement of the bloom in order to inform the public about the danger of the occurring bloom. In this study, the main focus will be on broader scale bloom phenology and event scale analysis of high biomass blooms of potential damage to the aquaculture industry, supported by available information on phytoplankton community composition.

1.2 Significance of the study

The oceans hold about 97% of the planet's water and covers almost 70% of the earth's surface (Silva and Palma, 2010; Felemban *et al.,* 2015). The South African coastline is surrounded by an ocean current system that exhibits rich biodiversity and is highly productive (Shannon, 2006; Hutchings et al., 2002), but has not yet realised the great economic potential of this valuable resource. Upwelling has been identified as the major source of seasonal and spatial phytoplankton variability along the SA coastline (Goschen and Schumann, 2011; Goschen et al., 2015). However, these coastal waters are frequently affected by HABs (Bernard et al., 2014; GlobalHAB, 2017) and it is estimated that about 58 % of coastal and inshore ecosystems, 43 % of estuarine ecosystems and, 41 % of offshore ecosystems in South Africa are threatened by HABs (Kirkman et al., 2011). There have been several reports of the closure of bays and aquaculture farms along the coastline of SA on the account of HABs (Bernard et al., 2006; Pitcher et al., 2008; DAFF, 2017).

Through the Operation Phakisa, the South African national government aims at unlocking the potential of South African's oceans through the implementation of priority economic, social programs and projects better, faster and more effectively (DAFF, 2014; Environmental, 2016; Mkhize and Mbhele, 2017). The key focus of Operation Phakisa is unlocking the economic potential of South African's ocean. In order to achieve this goal, four sectors were selected as new growth areas. These include offshore oil and gas exploration, Marine transport and Manufacturing activities (coastal shipping, transhipment, boat building, repair and refurbishment, etc.); Marine Protection and Ocean Governance; and Aquaculture (DAFF Annual Report, 2014; Operation Phakisa, 2014; Environmental, 2016).

The current research focuses on one of the key priorities which is aquaculture. Across the world aquaculture is the fastest growing food production sector, approximately producing 67 million tons (mltns) of fish, 25 mltns come from marine and 42 from freshwater (FOA 2014). To feed the world's population an addition of 50 mltns is required by 2030 and it is anticipated that this will primarily come from aquaculture. In South Africa, aquaculture is still in its early developmental stage, with a strong potential growth and larger contribution towards food security, GDP and job creation (Vandepeer *et al.*, 2010; DAFF Annual Report, 2014; Fao *et al.,* 2014). Aquaculture is seen as one of the quick wins to grow the oceans economy, as it is the fastest growing food production sector in the fishing industry, supporting millions of people around the world both in rural and coastal communities (FAO, 2016, 2018).

HABs can negatively affect the coastal environment and its associated resources that contribute considerable value to the South African economy in terms of recreation, employment, and tourism. The four major coastal cities in South Africa: Durban, Cape Town, East London and Port Elizabeth registered the fastest economic growth during the 1980s (DAFF Annual Report, 2014; SACN. 2016). The Phakisa Oceans initiative and the Ocean and Coastal Information System (OCIMS) in collaboration with CSIR and DEFF, had developed a HAB Decision Support Tool (DeST) to provide valuable information to the government and the aquaculture industry.

1.3 Research Aims and Objectives

The aim of this study was to characterise phenological changes in phytoplankton blooms using both historical satellite ocean colour data and phytoplankton count data from regional aquaculture facilities and DAFF. Consequently, to advance our understanding of HABs - specifically, it attempts to produce a long time series of consistent satellite data and phytoplankton count data which are essential for interpreting trends and variability in key parameters. There would be significant value to a systematic study assessing bloom occurrence along the south coast of South Africa as a major regional focus area for an emerging aquaculture industry.

Objectives

To investigate the frequency and causative taxa of observed phytoplankton blooms along the south coast of South African from 2003 to 2018

To investigate intra- and inter-annual trends and variability of the frequency, intensity, and persistence of HABs.

Map the geographical distribution, and the persistence of HABs along the south coast with ocean colour remote sensing data.

Assessing the capacity of the aquaculture industry to make profitable use of existing observational and early warning tools.

And lastly follow an assessment of the CSIR HAB Decision Support Tool (DeST) in terms of information uptake and use during daily aquaculture farm operation and risk assessment.

2. LITERATURE REVIEW

2.1 Introduction

This chapter reviews the regional oceanography of the south coast of South Africa, looking into the interaction between Benguela current (BC) and Agulhas current (AC) as they influence the ecological and nutrient variability along the south coast. It will also look at the growth of the aquaculture industry and its environmental threats being harmful algal blooms (HABs); the HABs typical impacts on aquaculture; the typical bloom occurrence; and the underlying bloom formation mechanisms, and lastly look at earth observation approaches in monitoring HABs.

2.2 Study Area: The south coast of South Africa

South Africa is situated at the southern tip of the African continent, surrounded by three oceans: namely the Atlantic Ocean on the west, Indian Ocean on the east and Southern Ocean to the south. The south coast area is subjected to weather storms generated in the Southern Ocean (WWF, 2016). The south coast of South Africa, here defined as the region between 18.5 and 27°E from Cape Hangklip - Port Alfred and it is relatively smooth with few natural harbours. The coastline is surrounded by two ocean current systems (Hutchings *et al.*, 2002). The Benguela current (BC) flows along the north-western margin of the country, exhibits rich biodiversity and is highly productive (Hutchings et al., 2002), whereas the strong warm Agulhas current (AC) flows along the south-eastern margin in close proximity to the coast. The physical characteristics, ecological variability and nutrient availability along the coastline are mainly influenced by the interaction between these two currents and various atmospheric forcing mechanisms (Smith, 2016).

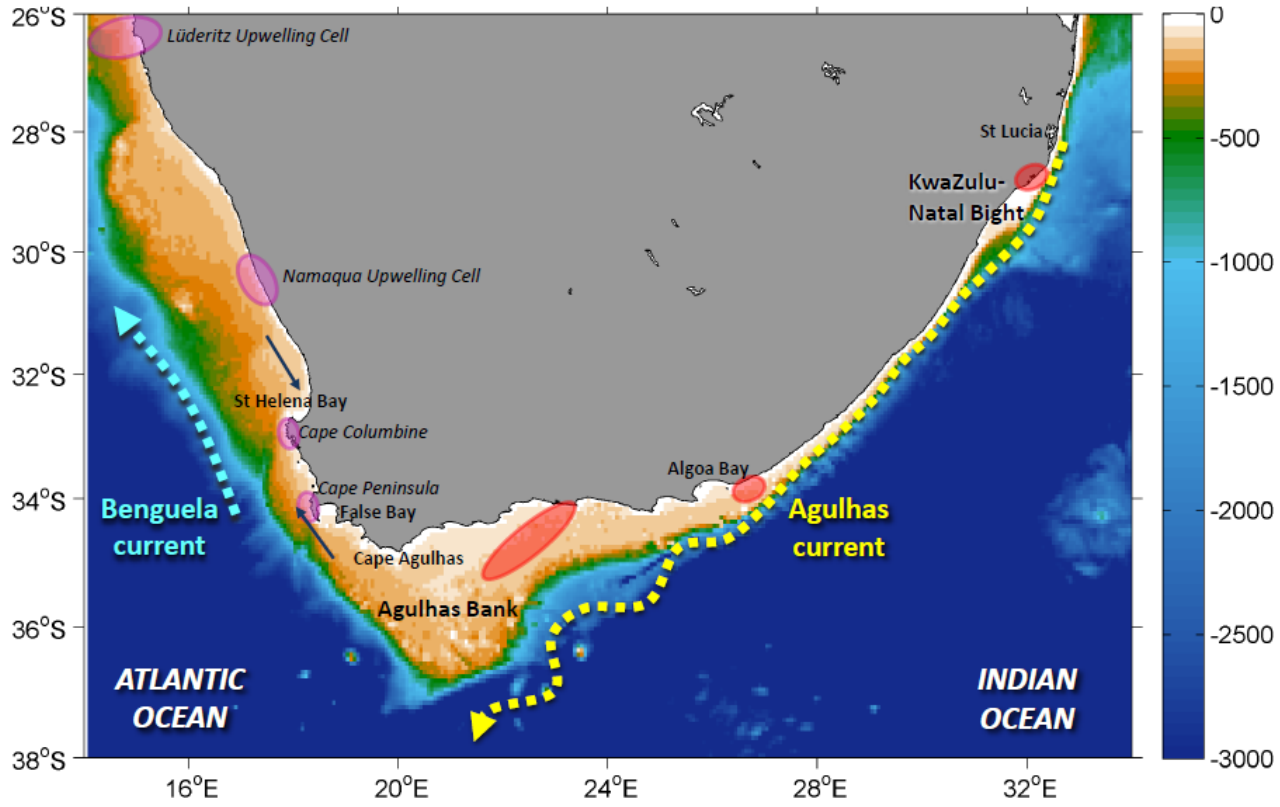

Figure 1: Physical oceanographic activities and active upwelling zones along the SA coastline. The BC is indicated by the blue arrows and the AC by the yellow arrows. The Benguela upwelling cells are shown in pink, and the zones of upwelling and/or periodic nutrient enrichment are shown in red, adapted from (Smith, 2016).

The BC forms one of the four major eastern boundary upwelling systems in the world (Hutchings *et al.*, 2009) known as the Benguela Current Large Marine Ecosystem (BCLME) (Pitcher and Nelson, 2006; Blamey *et al.*, 2015). It is divided into two parts, the northern and southern region, by the Luderitz upwelling cell (Hutchings *et al.*, 2002). The BCLME is unique compared to other upwelling systems because the southern region is strongly influenced by the Agulhas current retroflection at the southern tip of the African continent (Boyd *et al.*, 1998; Blanke *et al.*, 2005). As a marine ecosystem in the low latitudes, it experiences intra-seasonal variability both in physical and ecological dynamics (DEA, 2014). It is mainly influenced by eddies, filaments and rings that spawn at the Agulhas retroflection.

The southern Benguela is characterized by strong coastal upwelling due to south-easterly winds during austral summer; wind-driven divergence at the coast induces offshore movement of warm surface waters which are replenished with cold, nutrient rich water from depth creating a region of productivity (Hill *et al.*, 1998, Verheye *et al.*, 2016) associated

with cold sea surface temperatures at the coast (Miller *et al.,* 2006; Rubio *et al.,* 2009). These cold, nutrient-rich upwelled waters of the southern Benguela fuel most of South Africa's major commercial fisheries, including large-scale offshore pelagic and demersal fisheries, as well as the commercially valuable inshore line-fish, rock lobster and abalone fisheries (Blamey *et al.,* 2015). The physical environment of an upwelling system strongly influences the growth of phytoplankton. Under specific physical conditions typical to the southern Benguela, phytoplankton growth can be concentrated and large enough to form blooms.

The AC is the strongest and largest Southern Hemisphere western boundary current (Quartly and Srokosz, 2002). It is driven by the large-scale wind field and dominates the ecology of the southwest Indian Ocean (Jackson *et al.,* 2012). The current acts as a major barrier that separates the open waters of the Indian Ocean from the coastal waters of South Africa. It is mainly divided into two parts, the northern and the southern regions (Lutjeharms *et al.,* 2010). In the northern region the current is at its most intense velocity but stable due to the continental slope it flows on (Bryden *et al.,* 2005). In the southern region (Figure 1), the continental shelf widens southwards forming the Agulhas Bank; here the core flow of the current also moves offshore, bringing in sub-tropical warm water along the coastal environment, some of which penetrate into the bays. The agulhas bank region is one of the major nurseries and spawning areas on the south coast with diverse fish species (Hutchings *et al.,* 2002).

The upwelling in the AC occurs through Ekman veering, and a topographically induced upwelling, throughout the year (Rouault *et al.,* 2000). The south coast region is dominated by westerly winds, while the frequency of winds with an easterly component increases during summer; the strongest winds occur during around October and November, and the weakest during May and June (Shannon and Nelson, 1996; Schumann, 1998; Lutjeharms *et al.,* 2000; Schumann *et al.,* 2005), while winter is mainly dominated by strong westerly wind. The easterly components winds are responsible for upwelling initiated at Cape Recife. The primary productivity, nutrient availability, and stratification can be influenced by the alternating upwelled waters that occur more than 40% of the time and lead to dramatic changes in SST (Lutjeharms *et al.,* 2000).

The primary role of the AC is to influence the ocean's ecology and dynamics through the transport of ocean water and its biota into the southern part of southwest Indian Ocean (Lutjeharms and de Ruijter, 1996). The wind fields that drive the AC generate coastal

upwelling at the Agulhas Bank (AB), and these wind fields have a direct influence on the climate and weather in and around South Africa (Lutjeharms, 2006). The Agulhas Bank covers a large area on the continental shelf from 18^{o}E at Cape Point to 28^{o}E near East London. The hydrological characteristics of the Agulhas Bank include bottom water supply, surface water divergence south of Cape Agulhas, and biologically is known as the centre of warm temperate water species, from phytoplankton species to several endemic sparids, as it is both a spawning and a nursery area (Probyn *et al.*, 1994; Hutchings *et al.*, 2002).

2.3 Marine aquaculture in South Africa

Aquaculture is defined as the farming of aquatic organisms (Stickney, 2005) and involves the breeding, rearing and harvesting of aquatic plants and animals in controlled or selected environmental conditions, whether in a freshwater or marine environment (Karaan, 2004), for creation, commercial and subsistence purpose. In the world of ocean economic growth, aquaculture is seen as the quick win to grow the oceans economy, as it is the fastest growing food production sector in the fishing industry, supporting millions of people around the world both in rural and coastal communities (FAO, 2016, 2018). Aquaculture is an important food source, as fish is an important resource and source of protein and are in great demand for human consumption and is seen as the solution to sustain the ever-growing human population demand for fish and its products (Cressey, 2009). The aquaculture sector has expanded dramatically over the years and now almost producing half of the global fish supply (FAO, 2014), in countries like Asia, Indonesia and China aquaculture has improved productivity and country's economy (Ahmed and Lorica, 2002) with an estimate 89.1% of production occurring in Asia, with China contributing 62.3% (FAO, 2014).

South Africa aquaculture is a burgeoning industry; even though it's still in its developmental stage, with its positive potential for growth and contribution towards job creation, food security and rural development (particularly in marginalized coastal communities), it plays an important role in the country's blue economy (DAFF, 2014). Globally the aquaculture industry has shown a positive growth production of 7.2 percent from 1970 to 2012, and SA aquaculture has a steady growth of 6 percent from 2000 to 2014, and since 2014 the aquaculture has shown a positive growth with production from 5 fold to 20 000 tons (DEA, 2014). For long term purposes the aquaculture sector wants to increase the current production from 4 000 tons to 20 000 tons per annum and increase the current value from R400 million to R6 billion and create about 210 000 jobs by 2030. The potential contribution towards the

GDP by 2030 is estimated to be R177 billion compared to R54 billion in 2010 and potentially employ 1 million people by 2033 (DAFF, 2014; Department of Agriculture, 2016).

Marine aquaculture production in South Africa focuses primarily on shellfish, namely abalone *(Haliotis midae)*, oysters (*Crassostrea gigas*) and mussels (*Mytilus galloprovincialis*), with seaweeds (*Ulva* spp. and *Gracilaria* spp) being both cultivated and harvested for food for farmed organisms (DAFF, 2017; Smith and Bernard, 2020). Abalone are naturally found in the rocky coastal waters from Cape Columbine on the west coast to north of Port St Johns in the southeast coast, the majority of abalone farms are located on the west and southwest coast due to the fact that water temperatures are suboptimal for abalone growth and most farms are found at Hermanus and Walker Bay, water temperature in these areas ranges 13-16 °C. Farm production method operate on a land-based flow-through systems, which involves pumping large volume of water from the sea for removal and recycling of metabolic waste by using recirculating systems, temperature control, and optimal water exchange (DAFF, 2017; Smith and Bernard, 2020). While oyster and mussel farms mostly located in Saldanha Bay operate on in-water culture methods such as cages and rafts (DAFF, 2017; Smith and Bernard, 2020).

One of the major problems faced by the global marine aquaculture industry are environmental threats from harmful algal blooms (HABs), with their impact costing approximately 8 billion dollars per year (Brown *et al.,* 2019; Smith and Bernard, 2020). Within the South African aquaculture industry the HAB-related risk factors and mitigation strategies differ from one sub-sector to another. Herbivorous abalone are prone to injury and paralysis attributed to some dinoflagellate species (Pitcher *et al.,* 2019), while Pitcher and Calder (2000) believe filter-feeders (i.e. mussels and oysters) are vulnerable to growth arrest and the accumulation of biotoxins which renders them unsafe for human consumption as they become poisonous. On a larger environmental scale, even some non-toxic dinoflagellate blooms can result in marine mortalities and anoxia following the collapse of high biomass blooms (Ndhlovu *et al., 2017*). It is therefore important to minimise and manage any factors that may negatively impact on aquaculture operations, as an increase in aquaculture production depends on new research and improved management practices.

2.4 Harmful Algal Blooms

Phytoplankton are increasingly recognised as mixotrophic or heterotrophic and are the most predominant plants in the aquatic environment (Waibel *et al.,* 2019), present in all-natural waters. Phytoplankton are essential for life on earth; they produce half of the planet's oxygen (Kudela *et al.,* 2015; Palmer *et al.,* 2015; Anderson *et al.,* 2017) and form the base of marine and freshwater food webs that support fisheries and aquaculture industries across the world (Davidson *et al.,* 2014). These organisms are divided into taxonomic groups of algae, commonly known as classes, consisting of wide-ranging species. More than 5000 species of marine phytoplankton have been identified so far and new species are continually being discovered (Landsberg, 2002; Blondeau-Patissier *et al.,* 2014). All phytoplankton contain Chlorophyll-a (*Chl-a*), the key biochemical component responsible for photosynthesis. *Chl-a* is therefore often used as a proxy for total algal biomass and as a potential indicator of blooms; as a result, the spatial and temporal distribution of *Chl-a* has become an important aspect in the study of the biology and biogeochemical processes of the oceans (Reilly *et al.,* 1998; Shen *et al.,* 2012).

2.4.1 The Negative Impacts of HABs

Under certain environmental conditions, some of these phytoplankton species form high biomass (that lead to blooms) that often produces discoloration of the water (Garrison, 2005; Joan *et al.,* 2015; Lewandowska *et al.,* 2015) and some species can cause harmful negative effects even at low densities due to harmful bio-toxins (Gilbert *et al.,* 2005; Anderson, 2009; Kudela *et al.,* 2015). The high biomass forming and low density boi-toxic both are a threat to human health whether via toxic seafood consumption or direct exposure to water-borne toxins and aquatic ecosystems (Lewitus *et al.,* 2012; Grattan *et al.,* 2016; Anderson *et al.,* 2019). They also contribute to the reduction of water quality, affecting water resources, recreation, and ecosystems (Page *et al.,* 2018). During high biomass blooms, phytoplankton can reach high cell concentrations that block sunlight from penetrating the water, disrupting aquatic fauna, and hindering growth of aquatic plants underneath, causing mass mortalities through anoxia and hypoxia conditions after bloom collapse, and also through mechanical damage to fish gills. Those that produce potentially harmful bio-toxins can cause paralytic shellfish poisoning (PSP) (e.g., *Alexandrium spp.*) and diarrhetic shellfish poisoning (DSP) (e.g., *Dinophysis spp.*), diatoms known to cause amnesic shellfish poisoning (ASP) (e.g., some *Pseudo-nitzschia spp.*), as well as dinoflagellates known to produce yesso-toxins (e.g., *Lingulodinium polyedrum*).

HABs can adversely affect many aspects of the marine ecosystem; globally the most commonly observed impacts are massive fish kills, massive death of dolphins, whales, birds, sea lions, sea turtles, manatees, and wild and cultured fish and invertebrates (Landsberg, 2002), receiving toxins through the food chain via contaminated zooplankton or fish. In South Africa the highest mortalities of marine fauna due to low oxygen water occurred in 1994 in St Helena Bay where an estimated 1500 tons of fish and invertebrates were killed by blooms caused by *Prorocentrum micans* and *Ceratium furca* a non-toxic bloom, with *Alexandrium catenella* and *Dinophysis acuminata* (Matthews and Pitcher, 1996; Pitcher and Calder, 2000; Zingone *et al.*, 2006). In 2015 between February and March, St Helena Bay was again subjected to a large marine mortality associated with anoxia which led to mortalities of 415 tons of rock lobster; the causative species was *Prorocentrum triestinum* (Ndhlovu *et al.,* 2017; Pitcher, Kudela *et al.,* 2017). *Karenia cristata* in the Southern Benguela is not only responsible for faunal mortalities, but also has a negative impact on humans through skin irritation, eyes, throat (Bernard *et al.,* 2014). In 1999 some wild and farmed abalone on the west coast of South Africa showed signs of paralysis due the presence of PSP toxins (Pitcher *et al.,* 2019). In the summer of 2016 - 2017, blooms co-dominated by *Lingulodinium polyedrum* and *Gonyaulax spinifera,* both yesso-toxin-producers, for the first time significantly impacted farms of the abalone *Haliotis midae* on the southwest coast of South Africa, causing large mortalities and major stock losses (Pitcher *et al.,* 2017; Pitcher *et al.,* 2019).

Human health effects come from the consumption of shellfish or fish contaminated with the above-mentioned biotoxins (Pitcher and Calder, 2000; Etheridge, 2010; Silva and Palma, 2010). For an example: On the west coast of South Africa in 2005 about four people were treated at Tygerberg Hospital for PSP and another two people were treated at the Cape Town Medi-Clinic in Oranjezicht, people had allegedly eaten contaminated shellfish collected from Melkbosstrand and Blouberg, typical symptoms of PSP include tingling and numbness of the mouth, lips and fingers, difficulty in breathing, accompanied by general muscular weakness and lack of coordination, in Hermanus several people were treated for DSP, Symptoms of diarrhetic poisoning are vomiting, nausea and diarrhoea.

HABs can have serious economic consequences for coastal communities which rely on marine resources for their livelihood and income (Radford, 2012), as HABs impact several economic sectors. Human illness due to toxic HABs can lead to loss of income, workdays and medical expenses. The commercial fishing industry can also be affected by loss of

products, i.e. harvesting closure, fish mortalities, decrease consumer demand and high processing cost. Other economic effects due to HABs include loss of income from recreation and tourism as well as expenses associated with monitoring and management of HABs. HABs have the potential to cause devastating economic losses in the aquaculture and fisheries industries. Saldanha Bay in 1997–1999 experienced brown tides of *Aureococcus anophagefferens* causing an 80% reduction in monthly sales of oysters and mussels (Probyn *et al.,* 2001; Probyn *et al.,* 2010). Then due to the presence of biotoxins in shellfish, farms were closed 13 times in 2015 (DAFF, 2017). The largest recorded event in St Helena Bay of 2000 tons of rock lobster (*Jasus lalandii*) walkout in 1997 was caused by a bloom of *C. furca* (Pitcher *et al.,* 2014), with an estimated loss of 50 million US dollars (DAFF, 2017; Ndhlovu *et al.,* 2017). HABs are a constraint to the development of coastal areas across the world (Karki *et al.,* 2018).

2.4.2 HAB formation mechanisms

HABs have been observed to be increasing in intensity, frequency and in severity, and are geographically distributed across the world (Stumpf and Tomlinson, 2005; Kudela, Howard, *et al.,* 2010; Kudela, Seeyave, *et al.,* 2010; Kudela *et al.,* 2015; Zhao *et al.,* 2015). HABs are naturally occurring and are present in almost all aquatic environments. Blooms are triggered by a combination of environmental (Radford, 2012) and interaction between biological, chemical, and physical mechanisms which are poorly understood (Pitcher and Calder, 2000). However, oceanographic, and climatic conditions play an important role in HAB occurrence, which may be constrained by upwelling systems and stratification of the water column provoked by low wind stress and marine heat waves (Hallegraeff, 2010; Pitcher *et al.,* 2017; Borbor-Cordova *et al.,* 2019). In most areas, upwelling sources are the primary triggering factors for algal bloom formation in the marine environment and upwelling systems play a crucial role in ocean biological productivity of HABs because they are highly productive, nutrient-rich environments, prone to high-biomass blooms (Pitcher *et al.,* 2010).

Most HABs in the southern Benguela upwelling systems have in the past been attributed to one or another dinoflagellate species, but more recently harmful impacts have also been ascribed to other groups of phytoplankton, including the diatoms such as Pseudo-nitzschia species (Pitcher *et al.,* 2010). Diatom dominance in spring in high-nutrient and high-turbulence conditions is followed by a progressive shift toward an increasing contribution of dinoflagellates in late summer and early autumn under declining nutrient and turbulence

conditions (Pitcher and Pillar, 2010; Walker and Pitcher, 2010; Ndhlovu *et al.,* 2017). In South Africa, HABs are mainly associated with the latter part of the upwelling season and usually characterised with dinoflagellate species (Pitcher *et al.,* 1998; Pitcher and Calder, 2000), as these blooms tend to develop during late summer and autumn as seasonal stratification strengthens (Bernard *et al.,* 2014).

2.4.3 HAB transportation mechanism

Once a bloom is initiated, physical processes controlling bloom transport are of paramount importance. Coastal currents driven by wind, buoyancy, or other factors can transport blooms hundreds or even thousands of kilometres along the coast, often from one management area to another, even man-mediated events such as ballast waters and keels can transport algal bloom species. Wind forcing is essential to bloom transportation and development. Wind plays a crucial role in shaping and driving the surface currents that transport the algae (Davidson *et al.,* 2016). These local winds do not only drive the surface ocean current but also exert momentum to an object floating at the water surface making the object move relative to the surface current. Blooms are believed to develop offshore and migrate to the coast. When upwelling winds relax or down-welling winds occur the wind conveys the bloom patches onshore, and relaxation of upwelling wings also conveys the bloom patches coastal (Lewitus *et al.,* 2012). On the other side HABs species grow and as they grow they swim and there is a formation of long spiral chains of cells. Commercial ships and small recreational boats are therefore implicated as potential vectors for long-distance transport and local-scale dispersal of other species (Doblin *et al.,* 2004).

2.5 Remote sensing capability in monitoring HABs

Over the last few decades earth observation has been a useful tool for a number of disciplines based on the collection of routine spatial information. The application of earth observation through remote sensing (RS) has improved the study of marine, coastal and fresh-water ecosystems, by providing essential information for monitoring and managing these ecosystems. Ever since the 1970s, satellites have been used by scientists to detect the optical signatures of constituents present in sea surface water (Blondeau-Patissier *et al.,* 2014). In the 1980's Esaias (1980) recognized that ocean color could be used to derive global maps of oceanic *Chl-a* concentration. Since then ocean colour remote sensing has become an effective means of routinely monitoring coastal water quality and detecting algal blooms.

For remote sensing to be effective, the organism must be detectable, either directly through its effective colour on the water, or indirectly by correlation with other algal blooms or association with a water mass that can be monitored by other remotely sensed characteristics such as sea surface temperature (SST) (Tester and Steidinger, 1997; Stumpf, 2001). Various phytoplankton species, some of which may include HABs, have distinct spectral characteristics compared to that of water where the light is significantly absorbed and reflected at different wavelengths; the resulting spectral peaks and troughs may become increasingly evident as the phytoplankton concentration increases (Figure 2). For Case 1 waters (open ocean) phytoplankton is the primary water constituent. Because *Chl-a* absorbs strongly within the blue spectral regions, water with low phytoplankton concentration shows the highest water-leaving reflectance in the blue wavelengths, but as these concentrations increase the signal moves towards the green wavelengths (Srokosz, 2000). This allows *Chl-a* to be detected through changes in blue–green reflectance ratios (Blondeau-Patissier *et al.*, 2014). However, in Case 2 waters (coastal waters) suspended sediments and coloured dissolved organic matter (CDOM) varies independently of phytoplankton and can contaminate the water-leaving reflectance signal, making the blue–green reflectance band-ratios less sensitive or unreliable. The dominant phytoplankton-related signal shifts to wavelengths located in the red and NIR spectral region as the phytoplankton concentration increases above ~ 20 mg m^{-3}(Blondeau-Patissier *et al.*, 2014; Smith 2016). These spectral characteristics allow the detection of phytoplankton types across different ocean color satellite systems using various algorithms (Shen *et al.*, 2012).

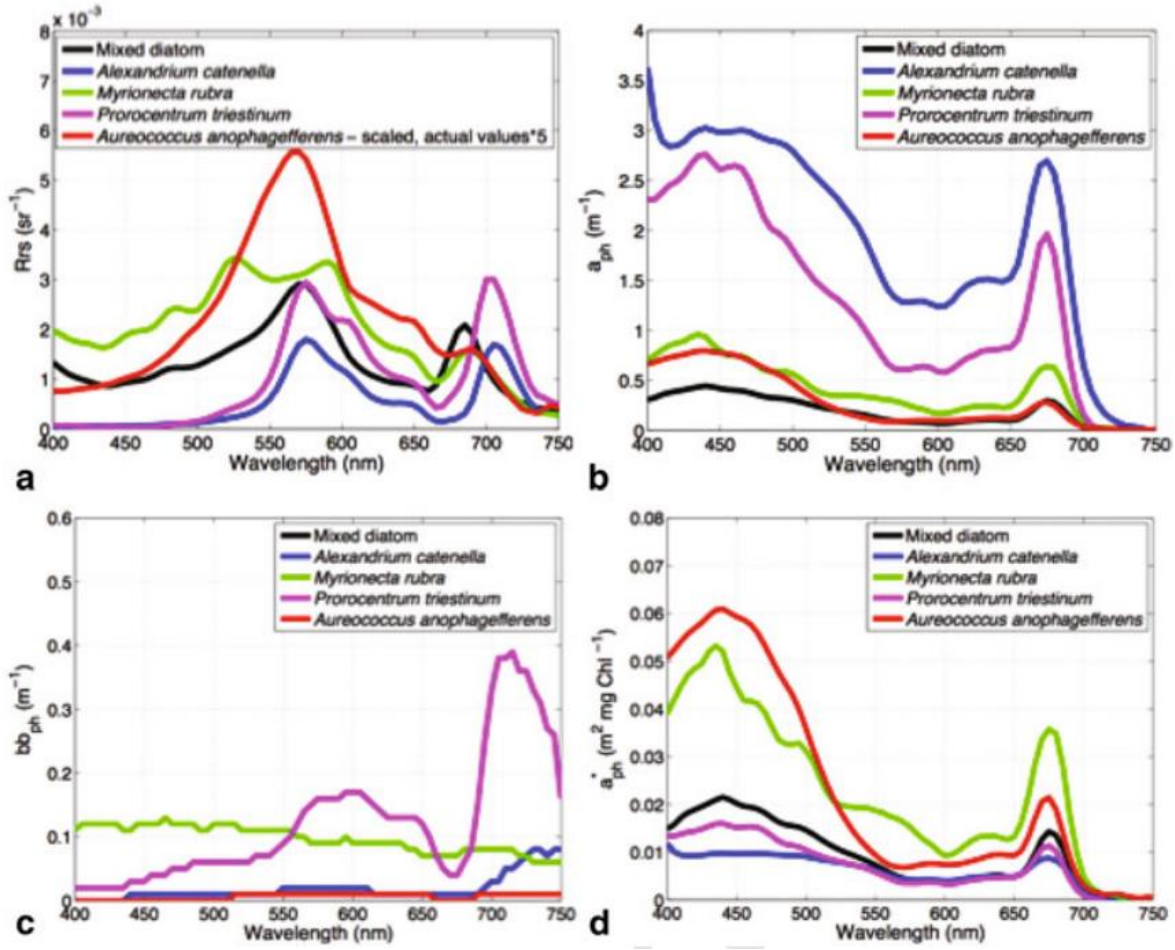

*Figure 2: Optical properties of five diverse blooms occurring between 1998 and 2005 from various locations in the southern Benguela: remotely-sensed reflectance Rrs (a), phytoplankton absorp- tion coefficients aph (b), phytoplankton backscattering coefficients bbph (c), and Chl-specific phytoplankton absorption coefficients a*ph (d) (adapted from Bernard et al., 2014).*

The ocean colour satellite sensors on board global polar-orbiting satellites are often multispectral with different radiometric and spectral setups. The wavebands are positioned to detect the spectral signatures of optically active constituents, including some photosynthetic pigments, making them useful for the detection of phytoplankton biomass (Richardson, 1996). Several multispectral ocean colour satellite sensors have been developed to measure and monitor ocean activities at a global scale, including the Coastal Zone Colour Scanner (CZCS, 1978-1986), Sea-viewing Wide Field-of-view Sensor (SeaWiFS, 1998-2010), and the Medium Resolution Imaging Spectrometer (MERIS, 2002-2012). Sensors that are currently operational include the Moderate Resolution Imaging Spectrometer on board the Aqua

(MODIS-Aqua, 2002-present) and Terra satellites (MODIS-Terra, 1999-present), the Visible Infrared Imager Radiometer Suite (VIIRS, 2011-present) and also the Ocean and Land Colour Imager (OLCI, 2016-present). These sensors are ideal for observing coastal water bodies as they provide daily, near-real time, and freely available ocean colour data, which can be used to derive quantitative *Chl-a.* Although the continuous ocean colour record reached 23 years in 2020, it is made up of individual sensors with different radiometric characteristics. For instance: VIIRS has good spatial resolution (750 m) but is not equipped with red bands that are useful for high biomass detection; OLCI has the ideal spectral setup for high biomass phytoplankton bloom detection and offers both reduced (1200 m) and full (300 m) resolution, but because these sensors were only launched in 2016 the dataset is too short for a comprehensive time series analysis; whereas MODIS provides a compromise with good spatial resolution (1000 m), some wavebands centered in the red-NIR, and an 18 year dataset.

Detection, prediction and early warning are fundamental for HABs and to minimize their effect is by developing near real time monitoring systems using satellite observations (Siswanto *et al.,* 2013). Numerical models are being developed almost every year to detect, monitor and predict HABs (Davidson *et al.,* 2016) based on bio-optical models (Claustre *et al.,* 2005; Brewin *et al.,* 2011), however most of these bio-optical algorithms are associated with uncertainty and error when it comes to differentiating coloured dissolved organic matter (CDOM) and bottom reflectance on coastal environments which are independent of the phytoplankton assemblage. For Case 1 waters O'Reilly *et al.,* 1998 utilise blue-green spectral for band ratio algorithms such as MODIS OC3 and SeaWiFS OC4, to detect *Chl-a*. However, as MODIS OC3 and SeaWiFS OC4 algorithms overestimate *Chl-a*, Hu *et al.,* (2012) use color index (CI) for MODIS and SeaWiFS to detect *Chl-a* concentration lower than 0.2 mg m^{-3}. In coastal waters MODIS Fluorescence Line Height (FLH) (Frolov *et al.,* 2013), and MERIS FLH (Gower *et al.,* 2005) were found successful in detecting phytoplankton concentrations under 20 mg m^{-3}, where FLH is the difference between the height of the reflectance peak at the middle waveband above a baseline between reflectance values at the two adjacent wavebands (FLH calculations for MERIS use bands 665, 681 and 709 nm, while MODIS use 667, 678 and 748 nm bands). For high-concentration bloom events MERIS Maximum Chlorophyll Index (MCI) was used successfully by Gower *et al.,* (2008) to monitor phytoplankton blooms globally; MERIS MCI is computed from MERIS bandwidth data at 681, 709 and 753 nm.

HABs can result from an outbreak of a single algae species that dominate the water column. MODIS normalized fluorescence line height (nFLH) has been used to detect *Karenia brevis* blooms in Florida (Hu *et al.*, 2005), Gulf of Mexico (Cannizzaro *et al.*, 2008; Hu and Feng, 2016), and in the U.S. West Coast and California (Frolov *et al.*, 2013) due to its advantage of detecting blooms in waters dominated by CDOM. MERIS MCI and MODIS FLH have been used in the Gulf of Mexico and on the North Atlantic Ocean to detect *Sargassum sp* (Gower and King, 2011b, Gower and King, 2008, Gower *et al.*, 2006). In the Southern Benguela Bernard *et al.* (2005) used a MERIS band ratio to detect high biomass dinoflagellate-dominated HABs, and also MERIS water-leaving reflectance signal (Bernard *et al.*, 2009). Smith and Pitcher, (2015) used a MERIS maximum peak height (MPH) to estimate *Chl-a* concentration in Saldanha Bay, and recently Smith *et al.*, (2018) used a regional switching and blending algorithm specifically designed for MERIS and OLCI, which use a weighted blending approach between two existing algorithms, the two-band red-NIR algorithm (Gilerson *et al.*, 2010) which operates in moderate to high (>10 mg m^{-3}) biomass waters and the OCI algorithm (Hu, *et al.*, 2012) for low to moderate (<10 mg m^{-3}) biomass waters.

3. DATA AND METHODS

3.1 Introduction

In this study several data sources were used to produce a long time series of consistent satellite data and phytoplankton count data in order to investigate the frequency and causative taxa of observed phytoplankton blooms along the south coast from 2003 to 2018. The first dataset includes phytoplankton count measurements provided by the Department of Environment, Forestry and Fisheries (DEFF) from aquaculture farms. The third dataset includes satellite ocean colour data where *Chl-a* is used as a proxy for high biomass. The fourth is the bloom analytic tool which assists in quantifying an areal extent of a bloom spatially. And lastly follows an assessment of the CSIR HAB Decision Support Tool (DeST) in terms of information uptake and use during daily aquaculture farm operation and risk assessment.

3.2 Selection of sub-regions

There have been less studies focussing specifically on the use of ocean colour data for HAB detection along the south coast of South Africa. Most of the studies have focussed on the west coast, specifically St Helena Bay (Fawcett, 2006; Pitcher *et al.*, 2008; Bernard *et al.*, 2014). The region of interest for this study is from the east of cape point, from Cape Hangklip to Port Alfred (Figure 3). The area is divided into four sub-regions; Overberg [Cape Hangklip to Cape Agulhas]; Langeberg [Cape Agulhas to Cape St Blaize]; Garden Route [Cape St Blaize to Cape St Francis]; Algoa Bay [Cape St Francis to Port Alfred]. The sub-regions coincide with upwelling areas (Figure 2).

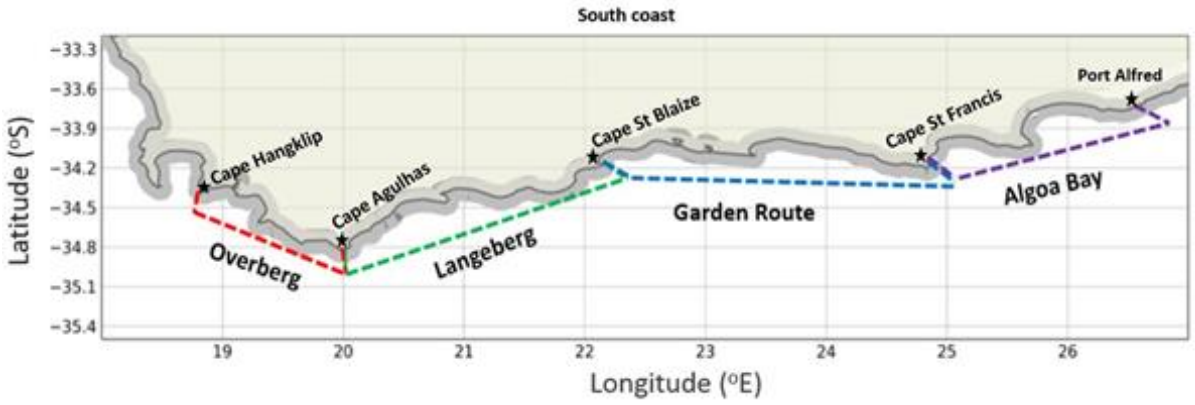

Figure 3: Schematic map of the 25 km buffer zone along the south coast of SA, which is divided into four sub-regions; ***Overberg*** *in red;* ***Langeberg*** *in green;* ***Garden Route*** *in Blue and* ***Algoa Bay*** *in purple.*

3.3 Phytoplankton Count Data

3.3.1 Collection and enumeration phytoplankton count data

Phytoplankton samples have been collected at various stations along the South African coastline since 2003 as part of a phytoplankton monitoring programme managed by DAFF in partnership with the aquaculture farms and other water quality companies. The sampling stations are generally located at aquaculture sites. 31 empty bottles of 250 ml that contain fixative are distributed monthly to each farm. The phytoplankton counts provide information used for water quality monitoring and HAB detection. Water samples are collected daily at the sea surface and the monitoring results include the sample location, date, species, cell count per litre (cells/l) and state whether the species is toxic or non-toxic toxicity.

The identification and enumeration of phytoplankton is carried out using an inverted microscope and the Utermöhl sedimentation technique (Hasle, 1978). The daily phytoplankton sample is mixed gently with repeated inversions of the sample bottle for 60 seconds. Then a 25 ml subsample is measured and poured into a settling chamber and allowed to settle for 24 hours. Once the phytoplankton has settled a coverslip is slid over the sample well, simultaneously discarding overlying water. The area around the coverslip is dried out with a paper towel and the sample is examined with an inverted microscope using an objective magnification of X16 or X40.

Phytoplankton are identified to species, genus or algal groups where possible. All harmful algal species listed in Pitcher and Calder (2000) are recorded and enumerated. The

phytoplankton concentration is enumerated by counting the number of cells for each species in at least three horizontal transects. Each transect is 15 mm in length. After the cells are counted in each transect the well is rotated by approximately 120 degrees to line up the next transect. Cells lying between the parallel threads of the counting eyepiece are counted as they pass the crossing thread. Only if more than half the cell lies within the parallel thread should it be counted. If organisms are not observed within the three strips, identification and enumeration are continued in strips until organisms are counted to a maximum of 12 strips. The area of the well analysed is recorded for conversion of counts into cells per litre, and the units are cells L^{-1}. Results are then communicated via an annual report and the information is saved on the database. If toxic species are observed, it is communicated to the relevant farm immediately.

3.3.2 Phytoplankton count data analysis

The south coastal water has quite a number of species that were sampled and recorded to track the new species that have emerged (Table 5), some of those species are harmful in certain parts of the coast (*Alexandrium catenella)*, but around the south coast some of these species exhibit low concentrations. However, for the current study only species that possess harmful effects and results in blooms were used for further analysis. Phytoplankton count data were sampled from different farms and compiled by DEFF from 2002 to 2018. Before 2012 the recording of samples only took place when there was an increase in phytoplankton, resulting in low oxygen in water and die off on the farms; as a result, there are occasionally large gaps in the datasets in all regions that resulted in huge gaps in data whereby there was no data between 2008 to 2010 (Figure 4) in all the farms. For seasonal interpretation and interannual variability, the seasons were defined as summer (December, January and February -- DJF), autumn (March, April, and May --MAM), winter (June, July, and August – JJA), and spring (September, October, and November -- SON).

There were five sampling stations each representing different aquaculture farms. The stations were grouped into bigger regions for instance Hermanus, Hermanus harbour and Gansbaai represented Overberg region, then Knysna represented Garden Route lastly there's Port Elizabeth which represented Algoa Bay region. All the sampled data for each region were combined, the daily maximum of each species, and the total cell concentration of these maximum values were used for that region. The species of interest that have a harmful impact were specified then grouped into their respective genera and also specified whether they were

toxic or non-toxic (Table 1). The monthly and yearly seasonal cycle was computed by resampling the data monthly/yearly then using the maximum concentration, and for visual analysis the data was plotted using a log scale.

Note that *Pseudo-nitschia* is a genera that includes toxic species, for the current study we present results of sampling for *Pseudo-nitzschia spp.*, without distinguishing the species level. It is also agreed that in South African waters it is known as a bloom-forming species, which has not led to any shellfish poisoning events in the southern Benguela *(*Pitcher *et al.*, 2020*)*.

Table 1: Phytoplankton species divided into toxic and non-toxic and grouped according to their respective genera.

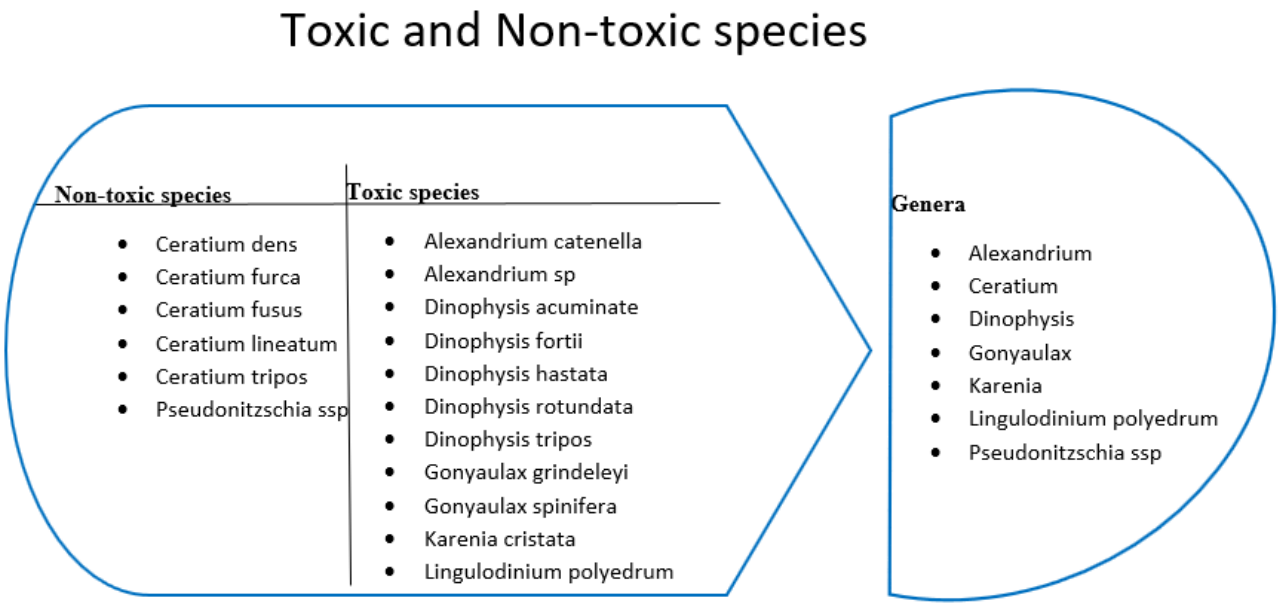

3.4 Remote Sensing Data

3.4.1 Deriving phytoplankton biomass from ocean colour

The *Chl-a* dataset used for time series analysis in this thesis was produced by the CSIR as part of the OCIMS project. The *Chl-a* data were derived using Level 2 Ocean Colour data from the Moderate Resolution Imaging Spectroradiometer (MODIS) on board the NASA Aqua satellite, available from the NASA Ocean color web portal (https://oceancolor.gsfc.nasa.gov/). Although global coverage was available from 2002 until the present, only the sub-regions of interest in Figure 2 covering the time period from 2002 to

2018 were used for analysis. The Aqua satellite is in a near-polar sun-synchronous orbit and has a swath width of 2330 km, which provides coverage of the study region every one-two days at approximately 1 km resolution. The MODIS *Chl-a* product used in this study is derived using a regional switching algorithm (Smith *et al.,* 2020_Earth obser DeST). This regional algorithm uses a weighted blending approach between three different *Chl-a* algorithms: the standard blue-green maximum band ratio algorithm, OC3M (Feldman & McClain 2017), which operates in low biomass waters (<3 mg m^{-3}), a nFLH-based algorithm (Smith *et al.,* 2020_Earth obser DeST), which operates in moderate biomass waters (>15 mg m^{-3}), and a two-band red-NIR ratio algorithm which operates in high biomass waters is implemented based on the 748/667 ratio. These three switching algorithms are blended to produce *Chl-a*.

Full resolution (300 m) Level 2 data from the Ocean and Land Colour Instrument (OLCI) on board Sentinel 3A and 3B were obtained from the EUMETSAT Copernicus Online Data Access portal (https://coda.eumetsat.int/) for the period of January 2019 to March 2019, which coincided with a 2019 HAB event in the Overberg region. The *Chl-a* product was derived using a regional switching and blending algorithm specifically designed for OLCI (Smith *et al.,* 2018). This regional algorithm uses a weighted blending approach between two existing algorithms, the two-band red-NIR algorithm (Gilerson *et al.,* 2010) which operates in moderate to high (>10 mg m^{-3}) biomass waters and the OCI algorithm (Hu, *et al.,* 2012) for low to moderate (<10 mg m^{-3}) biomass waters. Weighted algorithm blending offers the ability to smoothly transition between water-type appropriate algorithms while minimizing spatial discontinuities.

3.4.2 Sea surface temperature data

The Visible Infrared Imaging Radiometer Suite (VIIRS) sensor on board the NOAA Suomi National Polar-orbiting Partnership (NPP) satellite is considered as one of the key environmental remote-sensing instruments. The sensor uses few infrared bands in the 3.660-3.840 µm (M12) mid-IR also 3.973-4.128 µm (M13), and 10.263-11.263 µm (M15), 11.538-12.488 µm (M16) in the thermal IR on the spectral region that are mainly designed to derive SST and actually provides accurate SST results (Early On-Orbit Performance of the VIIRS On board (S-NPP) Satellite). These M- bands provide radiometric accuracy and have better signal-to noise-ratio than imaging bands which have high spatial resolution. Sea surface temperature is the crucial component in ocean dynamics conditions, it is used for derivation

of circulation patterns, structure of ocean fronts, behaviour of meanders, eddies and local upwelling regions (Ahn et al 2006). It is mainly needed for predicting and monitoring ocean dynamic changes (Ghanea *et al.*, 2015) this SST imagery gives better information of sea surface temperature fronts. For the case study Sea Surface Temperature was used to rationalize the existence of algae blooms in relation to upwelling events. The daily Level 2 VIIRS SST data were obtained from the NASA Ocean Biology Processing Group (http://oceancolor.gsfc.nasa.gov) for the Overberg region of South Africa for the date range of January 2019 to May 2019, coinciding with the 2019 HAB in Walker Bay (discussed further in section 4.7). Each of the SST data files were flagged for CLOUD, CLDICE, and HISATZEN, and subsequently re-gridded onto a common 800 m resolution grid.

3.5 Bloom Analytic Tool for Bloom Identification and Characterization

For the current study, the bloom analytic tool assists in quantifying an areal extent of a bloom spatially using a *Chl-a* threshold of 27 mg m^{-3}. The bloom analytic tool uses the derived MODIS *Chl-a* product as input. The *Chl-a* data were re-gridded onto a 1 km x 1 km grid; blooms were identified based on a per-pixel basis when *Chl-a* exceeded a threshold of 27 mg m^{-3}; this threshold was chosen by taking into consideration the low *Chl-a* values in the study region as opposed to coastline areas where the *Chl-a* levels are much higher due to suspended sediments and eutrophication due to river discharge. This threshold of 27 mg m^{-3} was used to identify bloom pixels in the four regions as identified in Figure 3. A convex hull (the smallest convex envelope that contains a "bloom" of a minimum size of two pixels) is used to represent the approximate spatial scale of the bloom in km^2; pixels within 3 km of each other are considered to be part of the same bloom.

3.6 Time Series Analysis Methods

To determine temporal and spatial changes of HABs, time series products for *Chl-a* concentrations (mg m^{-3}) were computed. To compute trophic status of the 25 km buffered region of the coast the mean and standard deviation was used to determine the average *Chl-a* value. The spatially average mean was used as the mean of pixels with *Chl-a*, which gives a good representation of integrated bloom variability over the main area of interest. The 25 km buffered zone was used to define the coastal area for this study, anything beyond was considered Open Ocean. The monthly and yearly average *Chl-a* concentrations were computed to determine temporal changes in phytoplankton biomass for the entire period (2003 – 2018). Climatology maps for monthly were also computed as the mean of all (yearly and monthly) composite images available. For seasonal interpretation and interannual

variability, the seasons were defined in session 3.3.2 The *Chl-a* seasonal anomalies were computed by subtracting monthly climatology from the *Chl-a* value of that month. The *Chl-a* trend for seasonal anomalies and yearly mean were computed using linear regression analysis, and the normalised anomalies was computed by dividing the anomalies by the climatological standard deviation. The *Chl-a* trend for seasonal anomalies and yearly mean were computed using least-squares regression, Theil-Sen regression, and the Theil-Sen 95% confidence intervals and the normalised anomalies were computed by dividing the anomalies by the climatological standard deviation. The least-squares regression is defined as (t) = at + b, where a is the regression coefficient and the linear trend with respect to time (t). Hovmöller plots of the *Chl-a* concentrations were also computed by averaging longitudinally to detect specific changes occurring in specific regions. To determine temporal and spatial changes of HABs using the bloom analytic tool, the monthly and yearly time series analysis was computed by sampling the data monthly and yearly then applied to the maximum function. The number of blooms per year were calculated by summing all the number of days the bloom was detected/present on the water.

3.7 Fisheries and Aquaculture Decision Support Tool (DeST)

Across the world, many countries run monitoring programs for the presence of HABs in their waters (Davidson *et al.,* 2016). These monitoring programs methodologies vary from country to country (Anderson, 1996; Davidson, Anderson, *et al.,* 2016a) and are formulated based on local or regional needs. Most of these monitoring systems are aimed at ensuring the survival and safety of finfish, fish, and shellfish. These systems are made freely available on the internet, they provide short term warnings to aquaculture (Davidson *et al.*, 2016) on the occurrence of the upcoming HAB, its spatial distribution, and direction.

The Council for Scientific and Industrial Research (CSIR) has developed a decision support tool (DeST) to routinely deliver near real-time products for use in locating, monitoring and quantifying algal blooms in coastal waters of South Africa, to assist in determining the water quality status for shellfish and other aquatic animals and plants. The program started functioning late December 2017 and from time to time it is still under construction to make it better and more understood by its stakeholders. During the initial development stages the near-coastal zone of South Africa (within approximately 25km from the shore) was divided into 12 regions of interest (however, for the purpose of this study the focus is on the four regions mentioned in Sec (3.2), based on the physical oceanography and presence of

aquaculture facilities, for the purposes of monitoring and assessing the risk of HABs within the DeST.

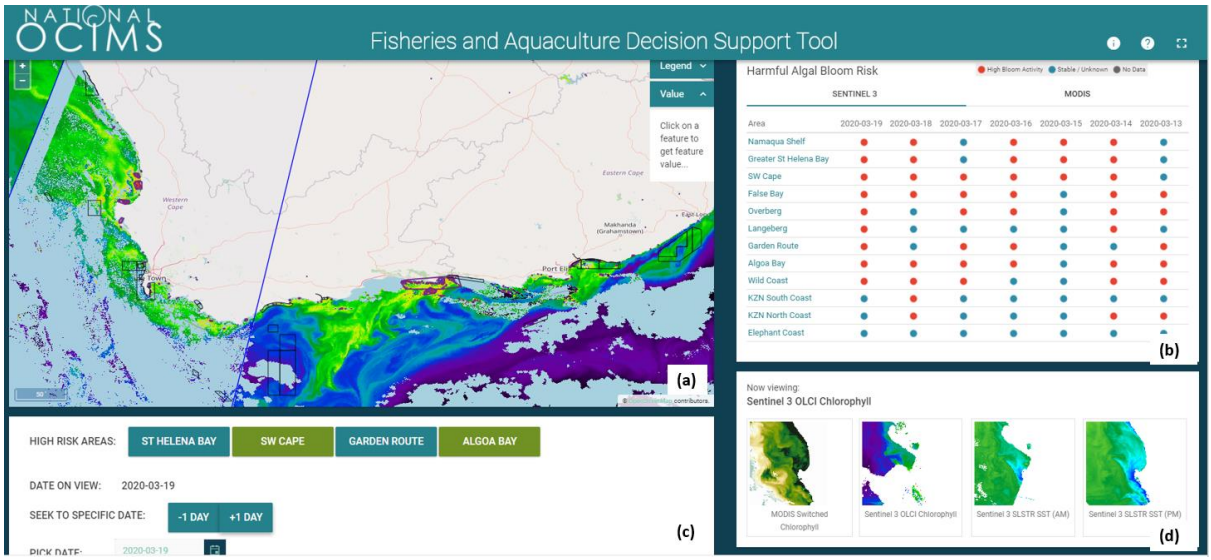

Figure 4: Graphical Layout of the South African DeST *bulletin, (a) View interface-Click on the map to get detail information for your area of interest, (b) HAB Risk-select an area of interest and view the risk, (c) Time series- select forecast time, and (d) Products-select which product variable to display: MODIS Switched Chlorophyll, Sentinel 3 OLCI Chlorophyll, Sentinel 3 SLSTR SST(AM,PM).*

The HAB DeST (figure 4) provides a simple and user-friendly interactive graphical interface that provides relevant information to the end users. The graphical layout is divided into four bulletins as shown in figure 21, (a) View interface: provides the opportunity for the user to zoom in/out and to get the values of a certain feature, and also to check the distribution of known HABs highlighting the impacted areas along the coastline; (b) HAB Risk: provides 12 regions of interest, it also show whether a certain area is in high risk or not based on the colour of a dot, grey with no data available for that particular day, blue for stable water column or unknown activities, and red being highly at risk or with high bloom activity; (c) Time series: provides a selection of a specific date, one can pick a date from the calendar or seek to specific date; (d) Products: the DeST provide four earth observation products the Chlorophyll-A derived from CSIR MODIS and OLCI Switched algorithm, Sea Surface temperature (SST) from SLSTR sensor (on board Sentinel 3 satellite), SST has a morning and an evening overpass, so there are two products available a day. These provide near real time risk thresholds. The temperature information helps in the identification of structures such as

upwelling fronts that may be related with high productivity areas, a brief description is found on https://www.ocims.gov.za/hab/app/#.

3.7.1 Engagement with stakeholders

There are various ways to understand the needs of stakeholders which include surveys, workshops and in-person or web-based meetings between the stakeholders and developers. The DeST development followed a user co-design approach, with iterative rounds of user testing phases, followed by user feedback, and improvements being made before the next version release. As a result, communication with the stakeholders is considered to be an important building block of the DeST.

A series of workshops were conducted to bring the stakeholders and the developers together to discuss the project aims and gather valuable information, insight, and feedback; this included (i) the type of information they need and how they would use it on a daily basis in their decision-making processes; (ii) their level of trust in the information provided; (iii) how they think the information would help them; (iv) what are their past experiences on HABs warnings. All identified stakeholders were contacted via email to invite them to the workshops or meetings, follow-up emails and telephone calls were used to ensure that all stakeholders were aware of the invitation to participate.

The structure of the meeting and for workshops was kept the same. A PowerPoint presentation was used to guide the discussion throughout the meetings. The developers would provide a short description of the background, rationale, and objectives for the tool, followed by a presentation of the scientific products/indicators, and functionality of the DeST. Comments, suggestions, and questions for clarity were welcomed at any point during the discussion.

After the first release of the DeST, an online questionnaire was generated in order to gather user feedback, assess how the information is used, and to evaluate the uptake and effectiveness of the tool. The online survey was designed and shared with the stakeholder via email to generate a user feedback evaluating the effectiveness of the tool, to understand our stakeholder and how each stakeholder makes use of the information provided on the DeST. Some questions on the survey were open-ended, to look at the specific views of each user on how they make use of the DeST. The results of the survey, together with suggestions during

workshops and meetings, were used to further develop and improve the indicators and products, HAB alerting, and to shape the DeST to better suit the needs of the stakeholders.

4. RESULTS

4.1 The Phytoplankton Count Data Analysis

Some phytoplankton names have not been updated according to the records in the World Register of Marine Species (for example some farms are still reporting *Karenia mikimotoi* as *Gymnodinium mikimotoi*). There is a lot of missing data in all the regions as shown in Figure 5 which limits the conclusions that can be drawn using these data. The missing data results from the fact that DEFF only started its routine monitoring operations in 2012, whereas before that the farms were collecting the samples for themselves (DEFF, pers. comm.), and most farms were only recording sampled data when there were some increase in cell concentration or if there were mortalities on their farms. The Overberg area had the most consistent sampling regime compared to other regions with the maximum concentration of *Pseudo-nitzschia spp*, and lowest concentration of *Dinophysis* and *Ceratium.* Figure 5 also shows that the Garden Route had the least samples, having only collected samples between 2003 and 2007. Routine sampling by DEFF only started in 2012 in the Algoa Bay region,with the maximum and minimum cell counts recorded for *Pseudo-nitzschia spp* and *Alexandrium,* respectively. The summarized statistics for all three regions are shown in Table 3. The total number of species counted and recorded along the south coast and their frequency of occurrence is shown in Table 5 (Appendix A).

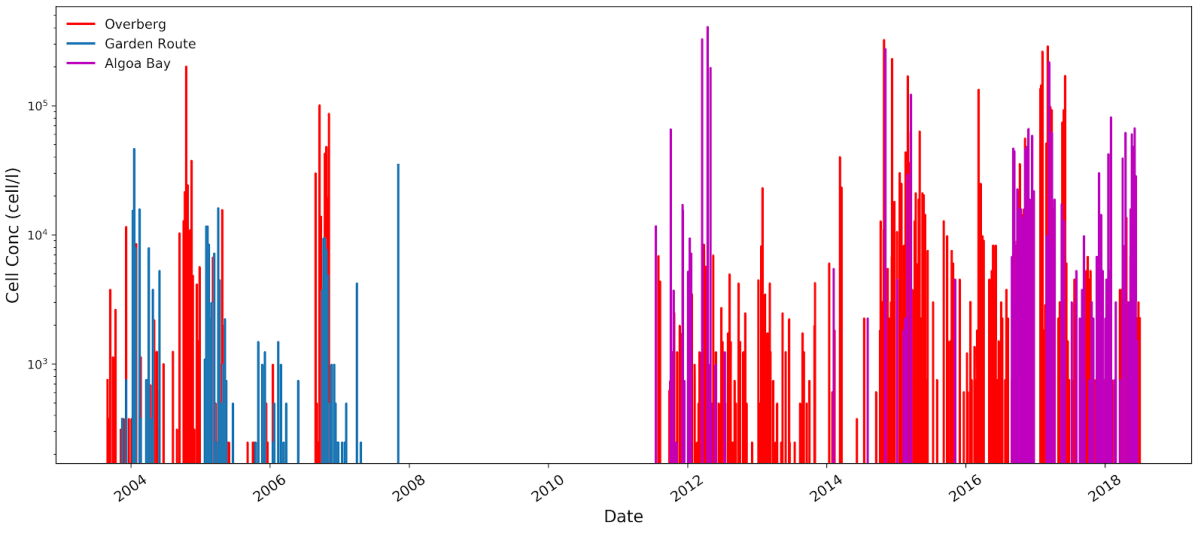

Figure 5: Daily time series plot of the recorded phytoplankton count data from three stations: Overberg in red, Garden Route in blue and Algoa Bay in purple.

Table 2: Summarized statistics table of all the sampled regions, showing the standard deviation, mean, median, minimum and maximum species cell concentration.

	Overberg	**Garden Route**	**Algoa Bay**
Max	321399	43758	104588
Min	246	246	246
Std	23832	6752	60428
Mean	7261	3129	24954
Median	1230	738	4488

However, we do acknowledge and understand that the conclusions that can be drawn from these data are fairly limited (or have high uncertainty) because of the known gaps in the data collection.

4.1.1 Overberg

4.1.1.1 Temporal variability of toxic and non-toxic species

To investigate the seasonal changes in bloom causative species, phytoplankton count data were grouped into toxic and non-toxic and summed up monthly and yearly. Figure 6 shows the monthly and yearly distribution of toxic cell concentration against non-toxic concentration. In figure 6 (panel a) the toxic species have a high concentration in midsummer (Jan) to early autumn (March), decreasing in late autumn and being at their minima in July (492 cells/L) starting to increase again in September. Whereas nontoxic species were always at their high concentration all year except also in July (2992 cells/l). Figure 6 (panel b) shows that the non-toxic species had high concentration throughout the sampled years, except in 2004 and 2013, and toxic species had the highest concentration in 2004, and in 2013 compared to that of non-toxic species, then in 2017 both toxic and non-toxic reached their maximum peak.

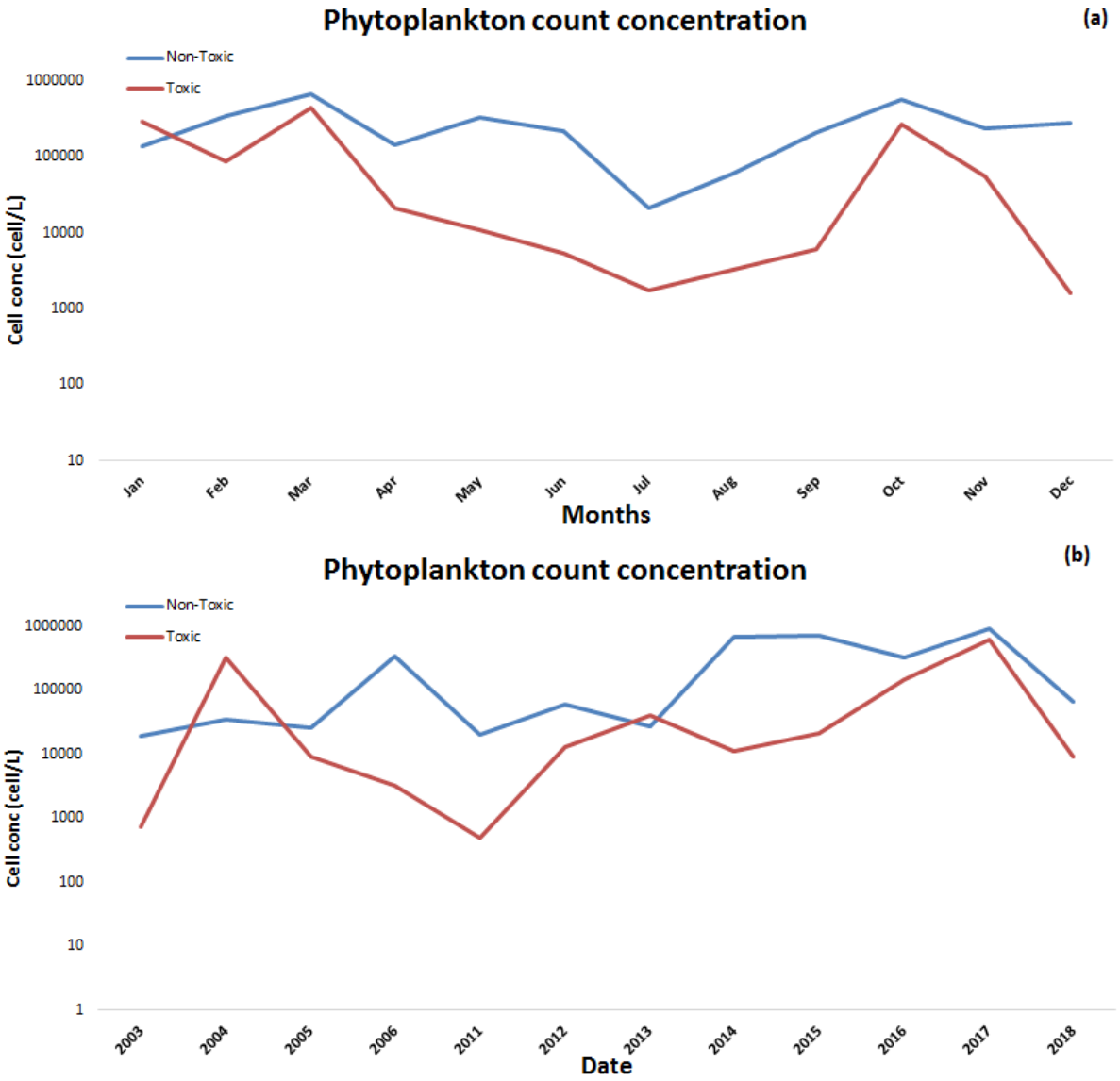

Figure 6: Monthly (a) and yearly (b) distribution of Toxic (red) and Non-toxic (blue) time series plot for temporal variations of phytoplankton cell count concentration in the Overberg region.

4.1.1.2 Temporal variability in species composition

For temporal variability and identification of the most frequent and dominant bloom causative species in the phytoplankton community, monthly and yearly distribution of species were plotted Figure 7. Figure 7 (panel a) shows the temporal variability in species is distinct; all potentially harmful species were present at some point within the samples from this region, with the lowest diversity (three genera) recorded during July. The species concentration changes over the season, with *Ceratium* is in its high concentration in May and June and is on its lowest in Dec, *Pseudo-nitzschia spp* experiences high concentration in spring and summer having high peak in October and starts to decrease in March till July and start to increase in August. The summer period experiences more species with the minimum concentration of 1147791 cells/l compared to that of the winter period with 310345 cells/l.

Figure 7 (panel b) shows the most frequent and dominant species over the years, the concentration of each species varied yearly. *Pseudo-nitzschia ssp*, *Ceratium* and *Dinophysis* are the most frequent species during all the years that were sampled, whereas *Lingulodinium polyedrum* was only sampled in 2004, 2017 and 2018. Between 2007 to 2010, there is no recorded data in this region.

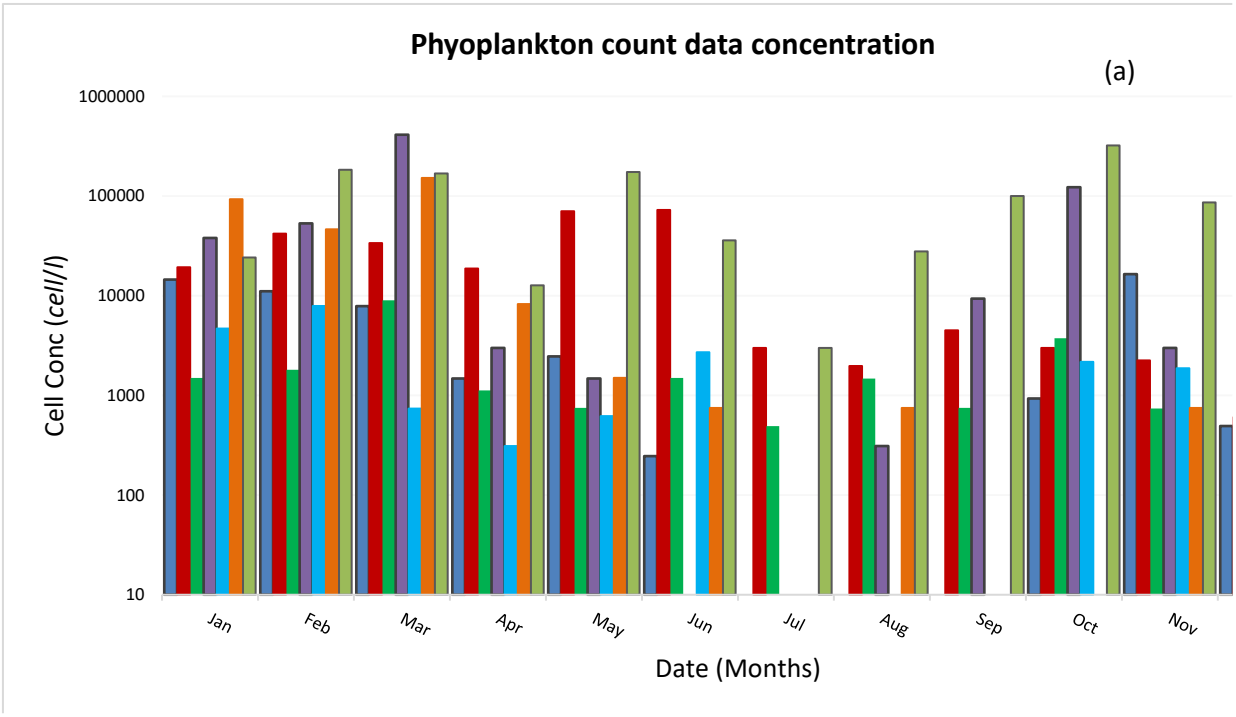

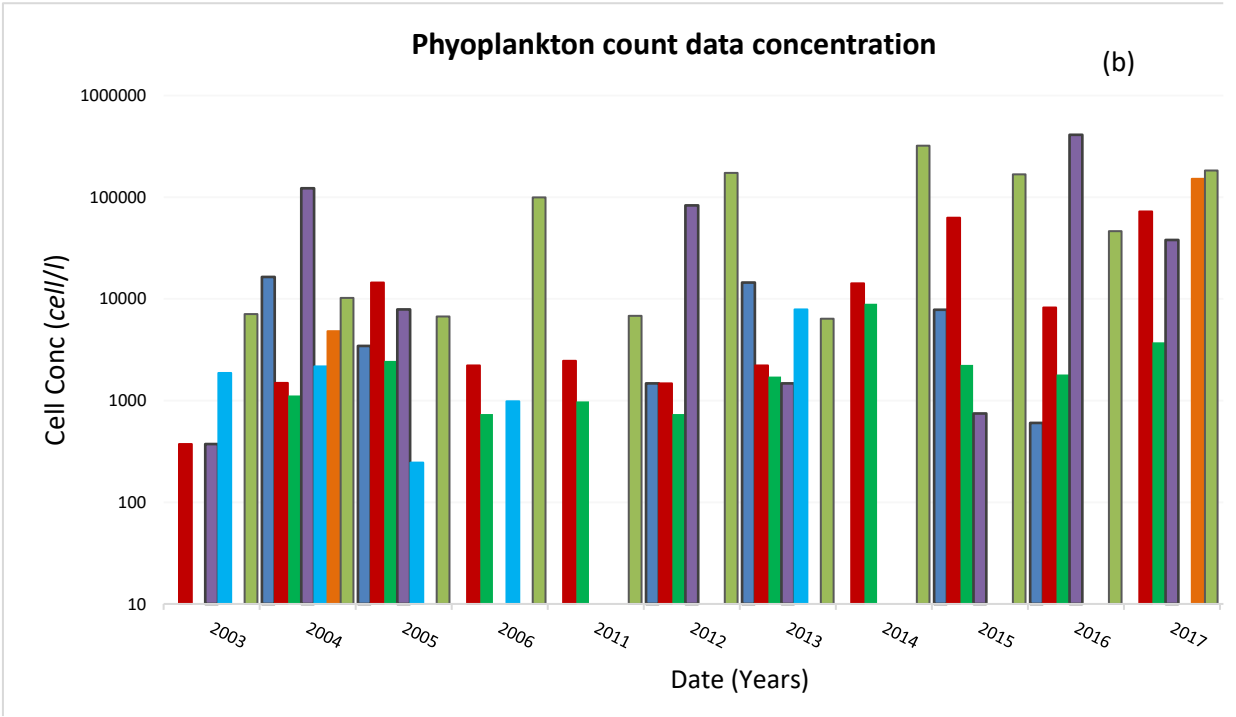

Figure 7: Average concentration for monthly (a) and yearly (b) seasonal abundance distribution of harmful causative species in Overberg.

4.1.2 Garden Route

4.1.2.1 Temporal variability in species toxicity

Figure 8 shows the monthly and yearly distribution of toxic cell concentration against non-toxic concentration. In figure 8 (panel a) there were months in which sampling did not take place for both toxic and non-toxic species, autumn (March), winter (June, July and August), and spring (September). Within the months that were sampled the toxic species had peaks in April and in October with relatively low concentrations of 6801 cells/l and 10558 cells/l respectively, whereas non-toxic had a peak in January (64796 cells/l) and November (34700 cells/l). Figure 8(panel b) shows that only five years were sampled (2003, 2004, 2005, 2006 and 2007), with toxic species having dual peaks in 2005 and 2006, and the highest concentration of toxic species measured during 2006 with a total of [10804 cells/l].

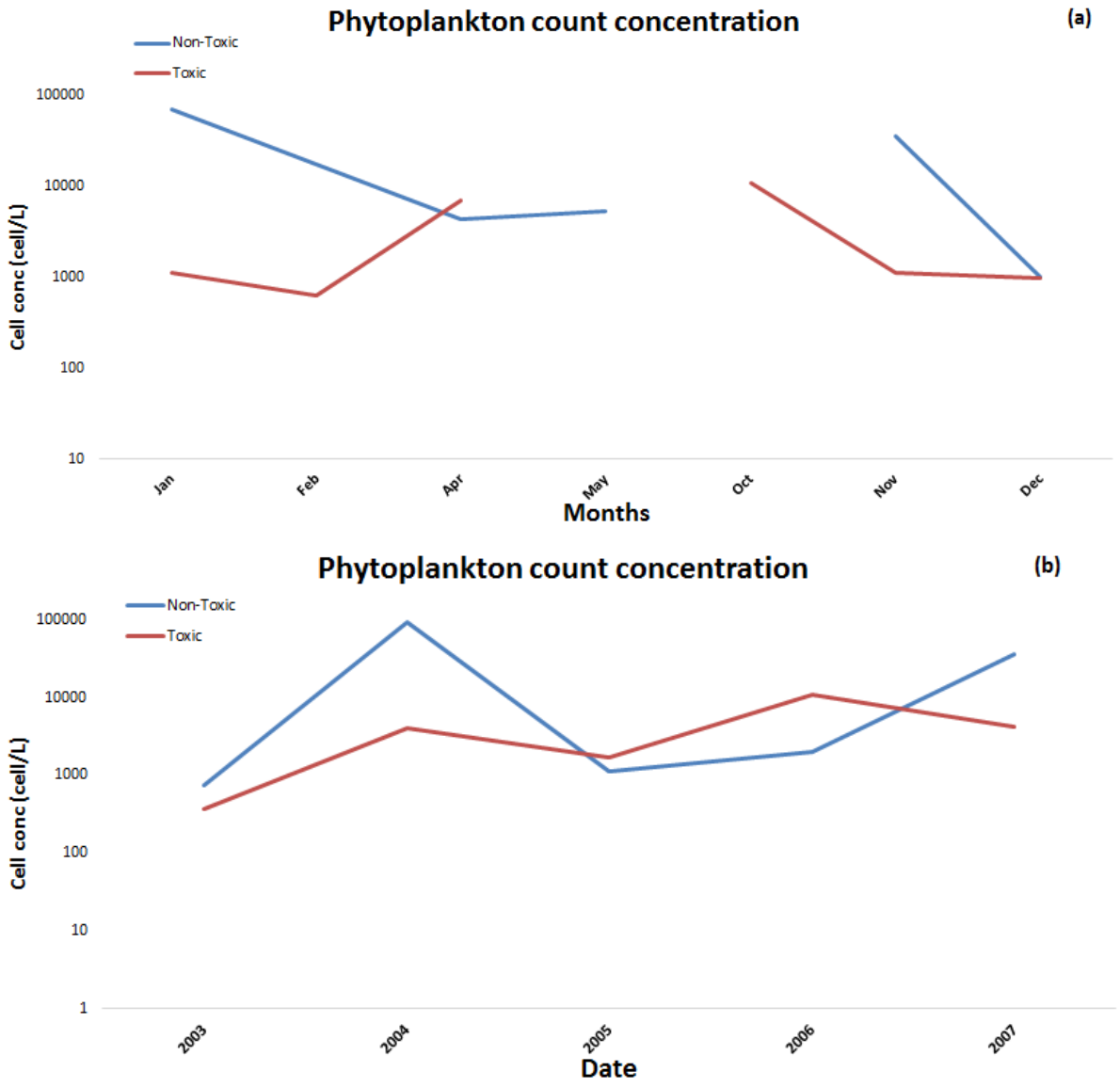

Figure 8: Monthly (a) and yearly (b) distribution of Toxic (red) and Non-toxic (blue) time series plot for temporal variations of phytoplankton cell count concentration in the Garden Route region.

4.1.2.2 Temporal variability of species composition

The concentration of each species varies season and yearly. In figure 9 (panel a) the most dominant species was *Pseudo-nitzschia spp* which was present in six of the seven months; it was also the only genus to reach concentrations of >10000 cells/l, doing so in three different months. *Dinophysis* was also present in six of the seven months, with the highest concentrations in October at 10558 cells/l. Then figure 9 (panel b) shows that the 2006 toxic counts mentioned in figure 8 (panel a) were attributed to *Dinophysis*.

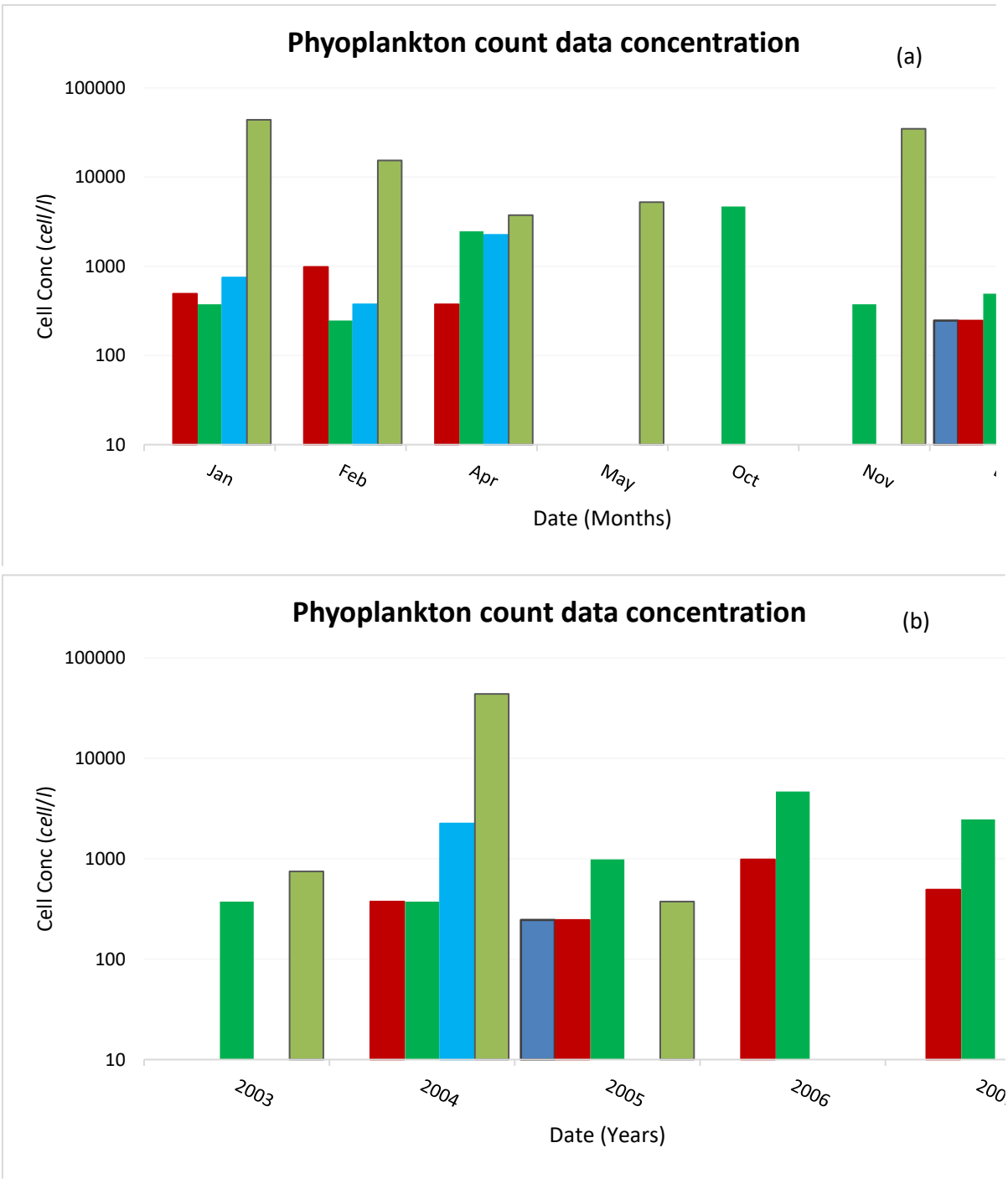

Figure 9: Average concentration for monthly(a) and yearly (b) seasonal abundance distribution of harmful causative species in Garden Route.

4.1.3 Algoa Bay

4.1.3.1 Temporal variability in species toxicity

Figure 10 shows the monthly and yearly distribution of toxic cell concentration against non-toxic concentration. In this region the sampling took place from 2011 till 2018, except in 2013. In Figure 10(panel a) both toxic and non-toxic species have a binomial pattern, they have the first high peak in autumn (March) and decrease in winter and start to increase in spring resulting in the second peak. Toxic species have high concentration only in February. Then in Figure 10 (panel b) non-toxic species dominated over the years except in 2017 when toxic species reached their highest peak and dominated with a total concentration of 320892 cells/l.

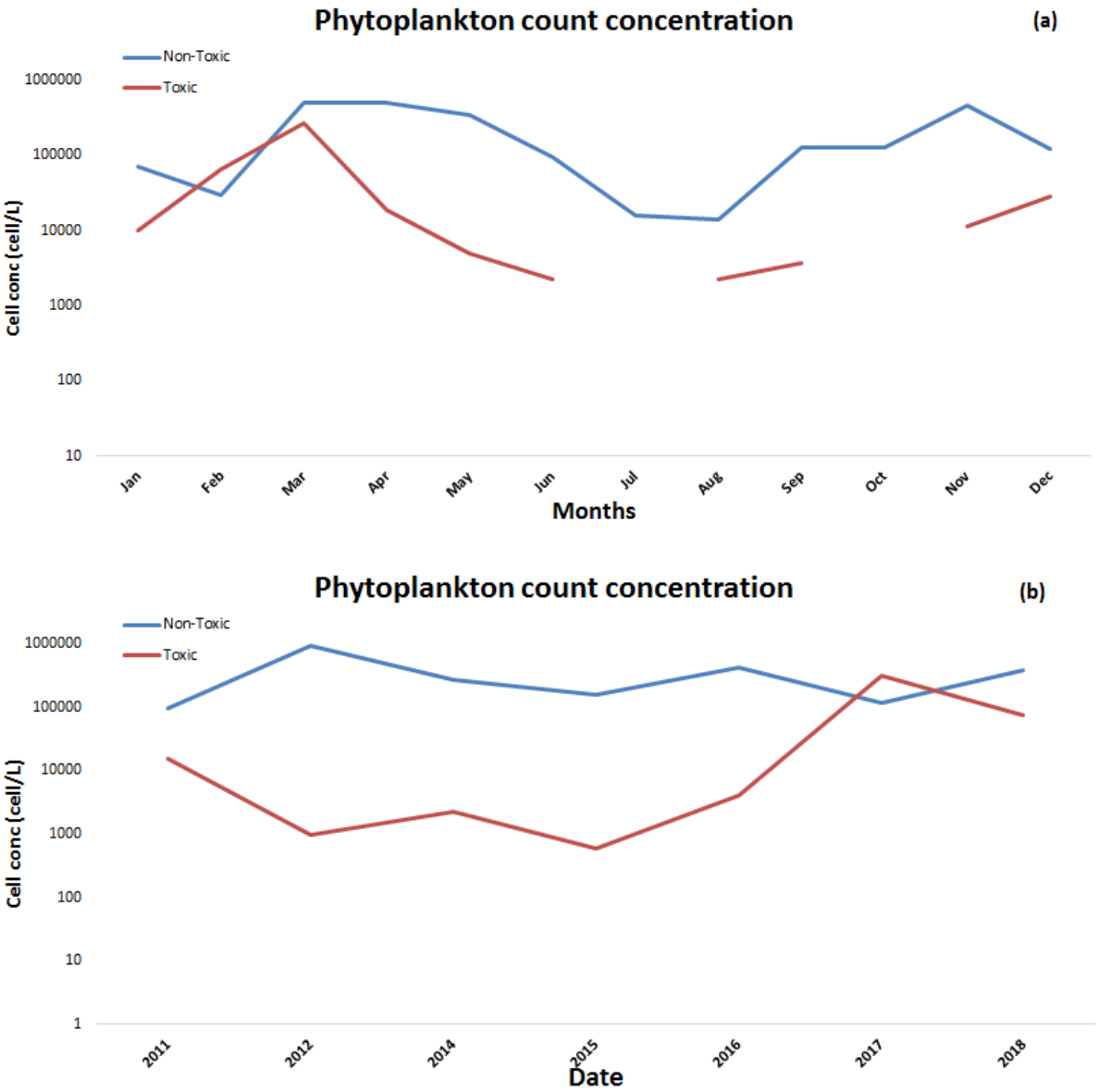

Figure 10: Monthly (a) and yearly (b) distribution of Toxic (red) and Non-toxic (blue) time series plot for temporal variations of phytoplankton cell count concentration in the Garden Route region.

4.1.3.2 Temporal variability of species composition

Figure 11 shows the seasonal frequent and dominant species over the years and through months. In Figure 11 (panel a) *Pseudonitzschia spp* was sampled all year long, reaching high concentrations during March, April and reaching its highest concentration in November of 459272 cells/l. *Gonyaulax* starts to increase in November and reaches its high concentration in summer (February) of approximately 63580 cells/L and reaches its lowest in 748 cells/l in May. *Lingulodinium polyedrum* is only present in autumn (march and April) and spring (Sep and Nov), having its highest concentration in March of ~257312 cells/l dropping to 1496 cells/l in November. Then in figure 11(panel b) *Pseudonitzschia spp* is present throughout the sampled years reaching its highest concentration of 948466 cells/l in 2012. In 2017 all the genera, except *Alexandrium,* were present, with *Lingulodinium polyedrum* being the dominant species with concentrations reaching 281248 cells/l. This was also the first time that *Lingulodinium polyedrum* was sampled at an aquaculture farm in this region.

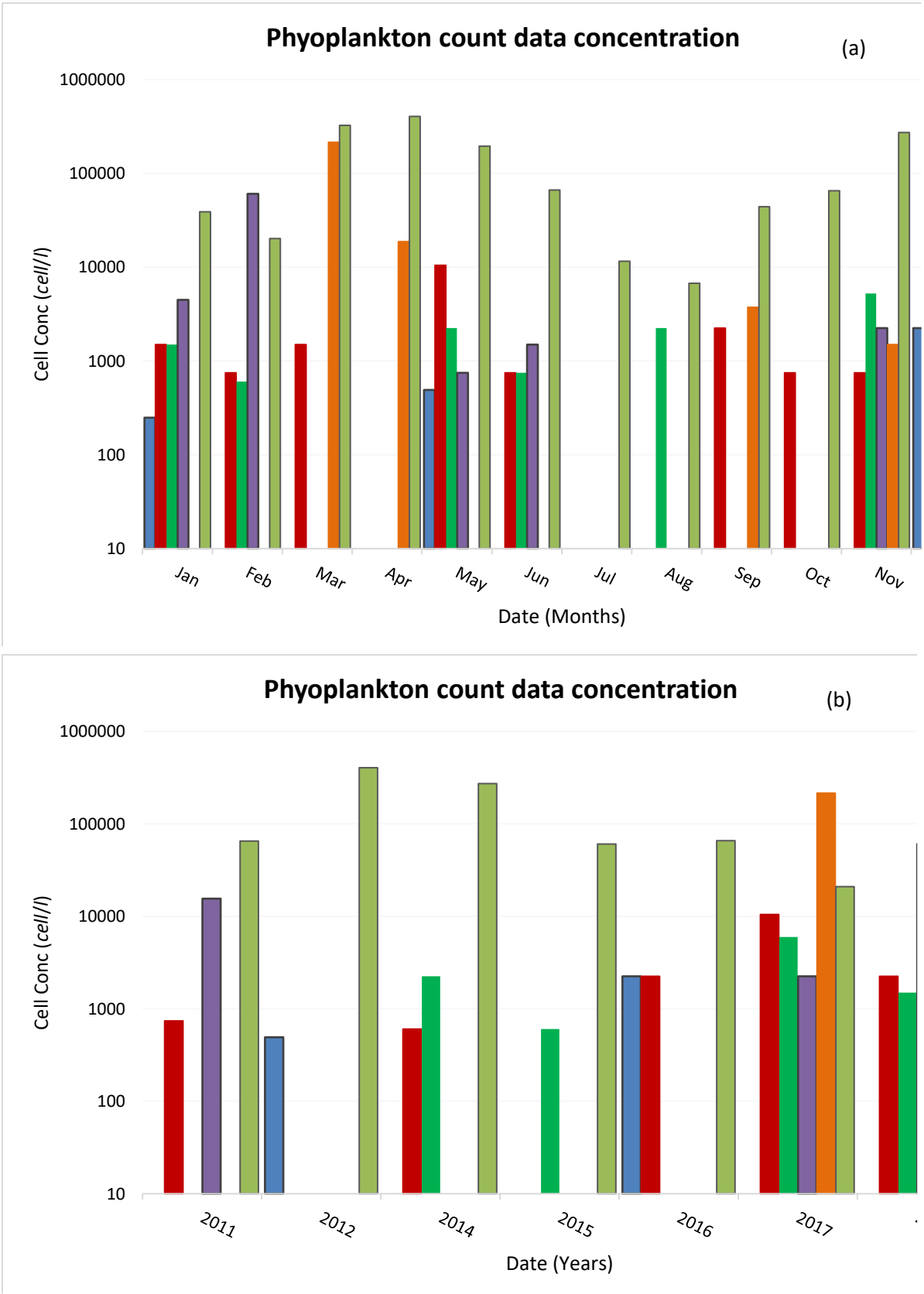

Figure 11: Average concentration for monthly(a) and yearly (b) seasonal abundance distribution of harmful causative species in Garden Route.

4.2 Chlorophyll *a* Distribution

4.2.1 Spatial Variability of *Chl-a*

A Hovmöller diagram (figure 12) was used to represent both the spatial and temporal variability of phytoplankton biomass along the entire south coast. It shows that there is inter-annual variability in the *Chl-a* concentration and a seasonal pattern which is more prominent between 19.5^0- 20.2^0 and also at 21^0- 23^0 longitude with high phytoplankton biomass levels. Several intense bloom events are clearly evident in the Langeberg and Garden route regions, specifically during 2003, 2004 and 2014 and also Algoa Bay experienced some blooms in 2004, 2013/2014 and in 2017.

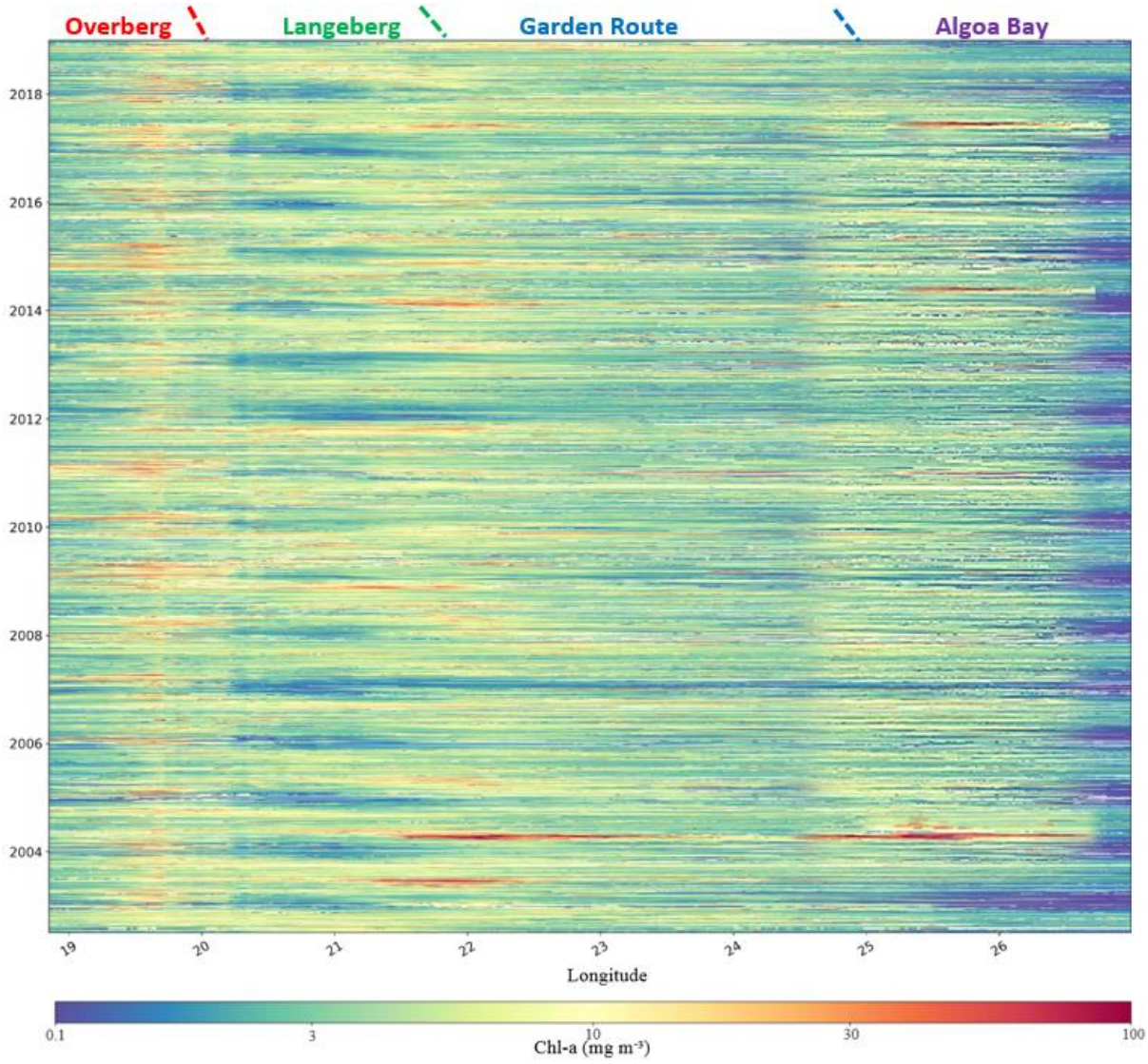

Figure 12: Hovmöller diagram of the daily latitudinally-averaged MODIS Chl-a concentration within the 25 km coastal zone for the period of 2002 to 2018 also highlighting regions with high interannual variations in Chl-a biomass.

Through the use of temporal average *Chl-a* concentration, the variability of *Chl-a* was obtained by computing the spatial mean using a regional shape (demarcated in figure 12) and then the standard deviation over time, to highlight the regions with the largest interannual variance (figure 13). The entire south coast experiences different physical forcing mechanisms and environmental conditions at different seasons and different years. Figure 13 highlights the regions of interest that include a continental shelf zone (Langeberg, shown in light green), a zone of intermittent coastal wind-driven upwelling (Garden route, shown in light blue), and a bay near a dynamic upwelling zone (Algoa Bay, shown in light purple). The Overberg region (shown in light red) illustrates the influence of the southern Benguela physical forcing mechanism in this region and the strong easterly winds stimulate more upwelling.

The *Chl-a* concentrations then tend to decrease eastwards, being lowest at the easternmost (towards Algoa Bay,) where the phytoplankton biomass drops with *Chl-a* concentration of about 0.25 mg m^{-3}. There is an apparent time shift from west to east which is also observed with figure 12. The highest spatial variability denoted by standard deviation ~3.8 mg m^{-3}, were observed on the west part of Langeberg (21.7°E). And the lowest spatial variability ~0.25 mg m^{-3} were observed in the Algoa Bay.

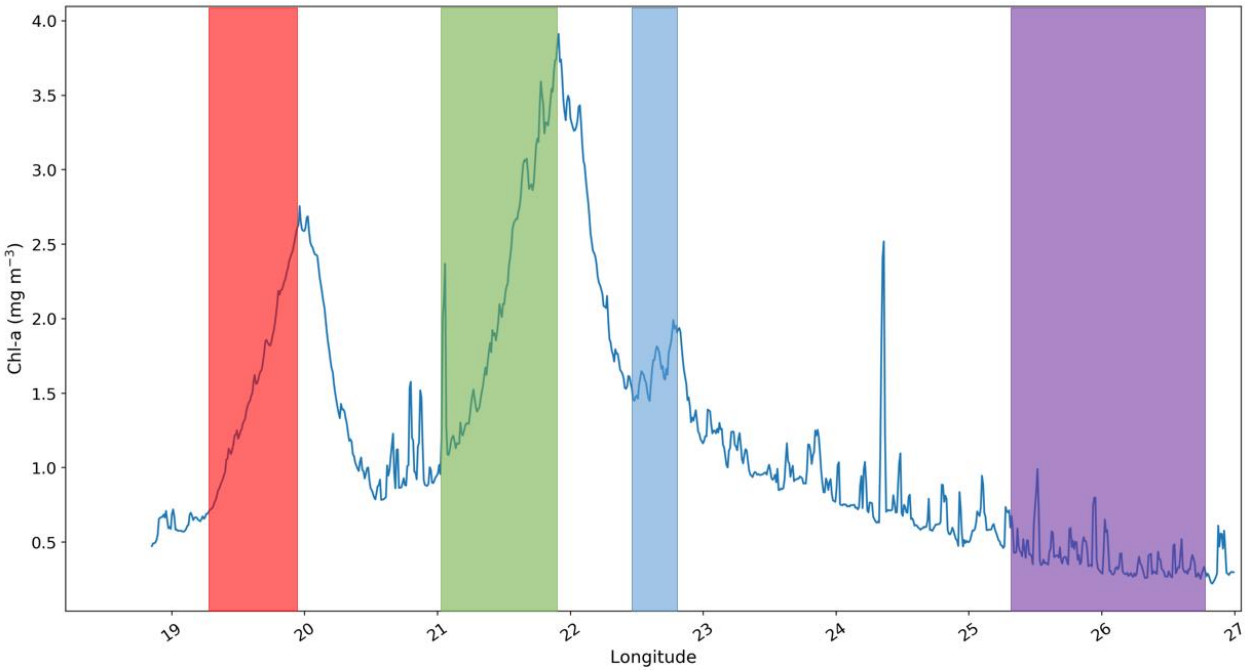

Figure 13: Spatial standard deviation of Chl-a overtime along longitude highlighting regions with high variations in phytoplankton biomass.

Figure 14 shows the monthly average *Chl-a* concentration for each of the regions (figure 13) over a period of 16 years, between 2003 to 2018. The *Chl-a* time series for each sub-region show high inter-annual variability. Algoa bay has four distinct highest *Chl-a* concentrations peaks observed in 2004 with *Chl-a* ~ 44 mg m^{-3} being the highest, 2005, 2014 and 2017. Garden route had two distinct high peaks in 2003 and 2004. Langeberg has relatively low concentration compared to other regions.

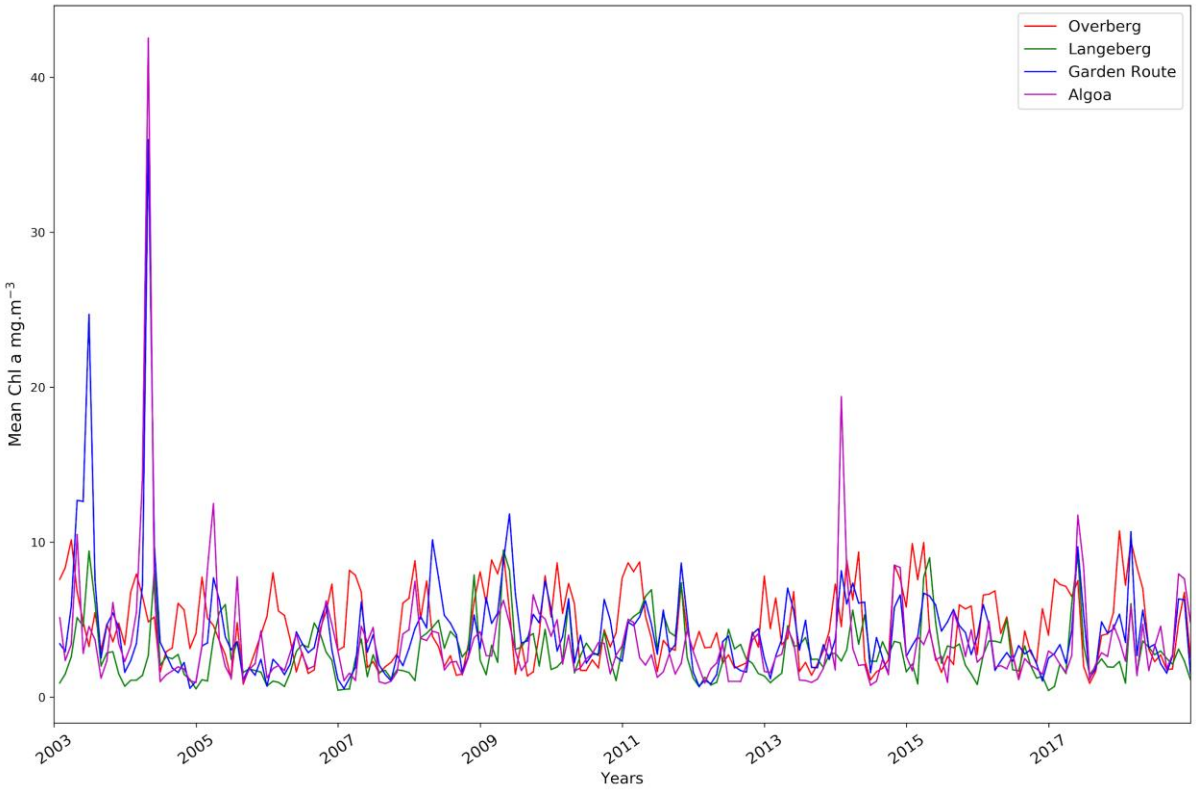

Figure 14: Monthly average time series plot of Chl-a (mg m^{-3}) Overberg (Red), Langeberg (green), Garden Route (blue) and Algoa Bay (purple).

4.2.2 *Chl-a* Seasonal Patterns

Figure 15 shows the monthly climatology plot of *Chl-a* for the four regions and their standard deviation. The seasonal cycle for each region has different shapes but are consistent in that they have an expected autumn *Chl-a* increase peak. For the monthly climatology each region experiences different monthly peaks, in which it corresponds to the upwelling season of that particular region. Although these regions have lower average concentrations compared to those of the west coast, they show similar seasonal trends of autumn maximum peaks and spring peaks of *Chl-a* due to the prevalence of long-shore winds that induced upwelling during these seasons (Smith 2016).

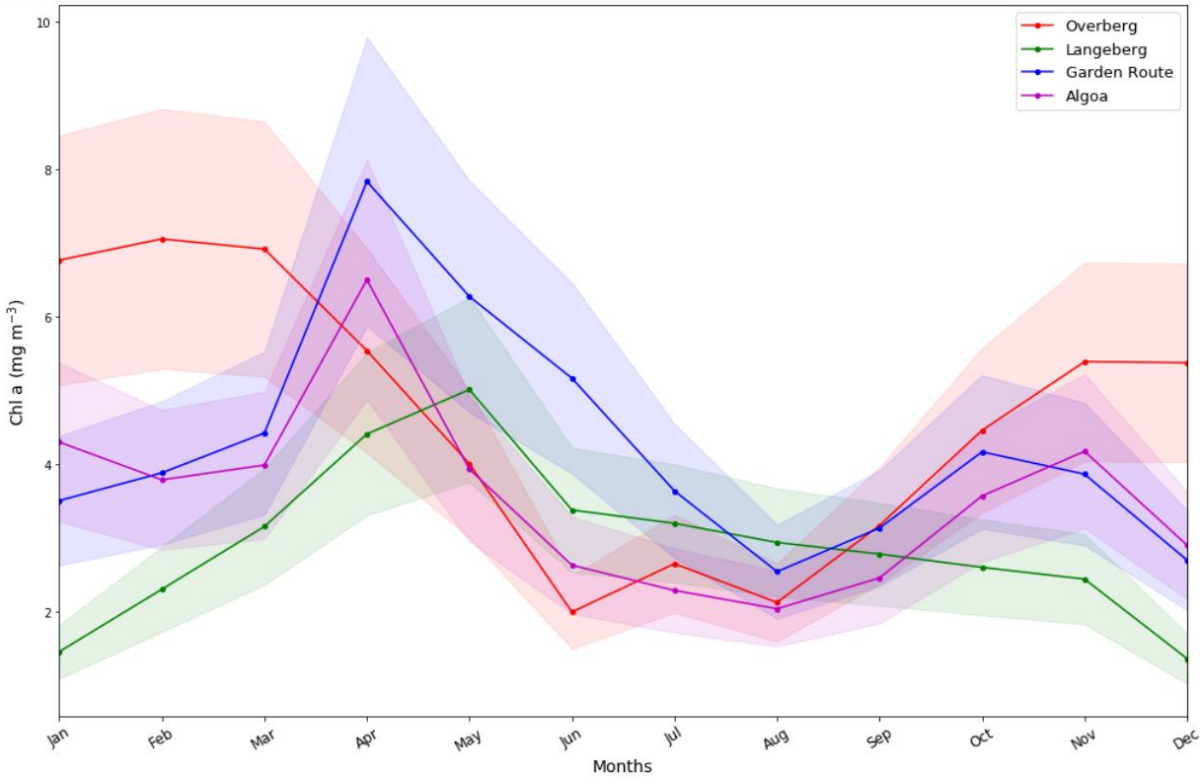

Figure 15: Averaged monthly climatology plot and their standard deviation (shaded colours) of Chl-a (mg m^{-3}) Overberg (Red), Langeberg (green), Garden Route (blue) and Algoa Bay (purple).

These four regions have strong seasonal signals, and they show the greatest variability in chlorophyll productivity throughout the year. All of them show a bimodal pattern, experiencing two seasonal peaks in autumn and in spring, except the Overberg sub-region, this area experiences long summer peaks, spring peaks and also in winter (July), during winter there's deeper water column mixing resulting in moderate biomass as previously observed by Beckley (1988).

4.2.3 *Chl-a* Trends

4.2.3.1 Yearly Chl-a averages

This analysis is meant to be an overview of the temporal trends to detect major differences between the regions. Figure 16 shows the time series of yearly *Chl-a* averages for Overberg (panel a), Langeberg (panel b), Garden Route (panel c) and Algoa Bay (panel d), the trend is calculated using the least-squares regression (dotted black line), Theil-Sen regression (solid green line), and the Theil-Sen 95% confidence intervals are also presented (dotted red line). The annual mean *Chl-a* concentration shows apparently increasing trends in Overberg and in Langeberg and decreasing trends in the other two regions. None of the trends is however significant, as shown by the confidence interval of the slopes that crosses the zero. There is a clear signal of large interannual variability in the means. The mean annual *Chl-a* concentration in Overberg fluctuated between ~3.2 mg m^{-3} and ~5.35 mg m^{-3} (lowest 2012, peak 2003 respectively). In Langeberg the mean annual *Chl-a* concentration showed fluctuation between ~1.76 mg m^{-3} lowest in 2007 and highest peak of ~5.57 mg m^{-3} in 2011. In Garden Route the mean annual *Chl-a* fluctuated between ~3.69 mg m^{-3} and ~8.76 mg m^{-3} (lowest 2007 and 2012, peak 2003, respectively). Then in Algoa Bay *Chl-a* fluctuated between ~3.76 mg m^{-3} and ~9.13 mg m^{-3} (lowest 2012 and 2013, peak 2004 respectively).

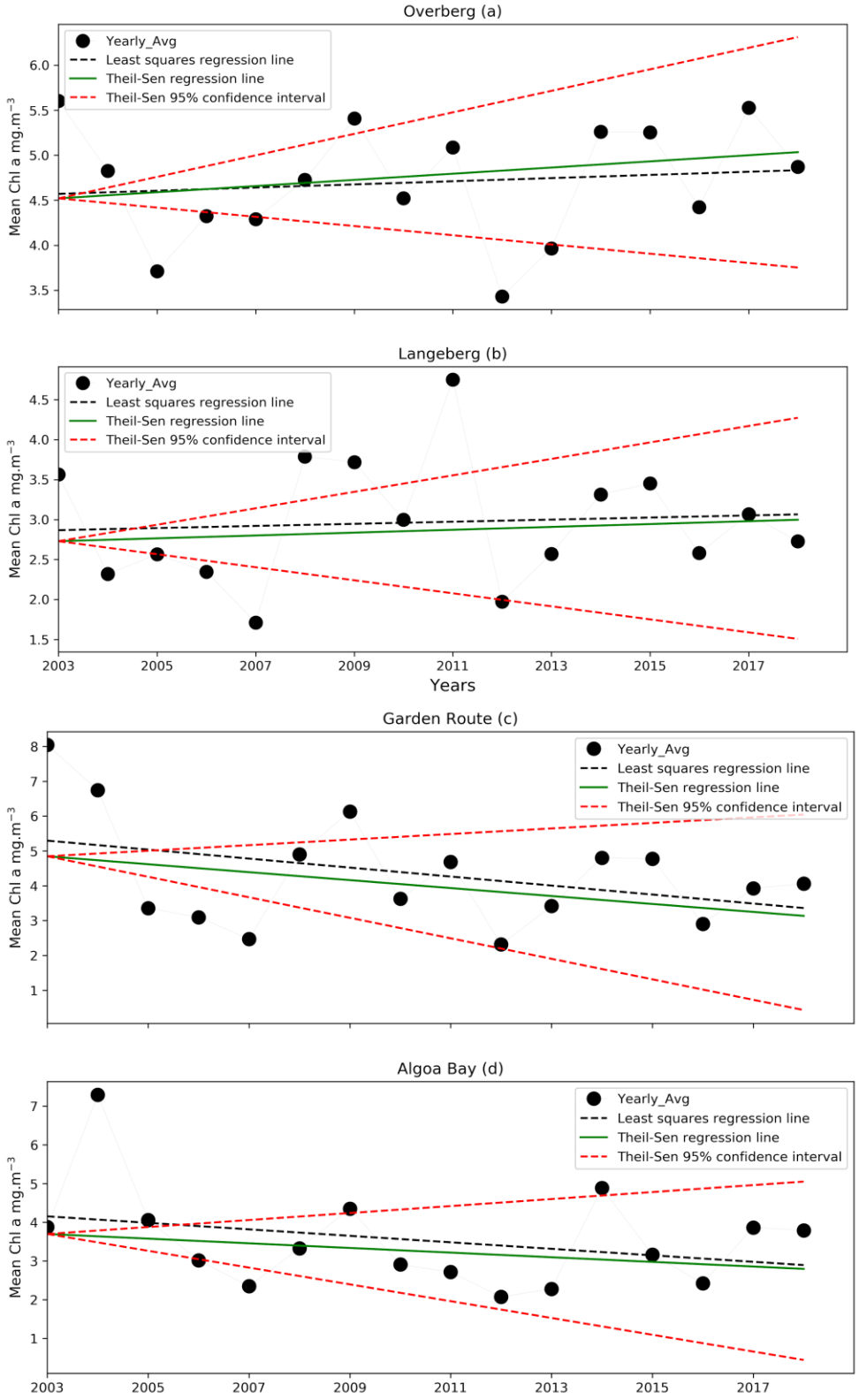

Figure 16: Time series plot of Chl-a yearly averages (black dots) with fitted trend lines: least squares regression line (dashed black line), Theil-Sen regression line (solid green line) and Theil-Sen 95% confidence intervals (dashed red lines) for Overberg (panel a), Langeberg (panel b), Garden Route (panel c) and Algoa Bay (panel d).

4.2.3.2 Chl-a Anomalies

The monthly climatological anomalies were plotted to show the information about the interannual changes in the magnitude of *Chl-a* concentration in Figure 17 (Overberg (panel a), Langeberg (panel b), Garden Route (panel c) and Algoa Bay (panel d)). For all the regions the positive anomalies were typically observed during periods of high *Chl-a* concentration. To better analyse the Garden Route and Algoa Bay regions, the time series for monthly anomalies are computed from 2005, due to the biases caused by the peaks in 2003 and 2004 as seen in figure 13.

The results in figure 17 show positive and negative anomalies in all-season, which is indicative of the issue in defining a climatology for the regions. However, the Overberg region (panel a) seems to present both summer and winter anomalies even though summer dominates. In this region after 2013 the summer positive anomalies prevail, even though in previous periods there was a bit of alternation. In 2003, 2009, 2014, 2017 and 2018 all summer months appear anomalous with respect to the climatology, which may be indicative of a summer trend in primary production.

Langeberg (panel b), with Garden Route (panel c) seem to have a similar anomalies pattern, where they both experienced persisting positive summer-autumn anomalies in 2008, 2009, 2014 and 2015 with negative anomalies in 2005-2006, 2007, 2012 and 2016. Moreover, Langeberg had an interesting period between 2008 - 2012 with anomalously positive *Chl-a* both in summer and winter, which were more productive than the entire climatology over the 16 years period. As for Algoa bay (panel d) there's low positive anomaly amplitude, and the years with persisted negative anomalies dominate.

The monthly anomalies of *Chl-a* highlight the dominant variability of *Chl-a* at certain years, the amplitude and frequency are different for each region and varies with time. The anomalies magnitude of *Chl-a* concentration fluctuate between ~ -3.61 mg m^{-3} in 2012 to ~ 5.2 mg m-3 in 2015 and 2018 (Overberg (panel a)), in Langeberg the *Chl-a* fluctuate between ~-3.0 mg m^{-3} in 2016 to ~6.3 mg m^{-3} in 2009 (panel b), in Garden Route the *Chl-a* fluctuate between ~-4.7 mg m^{-3} in 2007 to ~34.3 mg m^{-3} in 2004 (panel c), and then in Algoa Bay the *Chl-a* fluctuate between ~-4.3 mg m^{-3} in 2014 to ~38.6 mg m^{-3} in 2004 (panel d).

For further analysis on monthly *Chl-a* anomalies, the trend was calculated for each region focusing on the peak month of the climatology (figure 15). The trends shown in figure 18 were also calculated using the least-squares regression (dotted black line), Theil-Sen regression (solid green line), and estimating the 95% confidence intervals (dotted red line). The February monthly anomalies showed an increasing trend in Overberg (panel a) and the May monthly anomalies in Langeberg showed no trend. In Garden Route and Algoa Bay the trend was calculated using the April monthly anomalies, and both regions showed a decreasing trend. Despite the apparent increase in Overberg highlighted in figure 16, none of these trends are significant, as shown by the confidence interval of the slopes that crosses the zero.

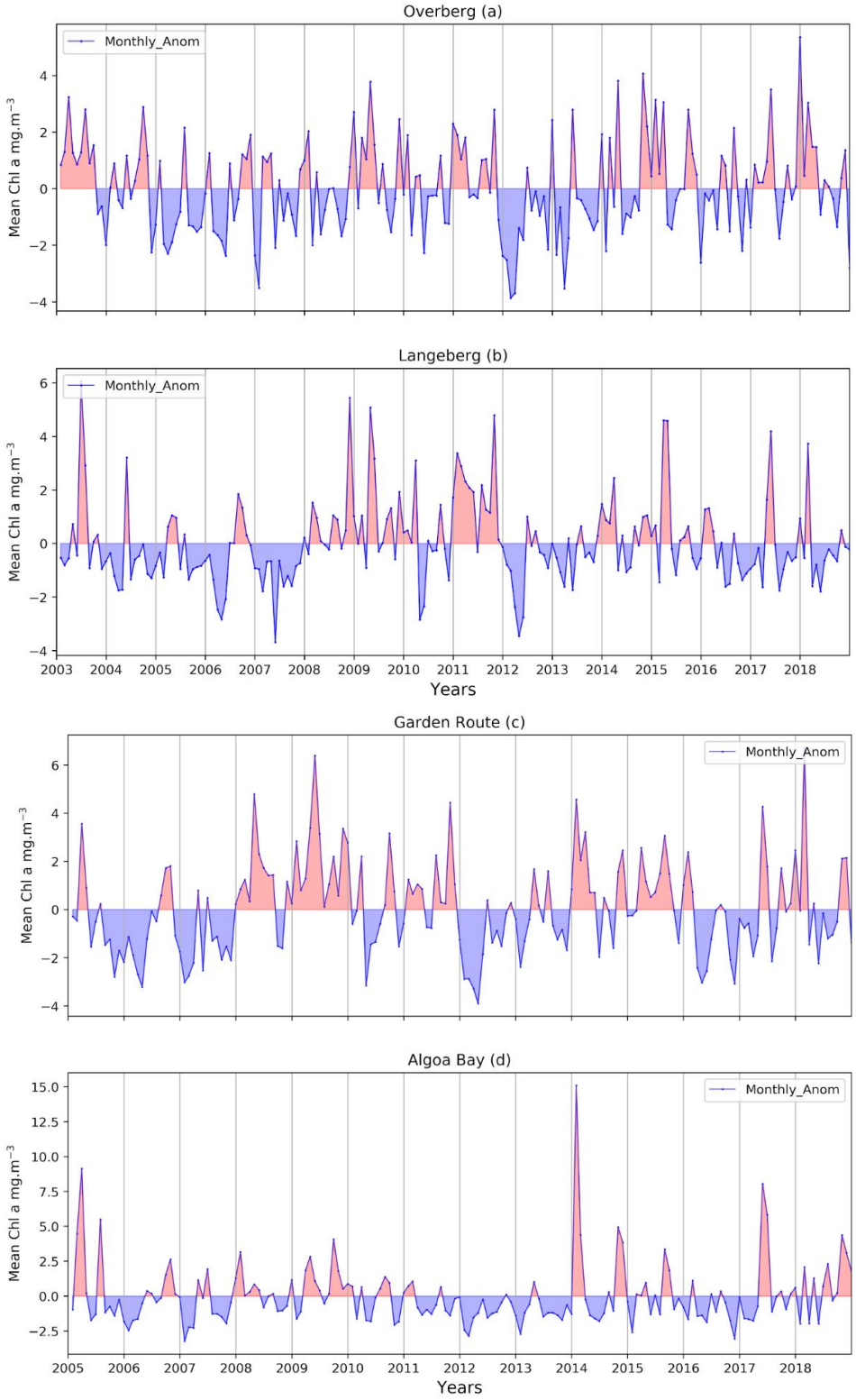

Figure 17: Monthly time series plot of Chl-a anomalies with positive anomalies (shaded red) and negative anomalies (blue line), for Overberg (panel a), Langeberg (panel b), Garden Route (panel c) and Algoa Bay (panel d). Panels c and d show anomalies over the period 2005-2018 to exclude the extreme events shown in figure 13.

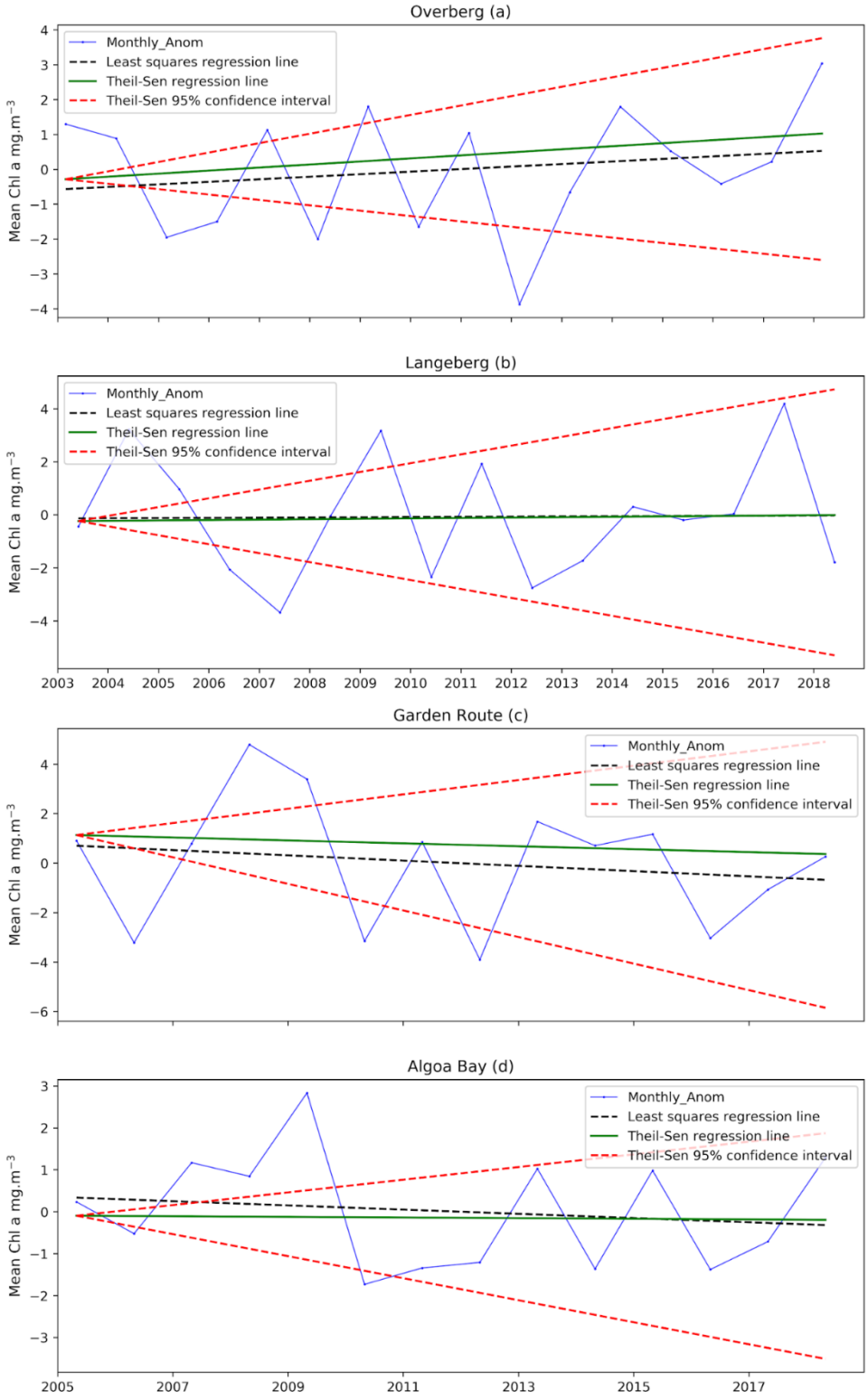

Figure 18: Climatological peak monthly time series plot of Chl-a anomalies for February in Overberg (panel a), May in Langeberg (panel b), April for Garden Route (panel c) and Algoa Bay (panel d). Panels c and d show anomalies over the period 2005-2018 to exclude the extreme events shown in figure 13.

4.3 The bloom analytic

4.3.1 Spatial extent of bloom distribution in time

The spatial extent, seasonality and frequency of bloom is analysed with the bloom analytic tool described in Sec. 3.6. It is evident that the south coast has experienced blooms more often than those recorded in Sec. 4.2, and these waters are vulnerable to HABs. Figure 19 shows the detected areal extent of spatial distribution and the number of blooms (second axis) annually in Overberg (panel a), Langeberg (panel b), Garden Route (panel c), and Algoa Bay (panel d) respectively, from 2003 to 2018. The year 2002 was excluded on further analysis as it starts in August. The number of blooms was calculated by summing up all the number of days the bloom was detected on the water column.

The Overberg (panel a) region had a total number of 546 blooms between 2003 and 2018, moreover 2015 had the highest number of 45 blooms, 2007 and 2008 have the same number of bloom occurrences of 42, even though the blooms had different spatial extents, and the year with the lowest number of blooms is 2012 with only 21 occurrences. In this region the two years that showed the largest spatial extent of total bloom coverage were 2010 and 2012, with ~5409 km^2 and ~3435 km^2 respectively, even though these years had about 20 blooms each.

Langeberg (panel b) had a total number of 409 blooms over the years, having 36 frequent occurrences of blooms as the highest number, that include 2003, 2008, and 2011 even though they had different bloom extent, and 2018 is the least year with only 12 blooms. In Langeberg two years that showed the largest spatial extent of total bloom coverage were 2003 and 2004, with ~2959 km^2 and ~3459 km^2, respectively. Garden Route (panel c) had a total of 880 blooms from 2003 to 2018, having 88 number of blooms in a year as the highest number in 2003, and 2006 being the least year with only 34 number of blooms. The year with the largest bloom extent Garden Route is 2004, with a bloom spatial extent of ~ 21979 km^2, followed by the 2003 bloom with a spatial extent of 12883 km^2. Algoa Bay (panel d) had a total of 850 blooms, having 73 as the highest number of blooms in 2014 but only 2 blooms been publicly recognised (Sec 4.2), and 2012 being the least year with only 36 blooms with a spatial extent of less than 471 km^2, furthermore, 2004 is recorded as the largest event with an areal extent of 15887 km^2 followed by the bloom in 2005 with a spatial extent of 9458 km^2.

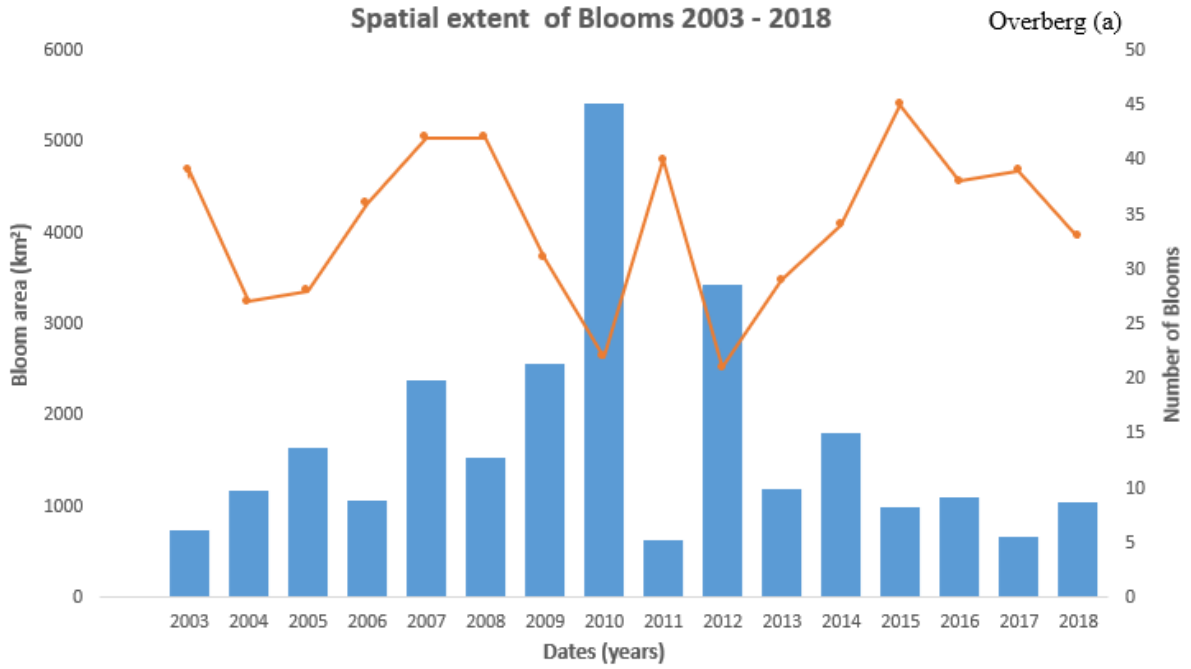
Spatial extent of Blooms 2003 - 2018
Overberg (a)
Bloom area (km²)
Number of Blooms
Dates (years)
6000
5000
4000
3000
2000
1000
0
50
45
40
35
30
25
20
15
10
5
0
2003 2004 2005 2006 2007 2008 2009 2010 2011 2012 2013 2014 2015 2016 2017 2018

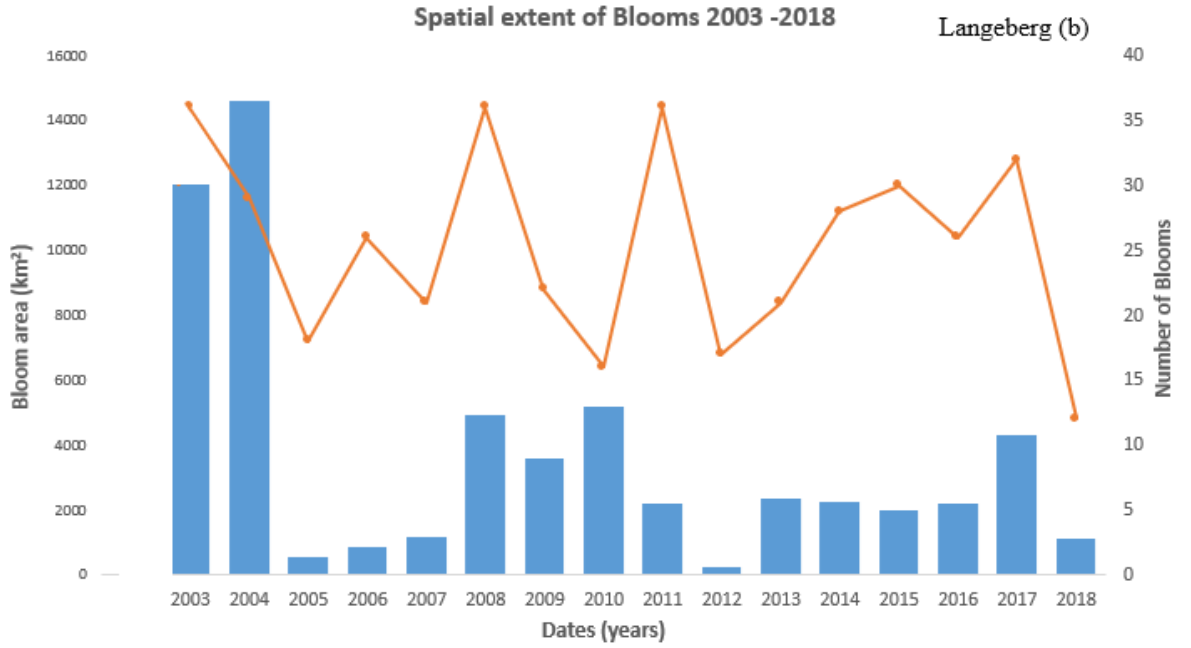
Spatial extent of Blooms 2003 -2018
Langeberg (b)
Bloom area (km²)
Number of Blooms
Dates (years)
16000
14000
12000
10000
8000
6000
4000
2000
0
40
35
30
25
20
15
10
5
0
2003 2004 2005 2006 2007 2008 2009 2010 2011 2012 2013 2014 2015 2016 2017 2018

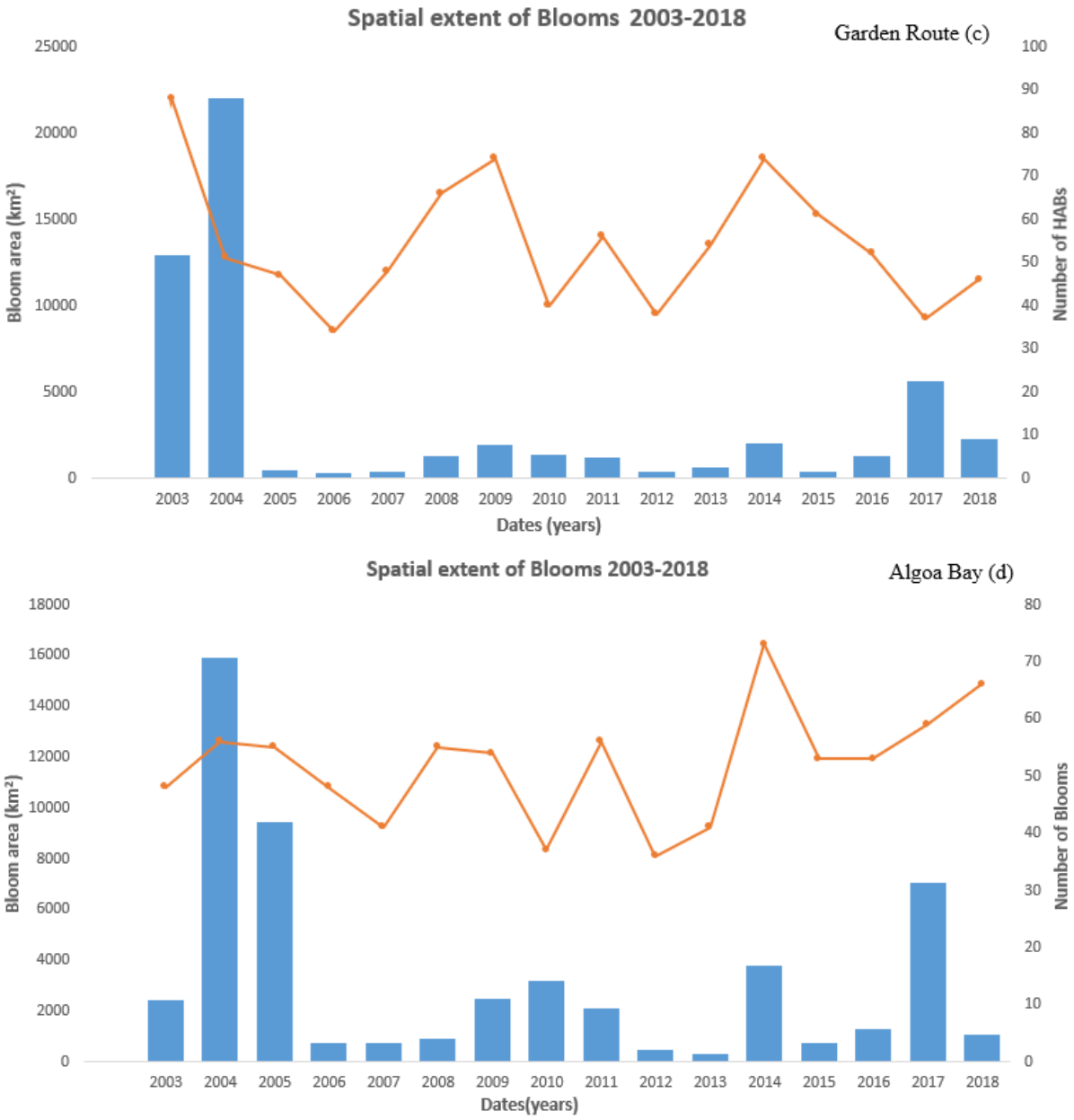

Figure 19: Yearly time series plot of bloom spatial extent (blue) and the number of blooms each year (Orange) for (a) Overberg, (b) Langeberg, (c) Garden Route and (d) Algoa Bay.

4.3.2 4.4.2 Seasonal variation

Figure 20 shows the monthly climatology and seasonal variations of the average total bloom spatial extent for each of the four regions. The seasonal cycle is similar to that of *Chl-a* in section 4.3.1, all the regions have similar seasonal patterns and have an expected autumn peak. However they experience some minor differences in their monthly climatology, Overberg (panel a) has a different seasonal and monthly variation compared to other regions, the average combined spatial bloom extent is larger in march, and starts to decrease around April, reaching the smallest average combined spatial extent in June. Whereas Langeberg (panel b), Garden Route (panel c), and Algoa Bay (panel d) reach their maximum average combined spatial bloom extent in April, and also in June. Moreover, the major difference is in the spring season, Overberg (panel a) experiences the second bloom peak from October-to end November, whereas Garden Route (panel c) only experiences some second bloom peak in October. Langeberg (panel b), and Algoa Bay (panel d) experience the second bloom peak in November.

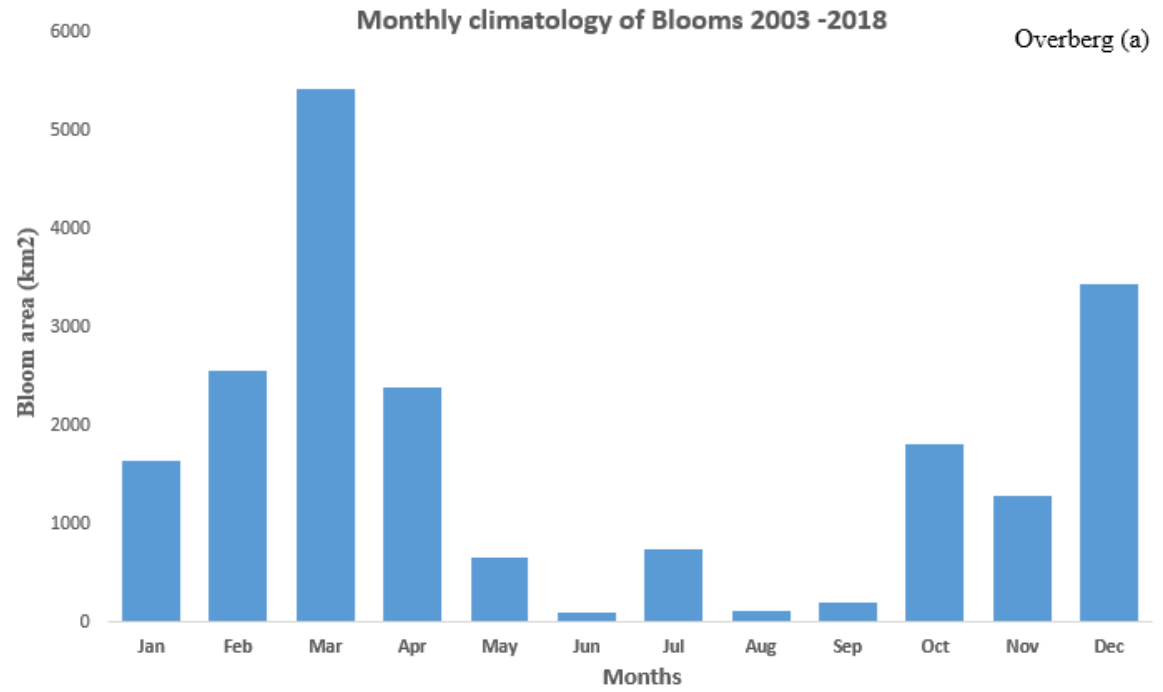
Monthly climatology of Blooms 2003 -2018
Overberg (a)
Bloom area (km2)
6000
5000
4000
3000
2000
1000
0
Jan
Feb
Mar
Apr
May
Jun
Jul
Aug
Sep
Oct
Nov
Dec
Months

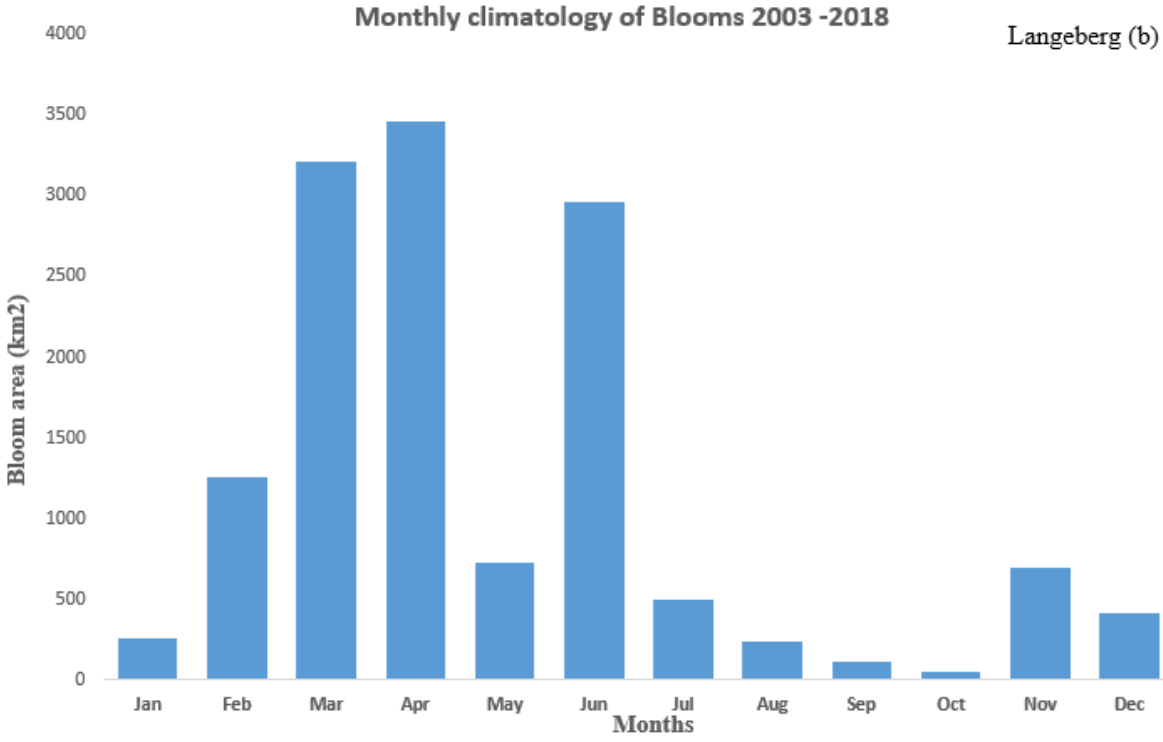
Monthly climatology of Blooms 2003 -2018
Langeberg (b)
Bloom area (km2)
4000
3500
3000
2500
2000
1500
1000
500
0
Jan
Feb
Mar
Apr
May
Jun
Jul
Aug
Sep
Oct
Nov
Dec
Months

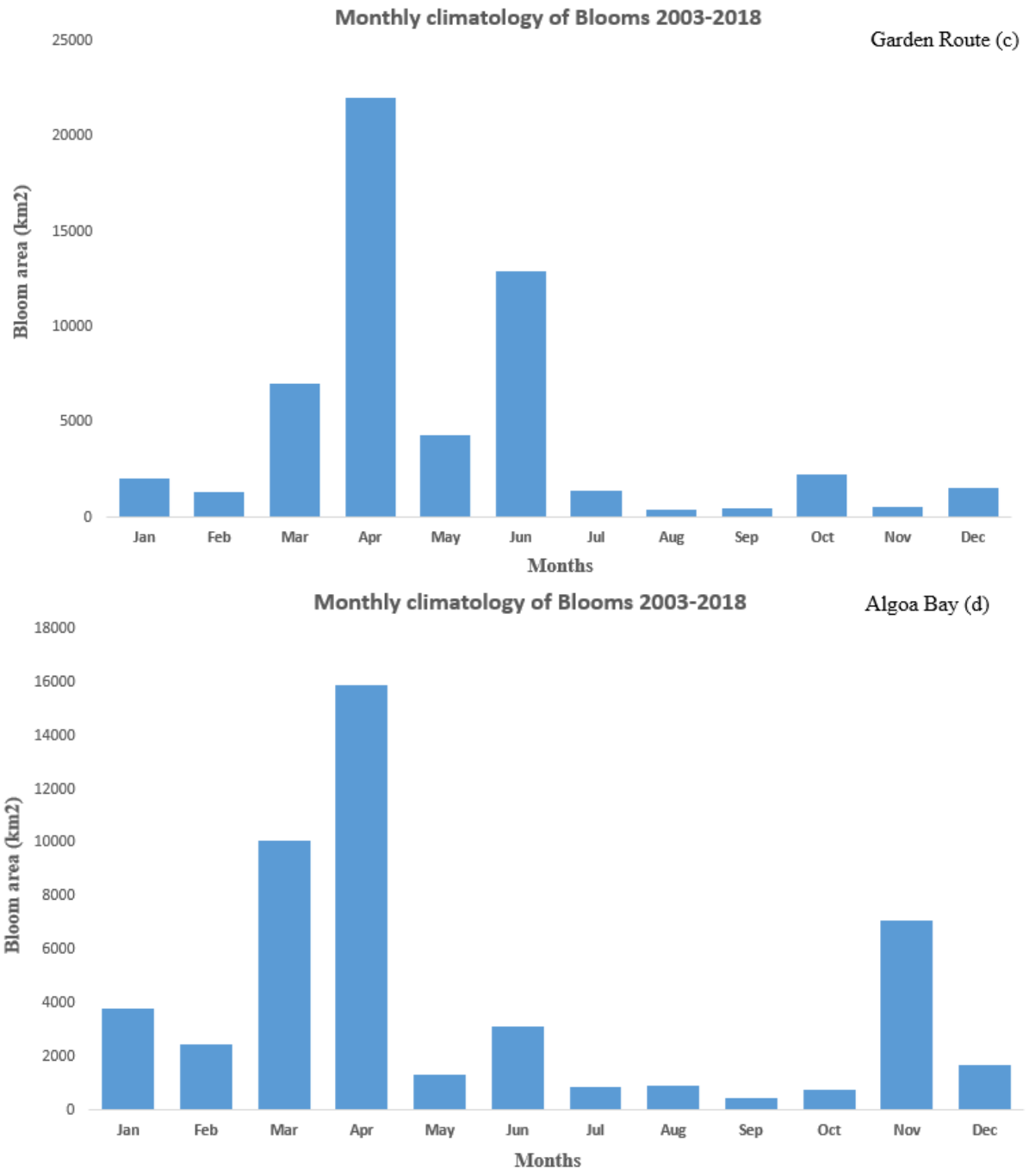

Figure 20: Climatological monthly time series of the bloom analytic spatial extent for (a) Overberg, (b) Langeberg, (c) Garden Route and (d) Algoa Bay.

4.4 Harmful Algal Bloom: Case Study

For this Case study, Overberg is selected as the focus area, as it is where most of abalone aquaculture farms are located, and recently it has been affected by numerous high-biomass dinoflagellate blooms that resulted in massive mortalities (Pitcher *et al.*, 2010; see Chapter 1). The case study focus will be on the massive biomass bloom that was observed from the beginning of February to the end of March 2019 in the Overberg area (Figure 21). The areas with bloom were identified using OLCI (as explained in section 3.5.1), over a period of two months (from February to March) of 2019. Figure 21 shows the average *Chl-a* concentration over the period of the bloom, also showing the farms where there are available phytoplankton count data, denoted by the black dots with numbers, they were referred to as farm 1, farm 2 and farm 3.

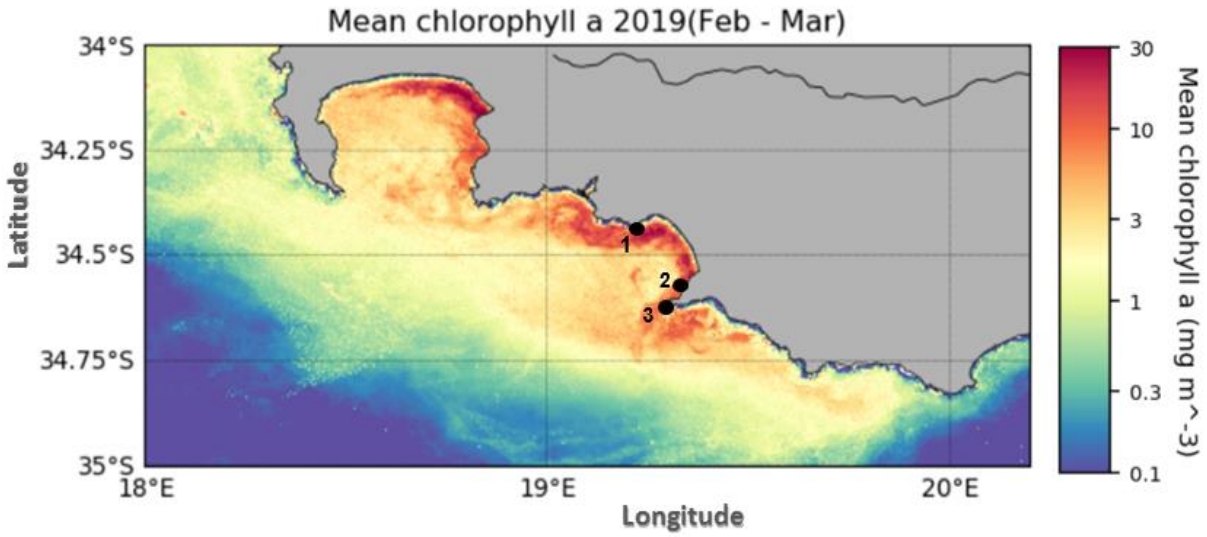

Figure 21: The average Chl a concentration over the Overberg region, for the period of two month (Feb-Mar 2019) showing a bloom.

The bloom dynamics and hydrographical conditions of the bloom were examined by different aquaculture farms that were affected around this area. Furthermore, the bloom movement and physical oceanography were examined with the use of *Chl-a* and SST images. Firstly, it is important to note that the phytoplankton count data do not record all the species in the water column but only those that have a negative or harmful impact on the farms and environment, while satellite *Chl-a* measurements represent the entire phytoplankton population present. According to the farms data, the bloom was mainly dominated by three dinoflagellate species identified by light microscopy (as explained in Sec.3.3.1) as *L. polyedrum*, *G. spinifera* and *Prorocentrum micans*, and these species caused discoloration of waters. Even though *L. polyedrum*, and *G. spinifera* species are common bloom-causing species in recent years, their toxic impact is still not fully understood except for the Yessotoxin that was detected on the abalones in the bloom event of 2016/2017 in this same area (Pitcher *et al,*. 2019). They caused mariculture loss and fish kill due to Yessotoxin and oxygen depletion in water. *L. polyedrum* concentrations exceeded those of *G. polygramma* throughout the bloom period in all 3 farms (per. comm from the farmers).

During the bloom period, the weather had clear skies to cloudy (as the satellite imagery shows in figure 22), and due to cloud cover, there were only seven OLCI overpasses that were actually showing Chl-a data useful to the farms, compared to fifty that were recorded over this study region. For the first week of February the bloom concentration was relatively low especially in farm1 and farm3. These two farms experienced the lowest concentrations of these species, while farm 2 started to experience the bloom on week 2 of February for a few days, then the species disappeared again until the 23rd (figure 22(h)). In the same period, end January beginning February before the bloom, the SST imagery showed a cold-water plume extending from the coast, followed by warming surface waters and an increase in *Chl-a* (not shown). This indicated that the phytoplankton species were induced and supported by larger scale upwelling that brings nutrients from the deep ocean to the surface and from coastal waters to offshore water. The bloom developed on week two of February and was spatially distributed westward from its point of origin, and on the 15 of Feb there was a mixing of water due to upwelling which led to more nutrients on the water surface that fuel the bloom to be more concreted (temperature - figure 22(d)). The spatial and temporal variation in *Chl-a* as detected through remote sensing (figure 22) coincided with the available phytoplankton count data from certain farms (figure 23). The development and spatial distribution of the bloom are shown in Figure 22.

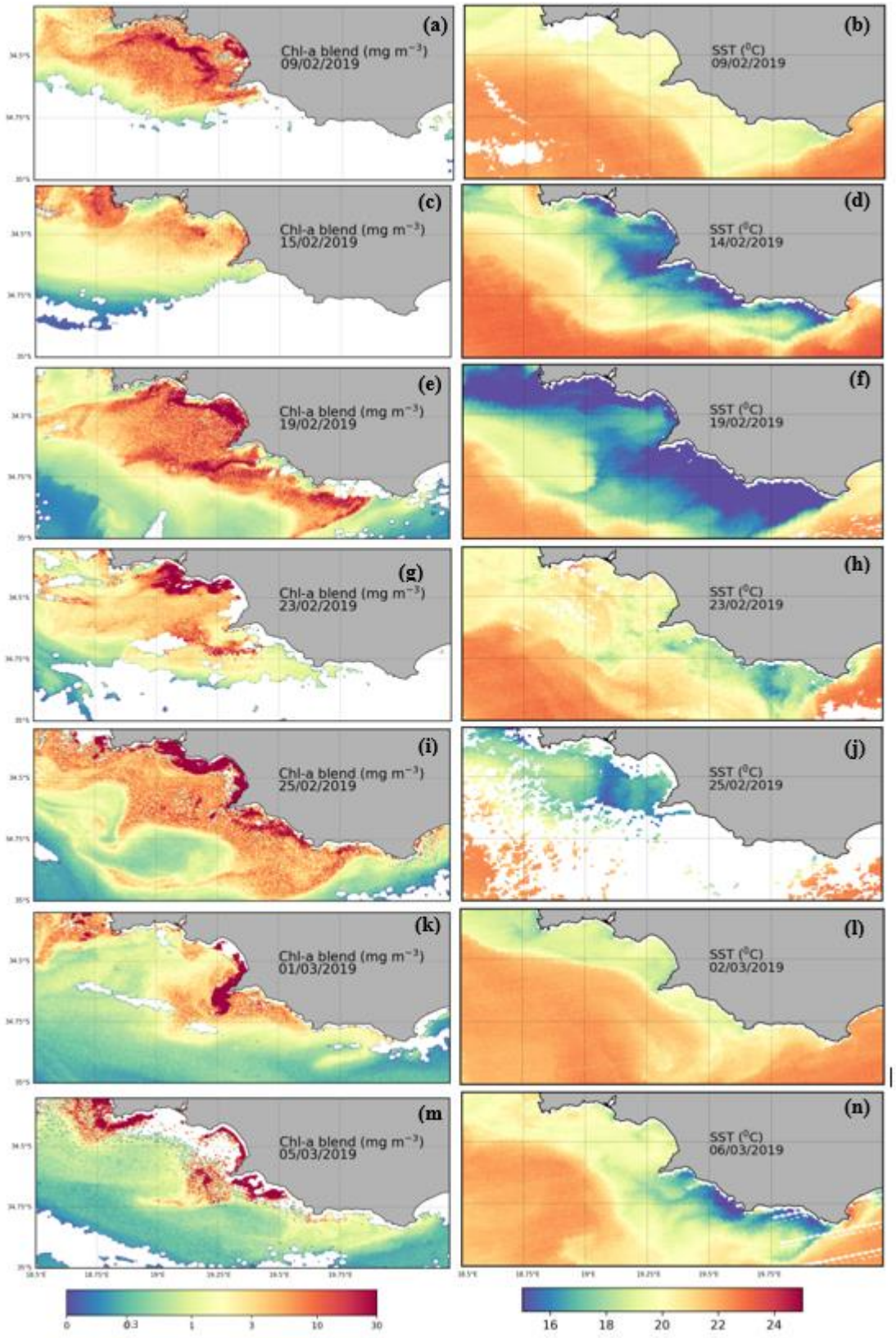

Figure 22: The spatial distribution of phytoplankton bloom and SST over the Overberg region, over the period from Feb-Mar 2019.

Farm 1 had multiple peaks, with the major one reaching the highest concentration of 2.4 million cells/l on the 23rd, on the 24th of March the concentration started to increase again (figure 22). On the 23rd of February farm2 bloom concentration started to increase reaching its peak of ~ 5 million cells/l on the 26th, which is the highest concentration at all three farms. Farm3 had the lowest concentration during the end of February bloom; it started increasing on the 25th reaching its highest peak of ~ 60051 cells/l on the 28th. I noticed that by the end of February and beginning of March the concentration of *Prorocentrum micans* showed a distinctive increase almost competing with *L. polyedrum.* The bloom persisted for 2 months, 1 week in this area, then it dissipated on the water column (Figure 22 and Figure 23).

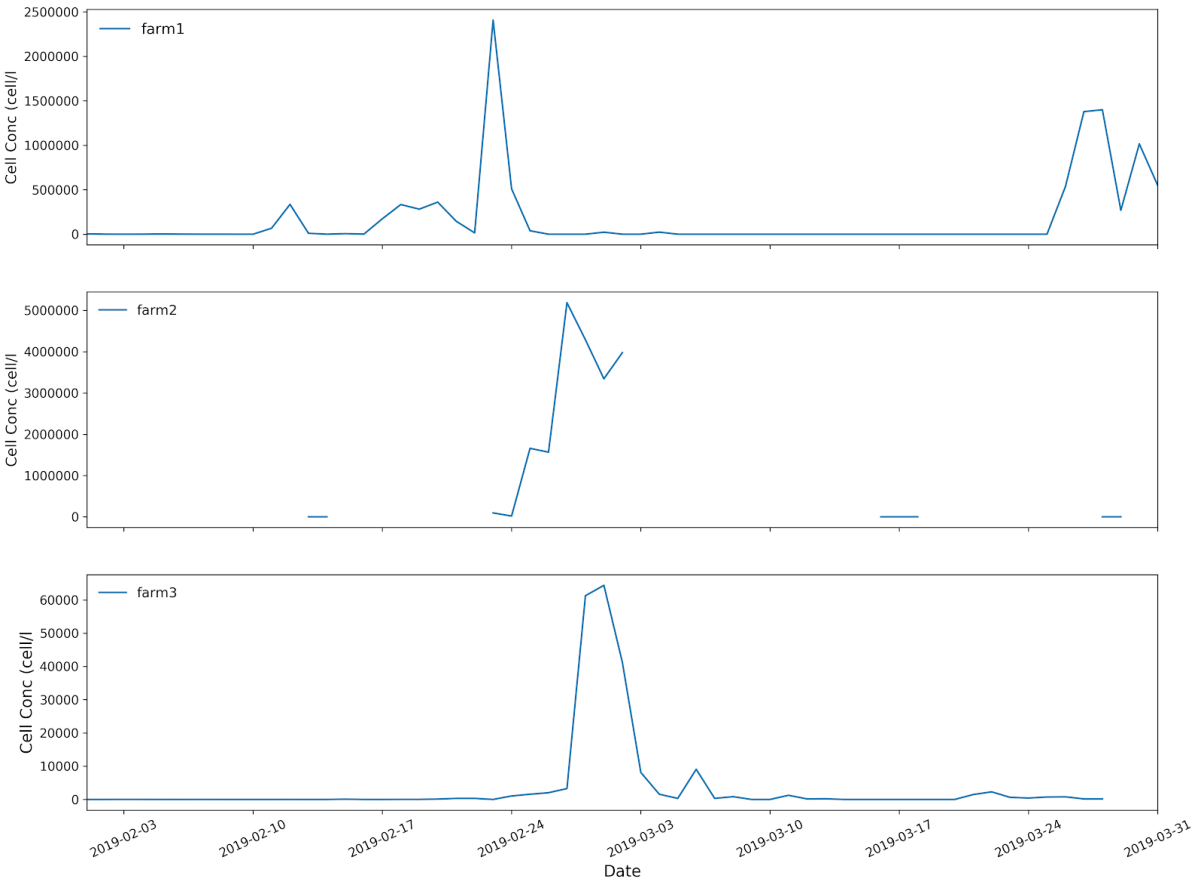

Figure 23: Total abundance of G. polygramma and L. polyedrum cell concentration (cell/l) measured at the three farms. Note the different y-axes.

4.5 Fisheries and Aquaculture Decision Support Tool (DeST)

This section of the results chapter outlines the use of the DeST for HAB-related monitoring and decision making within the South African marine aquaculture community. As illustrated in Sec 2.4, certain HABs can result in mortalities of abalone stock, loss of condition of oyster stock, and/or the accumulation of biotoxins in mussel stock, all of which can place economic strain on these industries and the communities that they support. To enable early warnings on the upcoming and occurring HABs to aquaculture farms and other end users, an information system based on the combination of optical remote sensing data (MODIS, OLCI) and model data is used (Sec 3.8). The complementary use of these different data sources compensates for the limitations of each of the data sources. Remote sensing gives the actual status on the phytoplankton algal bloom and the model data allows for the near real time forecast of the bloom. The information on the status of the bloom is reported to all stakeholders via website, email or WhatsApp daily to provide them with heads up of the bloom development/distribution as shown in figure 24, as to make viable commercial plans to reduce the commercial impact of these blooms. In these information sharing platforms, there are also discussions that take place about the occurring bloom.

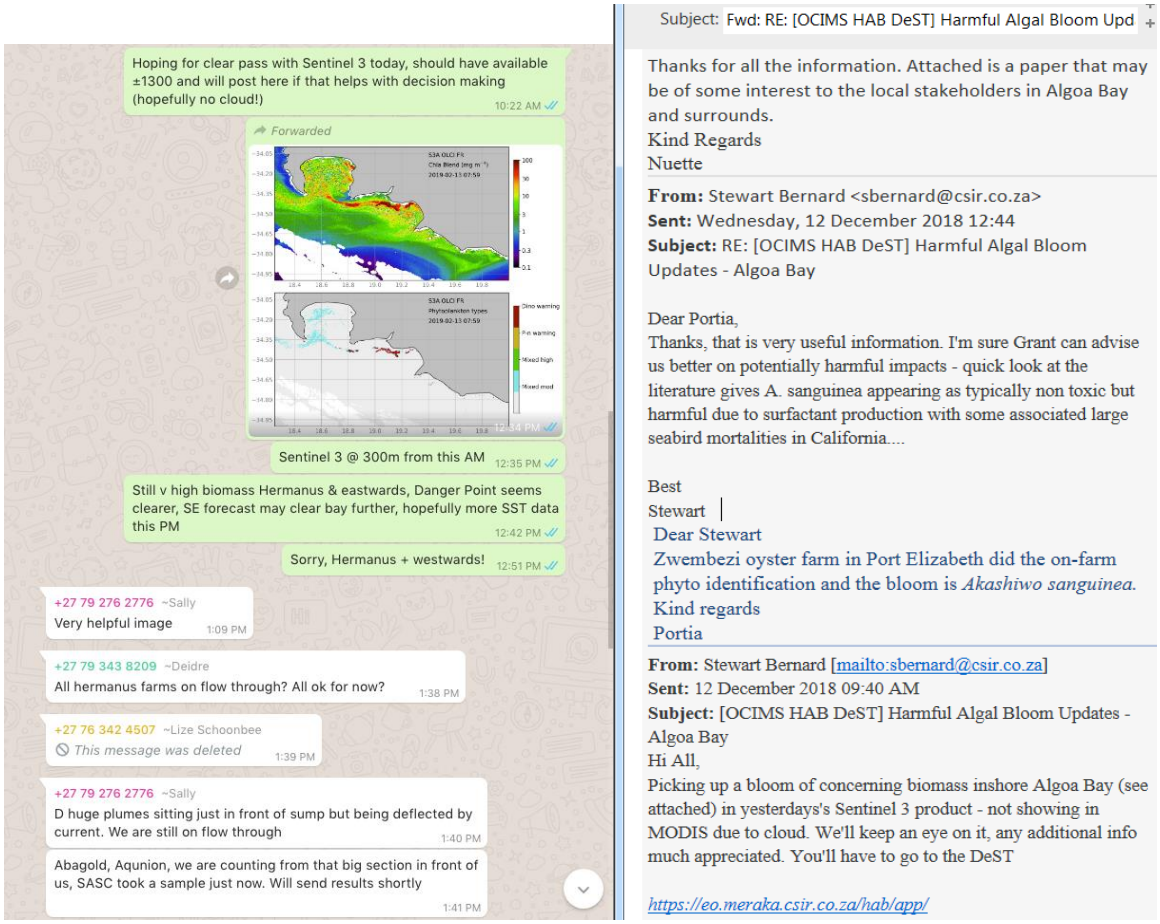

Figure 24: WhatsApp (walker bay area-2019) and email (Algoa Bay area 2018) snapshot of the development of HAB on the coast, with the input, and discussing the HAB distribution and causative species.

4.6 The Aquaculture user perspective

One component of the thesis was to propose and analyse the uptake on how this tool was actually taken up with new methodology into the day-to-day operations in the aquaculture farms. Part of achieving the aim of integrating this monitoring tool into the day today: I visited the farms and collected the following information. These are the day-to-day operations that I have connected and learned. Since the establishment of each farm, farms have managed to monitor the presence of phytoplankton blooms in their water. Management strategies have included regular monitoring of phytoplankton count data, water quality, temperature, and ocean colour remote sensing (*Chl a*).

4.6.1 Farm Operation

Marine aquaculture is a diverse production industry involving a variety of different species, production methods and farming operations. In this section the focus will be on abalone farm operation and assessment. As for all farming, marine aquaculture development have specific demands for the site selection and is well documented in (Final Abalone Feasibility) to avoid being situated near habitats of special interest (recreation, wildlife, and fishing zones) and near industries and sewage outfalls. In South African coastline abalone farming is based on a single species, *Haliotis midae*, which is land-based. The aquaculture monitoring and risk assessment strategies vary from country to country, depending on their regulatory control.

Figure 25: Land-based abalone farm structure they are situated close to the ocean

These land-based abalone farms use a flow-through system as their production system due to the knowledge on the system's productivity, its success and available resources. Flow-through systems require massive amounts of water, high levels of tech and engineering and thus can be expensive to run. The land-based abalone farms are licenced for 181 000 cubic meters a day for water, the farms pumps approximately 150 000 cubic meters per day under optimal circumstances. The farms pump seawater directly from the ocean into land-based tanks that run-in flow-through mode, even though recirculation technology is also used (in certain conditions). The most essential features of flow-through aquaculture systems include the rapid removal of waste, the first step of water treatment starts at the intake by decomposing organic material, like kelp. They dredge the sump at the intake pumps to get rid of some of these old organic materials.

Figure 26: The intakes pumps are normally 6 meter down, they all automated

The water is pumped up to the farm, mechanically filtered through 90 micron drum-filters to remove larger particles and suspended materials, and subsequently distributed to the rest of the farm; due to the high water quality in Walker bay this is the only treatment of the sea-water required during normal operations. Under red tide conditions the drum-filters screens can be changed to 25 micron, at which point water flow-through decreases to 25% of the normal rate; farm operations at the reduced flow-through rate can continue up to concentrations of 1.5 million cells per litre. Due to the potential biosecurity risk, recirculation of farm water is only used as a last resort if there are already abalone mortalities.

Figure 27: Drum-filter, the blue pipes are for the disposal of the suspended sediments

During red tides on the intake only two pumps are used or one depending on the concentration of red tide, but the best possible thing to do, try to filter out everything, don't get any stuff on the farm, the second option is the change of filter screens on the drum-filter reduced its size to 25 micros however the challenge is the finer your screen the less water comes through the farm, resulting in water rotation, or just close everything and do recirculation. Strategy is to increase the amount/number of drum filters, by all means the farms try not to do recirculation unless the abalone start dying. Biosecurity is gone if they go on recirculation.

After the water has gone through the farm, concentrations of suspended solids (including both organic and inorganic constituents) in the outflow water should not "exceed ambient levels by more than 10%". Effluent catchment with green grid to catch-up any accidental rubbish from the farm before it goes down to the turbine.

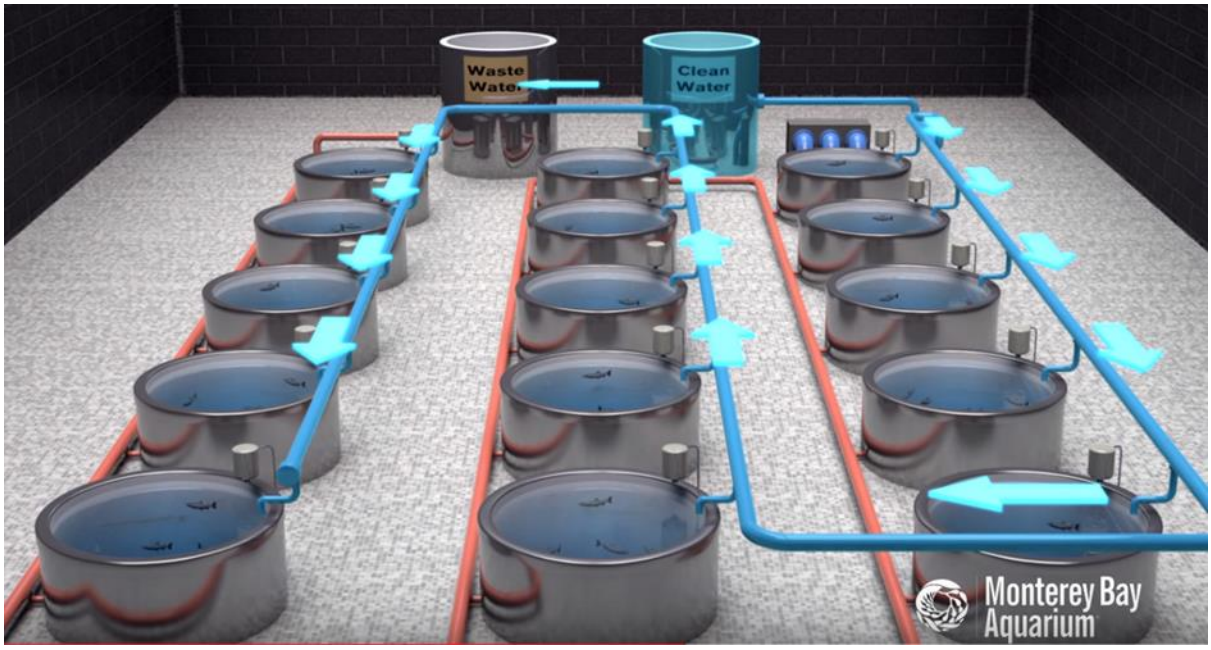

Figure 28: This is a graphic representation diagram showing how the fresh clean water is distributed on the farm tanks (blue), and the wastewater (red) is distributed out to the farm facility.

4.6.2 Monitoring parameters

The farms collect the water samples daily prior to drum-filtration to monitor the presence of HABs and do their own sample analysis as explained in 3.4; however, the samples are not left to settle, as the information is required immediately. Water samples are monitored for phytoplankton species, harmful/toxic species, and cell density through microscope analysis, whilst the water quality parameters of temperature, pH, turbidity and dissolved oxygen are measured with a skid. The sampling results are recorded on a hardcopy and on an online spreadsheet, while a monthly spreadsheet is sent to DAFF. The sampling is conducted every morning at 8 am; if an increased cell count is detected, an additional sample is taken at 12pm. During red tide events sampling may be increased to 1.5 h intervals, with supplementary sample analysis performed by Amanzi Biosecurity; additional water samples are also taken throughout the farm water supply to test the integrity of the filtration systems.

During an increase in phytoplankton cell count the farms try by all means to gather all the necessary information that might help them to understand the cause behind the increase. The farms enhance their monitoring on satellite imagery resources available www.ocims.gov.za/hab/# to check harmful algae proximity, spatial distribution and affected areas, secondly they conduct boat samples to observe what exactly they are dealing with so that they can prepare animals and when they might need recirculation.

4.6.3 Risk assessment flow chart

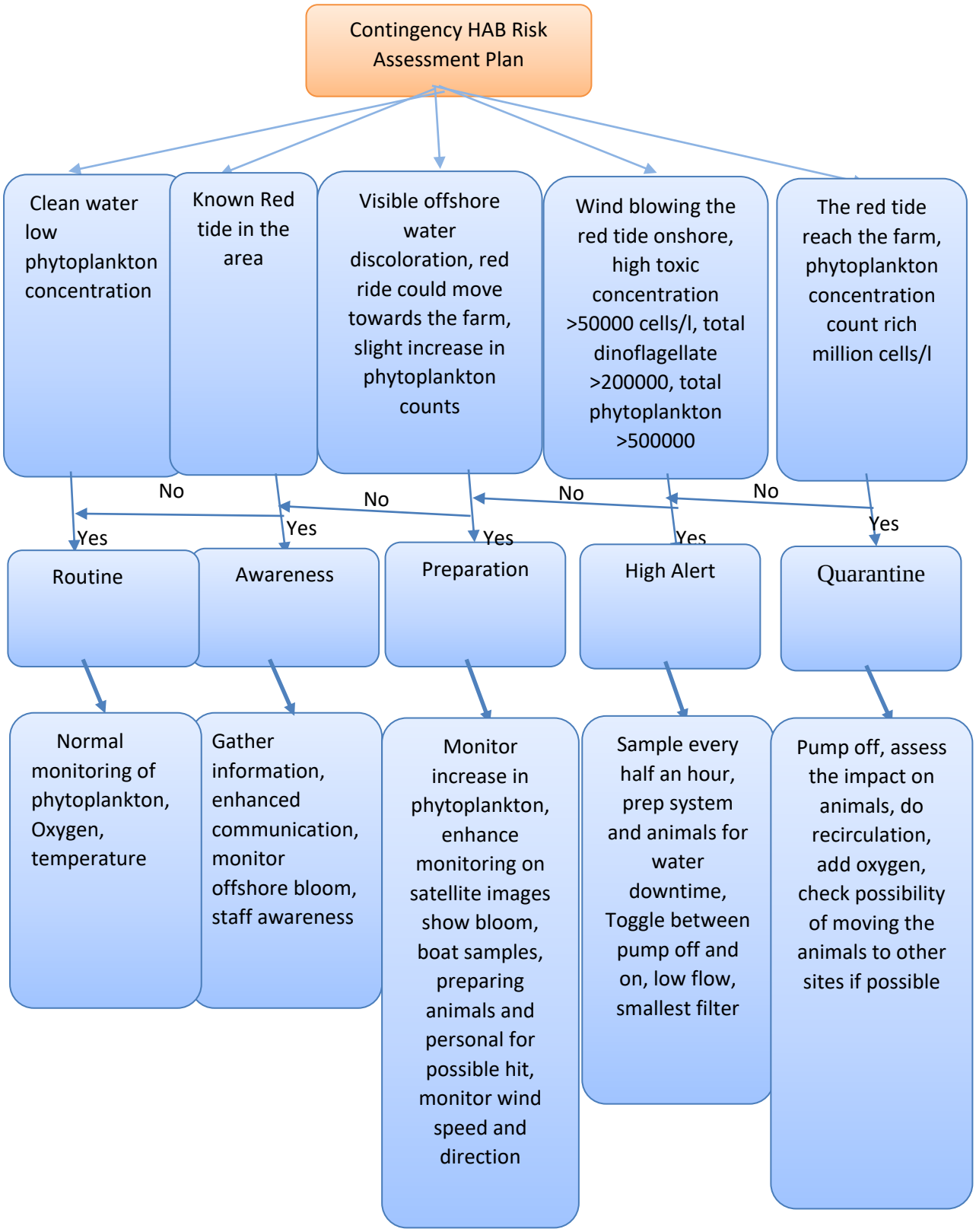

Figure 29: Flow chart for Contingency HAB Risk Assessment Plan

5. DISCUSSION

The geographic distribution of HABs has been increasing worldwide. Reports on HABs at different workshops, international conferences and publications have been recorded since the 1970s (Shen *et al.,* 2012, Anderson *et al.,* 2014; Blondeau-Patissier *et al.,* 2014; Borbor-Cordova *et al.,* 2019). Every year many coastal regions throughout the world are threatened by the series of ecological problems associated with huge economic losses and health issues caused by HABs (Anderson *et al.,* 2002; Pitcher *et al.,* 2017). Almost all the coastal and freshwater environments have experienced HABs over the last decade, and new species have emerged in some locations that were not previously known to have problems e.g. Wells *et al.,* 2015. As with all blooms, their proliferation results from a combination of physical, chemical, and biological processes and their interactions with other components of the food web.

Given the fact that blooms in the Benguela are a natural phenomenon and it is impossible to prevent them in the environment, an improved understanding and scientific method to monitor them is of crucial importance to the fisheries and coastal management practices. The time series analysis for the South African south coast provides valuable information on bloom frequency and distribution in support for the widespread observation that HABs have become more severe than previous years (Pitcher *et al.*, 2017; Pitcher *et al.,* 2019). In this thesis, time series are used to assess long-term changes, such as frequency, trends, and seasonal changes of a specific variable (*Chl-a*) that can be obtained from Earth Observation. In assessing long term changes in coastal waters, knowledge of *Chl-a* dynamics and phytoplankton composition with their long-term changes is of high importance. In doing so, long-term variability requires the availability of consistent and homogenous data. Therefore, satellite data through ocean colour studies using *Chl-a* as a proxy, provides the spatial and temporal continuity. Whereas in-situ data provide a solid anchor for the interpretation of satellites (Balsamo *et al.,* 2018) as well as to correct satellite biases (Reynolds *et al.,* 2005).

5.1 Satellite *Chl-a* versus *in situ*/count data limitations

Although ocean colour satellite sensors provide information on the location, spatial extent and temporal variation of bloom events, they have their own limitations. The ocean colour satellite sensor's ability to detect blooms depends on many factors regarding the satellite sensor specifications, algorithms etc, and on the actual properties and size of the bloom. Even the exceptional 1000 m resolution of MODIS with a long dataset that can detect large blooms, is still spatially sub-optimal for detecting blooms with less than a hundred square meters. Secondly the sensor revisit time also determines how well a bloom can be monitored. Apart from the instruments abilities the major concern is cloud cover, which results in a lot of missing data and the lack of sequential images to trace the spatial distribution and persistence of HABs (Anderson, *et al.,* 2016a; Davidson *et al.,* 2016). In addition, atmospheric corrections interfere with the accuracy of ocean colour concentration estimates (Cole *et al.,* 2012). Moreover, the greatest limitation is determining whether a "bloom" is a "HAB". Furthermore,there is still a gap between data availability and user skills which can restrict the use of this data in potential applications. Another fact to consider is the discrepancy between *Chl-a* concentration and phytoplankton biomass, since *Chl-a* is only a proxy for phytoplankton cell biomass (Devlin *et al.,* 2019).

Traditional in situ sampling, on the other side, usually provides very precise measurements (concentration count, species type, etc). However, the measurements vary in level of detail, scale and applied approach and are only available infrequently for a few distributed locations causing temporal and spatial gaps between measurements. Due to the high costs, data are often not collected for larger areas and due to regional differences, the information is not suitable for direct spatial upscaling. In situ sampling is nevertheless required in order to add value to imaging remote sensing observations. Phytoplankton count data sampling also comes with a human error (error in compiling the data) and also counting protocols may differ, especially when done at business companies. However, a combination of traditional in situ sampling and remote sensing observations can reduce these uncertainties.

5.2 Spatial and Temporal Variability of Count Data Distribution

As introduced in Chapter 1, there has been a significant increase in the frequency, intensity and geographic distribution of HABs along the coastline of SA, with a substantial loss on the environment and on the country's economy. According to Stephen and Hockey (2007) since the 1960's HAB events have been increasing. Moreover, between the years 1990 and 2005, the coast has experienced the greatest number of HABs with the most severe damage. Pitcher and Calder (2000) conducted a review of the areas that have been hit by HABs in the Southern Benguela, in which they documented the incidence and consequences in those areas (Sec.2.4).

The presented results (Sec.4.1) indicate that HABs occur most frequently in the latter half of the upwelling season in late summer and early autumn, as indicated by Pitcher and Calder, 2000, and have in the past been attributed to one or another dinoflagellate species such as *Scrippsiella trochoidea, Gymnodinium cf. mikimotoi, Noctiluca scintillans, Prorocentrum rostratum and P. triestinum* (Pitcher and Weeks, 2006). More recently harmful impacts have also been ascribed to other groups of phytoplankton, dinoflagellates (such as *Ceratium, Gonyaulax, Dinophysis,* and *Lingulodinium polyedrum*) on the south coast (Pitcher *et al.,* 2010, Pitcher *et al.,* 2017). On the presented results, phytoplankton community distribution is largely dominated by non-toxic species with relatively infrequent appearance of toxic species over the sampled years. Species concentration and their frequentness are largely influenced by seasonal forcing and are subjected to different environmental conditions and processes in each sub-region.

From the count data analysis presented in Sec.4.1 seven genera of species were identified and classified according to their seasonal occurrence: each region having different seasonal species abundance and distribution. The toxic species had a higher abundance in summer and throughout other seasons non-toxic species dominated. Some species were consistently present throughout the sampled years showing no seasonal variation (*Dinophysis),* but some species showed a distinct seasonal cycle defined by their presence in one season only or all year round but with the most frequent occurrence at a given season, accompanied by the highest concentration. From the count data analysis, the species abundance distribution varied greatly in all three areas, with low abundances and few species in Garden Route, intermediate abundance in Algoa Bay, and high abundance of all potential harmful species in the Overberg area. The count data suggest that blooms are in their highest concentration in late summer, while maintaining a low steady profile throughout the year.

Pseudo-nitzschia species contributed significantly to phytoplankton abundance in all areas as shown in Sec .4.1 and in figure 7, figure 9 and figure 11 (panel a, panel b), the monthly variations in phytoplankton cell concentrations results indicate that *Pseudo-nitzschia spp* species were dominating throughout the years, and this happened in all regions, even though other species occasionally dominate in summer and autumn. The high abundance of *Pseudo-nitzschia spp* during summer and autumn corresponded to a periodic nutrient enrichment indicative of coastal upwelling fits the ecological profile of *Pseudo-nitzschia* occurring during periods of high turbulence and nutrients (Fawcett et al., 2007; Trainer et al., 2012). The seasonal species distribution varies monthly, and the phytoplankton concentration for all regions is relatively low in winter and then starts to increase in spring. The analysis also presented a similar composition of dominant phytoplankton species recorded in the Overberg and Algoa Bay area's specifically in 2017 (Figure 7 (panel b), Figure 11 (panel b)), with some minor differences in seasonality and biomass concentration. Based on these results and given the fact that this is a typical period of upwelling it would appear that the shift in phytoplankton abundance and community structure coincides with changes in nutrient input due upwelling events of a particular region, as previously indicated by Lips and Lips (2010).

5.3 Spatial and Temporal Variability of *Chl-a* Distribution

The availability of ocean remote sensing-derived phytoplankton biomass data makes it possible for an assessment of synoptic climatology of regions, biogeography of the primary productivity and potentially harmful phytoplankton biomass using *Chl-a* as proxy (Borbor-Cordova *et al.,* 2019). Spatial and temporal variability of *Chl-a* concentration on the south coast of SA was investigated in Sec. 4.2 using 16-year (2003–2018) ocean colour derived products from MODIS. The results in Sec. 4.2.1 and figure 12 indicated that the scale of magnitude in *Chl-a* concentration varied temporally and spatially, showing a magnitude varying from 5 to >40 mg m^{-3} *Chl-a* it also shows that there is inter-annual variability in the *Chl-a* concentration which is more prominent between 19.5^0- 20.2^0 and also at 21^0- 23^0 longitude.

It is important to understand the suitability of *Chl-a* for future site suitability requirements for abalone aquaculture farming, as the physical and biological forcing mechanisms with environmental conditions at different seasons differ due to climate and geographical conditions. Results in figure 13 show the areas with high *Chl-a* variability (19.3^0- 19.82^0 , 21.1^0- 21.78^0 and 22.5^0 - 22.76^0) along the southern coast, and these areas are not suitable as

they are prone to the present and outburst of HABs. Within the constraints of needing suitably cold water for optimal growth, the farm sites need stable oceanographic conditions with the primary production of *Chl-a* that is less at risk of blooms. The analysis also presented a seasonal cycle with high intra-seasonal and inter-annual variability (Figure 14). Even though Overberg had relatively low *Chl a* concentration, this region experiences high *Chl-a* variability which is due to more blooms events. In the literature (see Sec.2.4.2) this area has been linked to more stratified water conditions, with blooms usually attributed to dinoflagellate species (Pitcher and Weeks, 2006).

As shown in Sec. 4.2.1 and Sec. 4.3.2 with their respective figures, distinct seasonal patterns of *Chl-a* exist in these four regions analysed, and they all displayed a bimodal pattern, experiencing two seasonal distinctive peaks in late-summer-to-early-autumn and in spring. The Overberg sub-region is different from other regions as it experiences long summer peaks, with big bloom spatial extent in March, through intermittent coastal wind-driven upwelling leading to higher biological productivity on the shelf (Smith 2016), and also it does experience some winter (July) blooms, due to deeper water column mixing resulting in moderate biomass as previously observed by Beckley (1988). Langeberg, Garden Route and Algoa Bay experience the highest *Chl-a* peaks in autumn, however in summer (the second peak) *Chl-a* concentration is relatively low, the blooms in these areas reach their maximum spatial extent in April. This bloom was observed by other authors and they explained it through thermal stratification prompting the formation of subsurface *Chl-a* maxima over much of the Agulhas Bank in close proximity to the thermocline (Probyn *et al.,* 1994), when nutrients supply to the surface waters was limited (Shannon *et al.,* 1984). Moreover Jarre *et al.,* (2015) also observed the bimodal pattern in *Chl-a* satellite time series, which is associated with upwelling events (Goschen and Schumann, 1988; Lutjeharms *et al.,* 2000a).

The linear regression analysis presented in Sec. 4.2.2 showed that the south coast experiences quite a large variability in the seasonal signal, mostly in the westernmost regions, rather than the easternmost, and also there are no significant trends, but a very large variability, which is different from region to region. In a global scale analysis conducted by Boyce *et al.,* (2010) the Chl trend indicated a decreasing slope, however the coastal regions may show otherwise. The coastal alignment and its interaction with atmospheric systems have apparently led to contrasting changes in biological and physical condition for each sub-region. Figure 16 and 17 both shows that the interannual variations of *Chl-a* concentration were spatially heterogeneous and difficult to constrain to any specific month. Furthermore, results show that

in Overberg *Chl-a* concentrations during summer months are associated with high phytoplankton activity, however in Langeberg, Garden Route and Algoa Bay the high phytoplankton peak occurred during autumn months.

5.3.1 Suitability of bloom analytic

For the identification and characterization of a bloom, a threshold method was developed. These threshold methods have been a common way to define the start of a bloom (Blondeau-Patissier *et al.,* 2014; Evers-King 2014) in relation to a seasonal average value. However, throughout literature there are no standard threshold techniques to characterise a bloom as Fawcett (*et al.,* 2007) explained, each author uses a different method depending on the specific species and its concentration on the water column. For instance, to define the bloom outbreak Siegel *et al.* (2002) and Henson and Thomas (2007) use the mean of *Chl-a*, whereas Ryan *et al.* (2008) used a threshold applied to the fluorescence based Maximum Chlorophyll Index (MCI) to indicate when biomass had exceeded a concentration of 75 mg m^{-3}.

5.4 Evaluation of Decision support tool (DeST)

The online survey was designed and shared with the stakeholder via email (section 3.8.1). It was quite difficult to get responses to the survey as I had to send follow up email until almost all the stakeholders responded. From the meetings that were held during this whole process of the DeST development, we had such a good number of people attending the workshops, maybe it was due to the fact that some companies delegated 3-5 people attending the meetings. However, when it came to the online survey responses, only 28 people responded to the survey. About 50 % of the stakeholders are from the abalone farms, the other 50% are divided among other aquatic farms (Mussels, Oysters, etc…), water quality and environmental managers (Figure 30).

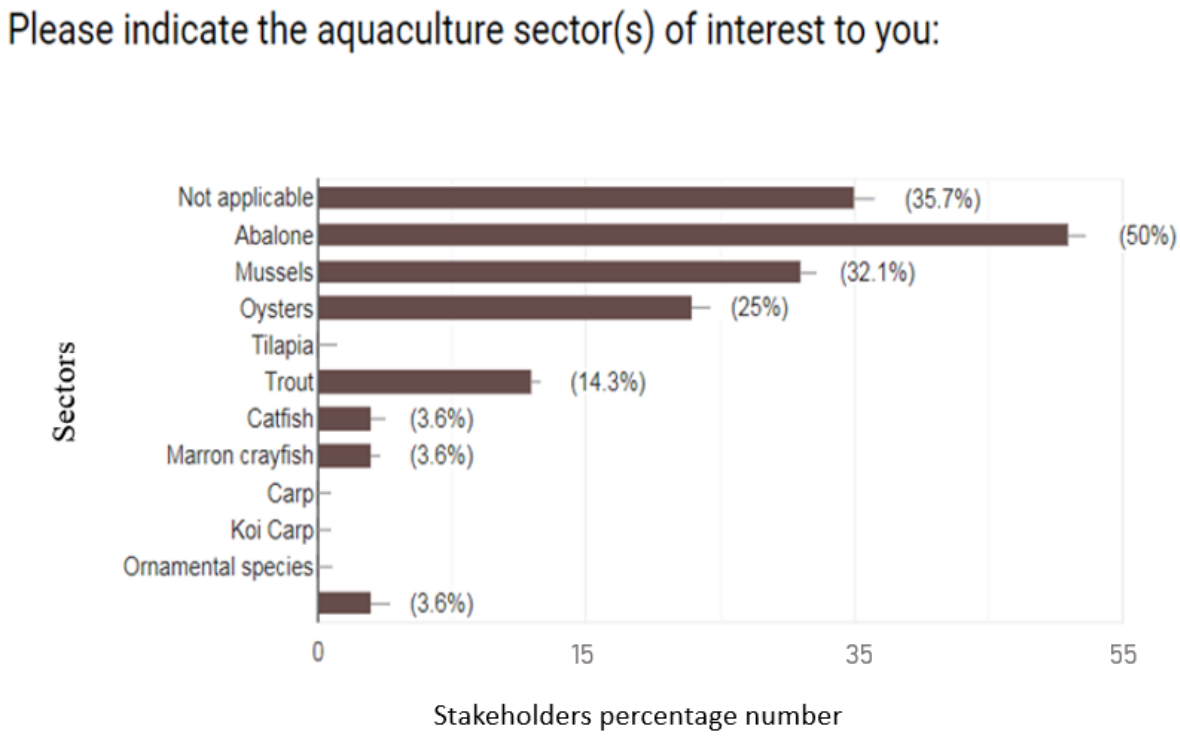

Figure 30: Sectors that make use of the DeST

Stakeholders had different interests on the DeST: some resort to the tool when they are experiencing risky conditions during harmful algal bloom period, for Operational Risk Management, Resource Management, some for Research (Figure 31, Figure 32); some out of the current available products provided on the DeST, they are mostly interested in the sea surface temperature (figure 31) to optimise growing conditions of their stock and for risk mitigation for Operational optimization, Environmental Impact and others for Site Selection for new facilities (Figure 31, Figure 32). The DeST developments have been driven by the end users' requirements and are still evolving, the feedbacks are used to reformat the presentation of data and information, including model based.

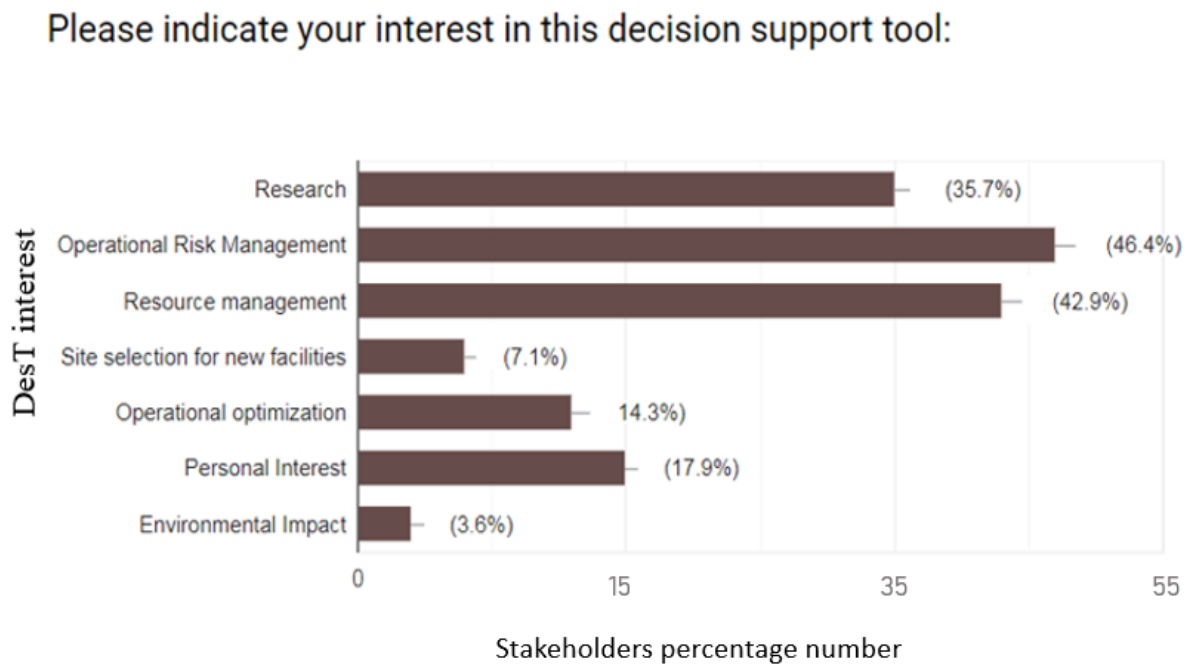

Figure 31: Different stakeholder's interest on the DeST

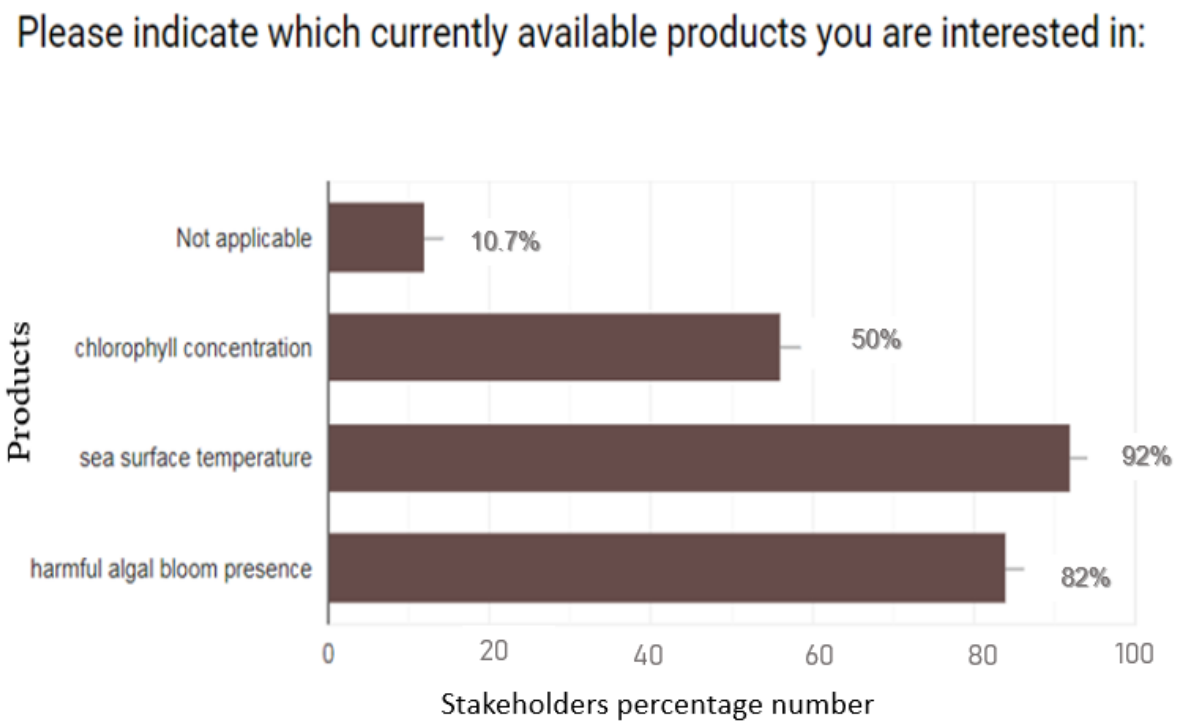

Figure 32: Different stakeholder's interest on the products available on the DeST

6. CONCLUSION

The south coast area is characterised by extensive mixing and variability, which strongly influences the dynamics of these waters. The related upwelling events fuel the formation of HABs in the coastal environment and maintain its productivity. Coastal environments are important areas for marine aquaculture and fisheries, as marine aquaculture has demonstrated potential of providing jobs and growing the South African economy.

Understanding the variation of species composition and biomass abundance provides an insight into the structure and dynamics of productive aquatic ecosystems (Oseji *et al.,* 2019) and the knowledge on which ranges of species are more likely to result in harmful impact.

In this study I have analysed 16 years (2003-2018) of MODIS satellite data describing the temporal and spatial variability of *Chl-a* concentration, and the spatial areal extent of the blooms using a bloom analytic tool in combination with in-situ phytoplankton count data for the same period. There is a crucial need in studying seasonal and temporal spatial variation/pattern of phytoplankton composition and abundance in coastal environments as fishing and profitable marine aquaculture depends on them. Phytoplankton in high biomass results in bloom, and blooms have been recognised to negatively impact commercial and recreational activities. Also, understanding *Chl-a* time series and the related analyses of bloom occurrence and phenology provide substantial insight into possible bloom prediction.

Phytoplankton count data were analysed to describe the temporal and spatial variability of harmful species in four regions of the southern coast of South Africa. Each region showed different seasonal species abundance and distribution. The data set for phytoplankton count data is affected by some limitations: it covers a relatively short time interval in most areas; it has no consistency in data format and occasional large gaps and it is spatially restricted. Nevertheless, it brings new information on the average yearly and monthly fluctuation and composition of the phytoplankton assemblage at sites of interest for the aquaculture industry. Past events showed that the toxic species even in low concentration had a negative impact on the environment and led to mass mortalities. However, we do acknowledge and understand that the conclusions that can be drawn from these data is fairly limited (or has high uncertainty) because of the known gaps in the data collection. Short-term and seasonal variability can be challenging to study in terms of accurate quantification because the spatial and temporal scales of sample observations are limited to a certain event. In this regard, the impact of environmental variables on phytoplankton structure and abundance vary from one

coastal region to another as also Zingone *et al.,* (2010) identified. Moreover, it is clear that a lack of consistent sampling makes it challenging to understand the seasonal characteristics of phytoplankton community structure. Therefore, full year and long term in situ observations should be strengthened and combined with data from buoys, satellites, and modelling studies (Hao *et al.,* 2019) to fully assist the aquaculture industry.

Further, the scale of magnitude in *Chl-a* concentration and count data varied temporally and spatially, and distinct seasonal patterns of *Chl-a* existed in these different sub-regions. Regions of high phytoplankton biomass are usually characterized by high variability, but also regions with intermediate concentrations can develop extreme blooms that may lead to HAB development. Based on a linear regression analysis at the annual scale and during the periods of the climatological blooms, there are no significant long-term trends in *Chl-a* concentration, although Overberg and Langeberg show an apparent increasing trend in summertime.

The bloom analytic tool assists in quantifying the areal extent of a bloom spatially. At times, some blooms developed in one region then they were distributed to other sub-regions by currents or wind. The use of MODIS data has shown promising results; however, we cannot deny the fact that at times it fails to detect small blooms that could lead to devastating economic loss. Hence it is recommended the use of the OLCI platform, with its higher resolution and improved spectral response.

To characterize the seasonal and interannual variations of *Chl-a*, ocean colour satellite data provide valuable information when compared to in situ data. However, with a regionally appropriate algorithm, ocean colour satellite data combined with in situ historical data is a powerful tool to understand the spatial and temporal phytoplankton dynamics. The occurrence of HAB and developing monitoring strategies has been the subject of many studies (Käse and Geuer, 2018 and the reference within). The interest in using computer-based models as tools to manage coastal ecosystems has increased worldwide, especially for aquaculture and fisheries. These models enable end-users to make more informed management decisions (Dabrowski *et al.,* 2015), for example the survey on the DeST tool presented in this thesis indicated that such a tool has helped managers to make decisive decisions to grow the ocean's economy and protect the environment. The South African aquaculture contribution to the global aquaculture is still minimal, as not all its aquaculture farms produce at commercial scale (Rainier *et al.,* 2016; DAFF, 2015; WWF 2016), however it could achieve substantial results if management and strategic planning are properly set up.

7. REFERENCE

Al Gheilani, H.M., Matsuoka, K., AlKindi, A.Y., Amer, S., and Waring. C., (2011). Fish Kill Incidents and Harmful Algal Blooms in Omani Waters. *Journal of Agricultural and Marine Sciences [JAMS]* 16: 23.

Al-Azri, A.R., Al-Hashmi, K.A., Al-Habsi, H., Al-Azri, N., and Al-Khusaibi, S., (2015) Abundance of Harmful Algal Blooms in the Coastal Waters of Oman: 2006–2011, *Aquatic Ecosystem Health and Management*, 18, 269–81.

Anderson D.M., Cembella A.D., Hallegraeff G.M., (2012). Progress in Understanding Harmful Algal Blooms (HABs): Paradigm Shifts and New Technologies for Research, Monitoring and Management, *Extension Publication*, Shelves, pond management.

Anderson, C.R, Moore, S.T., Tomlinson, M.C., Silke, J., and Cusack, C.K., (2014). "Living with Harmful Algal Blooms in a Changing World: Strategies for Modeling and Mitigating Their Effects in Coastal Marine Ecosystems." In *Coastal and Marine Hazards, Risks, and Disasters*, 495–561. Elsevier Inc.

Anderson, C.R., Berdalet, E., Kudela, R.M., Cusack, C.K., Silke, J., O'Rourke, E., Dugan, D., *et al.*, (2019). "Scaling up from Regional Case Studies to a Global Harmful Algal Bloom Observing System." *Frontiers in Marine Science* 6 (May).

Anderson, C.R., Moore, S.k., Tomlinson, M.C., Silke, J. and Cusack, C.K., (2015) Chapter 17 - Living with harmful algal blooms in a changing world: strategies for modeling and mitigating their effects in coastal Marine ecosystems. *In Coastal and Marine Hazards, Risks, and Disasters*, pp. 495-561.

Anderson, D.M., Boerlage, S.F.E., and Dixon, M.B., (2017). Harmful Algal Blooms (HABs) and Desalination: A Guide to Impacts, Monitoring, and Management, *Paris, Intergovernmental Oceanographic Commission of UNESCO*, p. 539.

Anderson, D.M., Glibert, P.M., and Burkholder, J.M., (2002). Harmful algal blooms and eutrophication: Nutrient sources, composition, and consequences', *Estuaries*, 25(4 B), pp. 704–726.

Anderson, D., (2009). Approaches to monitoring, control and management of harmful algal blooms (HABs). *Ocean Coastal Management*. 52, 342–347.

Anderson, D.M., Andersen, P., Bricelj, V.M., Cullen, J.J., and Rensel, J.E., (2001). *Monitoring and Management Strategies for Harmful Algal Blooms in Coastal Waters.* Paris: Intergovernmental Oceanographic Commission.

Atkinson, L. and Clark, B., (2005). Background Research Paper produced for the South Africa', *Marine and Coastal Ecosystems*, (October), pp. 1–35.

Balsamo, G., Agusti-Panareda, A., Albergel, C., Arduini, G., Beljaars, A., Bidlot, J., Bousserez, N., Boussetta, S., Brown, A., Buizza, R., Buontempo, C., Chevallier, F., Choulga, M., Cloke, H., Cronin, M. F., Dahoui, M., Rosnay, P. De, Dirmeyer, P. A.,

Drusch, M., … Zeng, X. (2018). Satellite and in situ observations for advancing global earth surface modelling: A review. Remote Sensing, 10(12), 1–72.

Bernard, S., Kudela, R.M., Franks, P., Fennel, W., Kemp, A., Fawcett, A., and Pitcher, G.C., (2006). The Requirement for Forecasting Harmful Algal Blooms in the Benguela. *Large Marine Ecosystems* 14: 273–94.

Bernard, S., Pitcher, G.C., Evers-king, H., Robertson, L., Matthews, M., Rabagliati, A., and Balt, B., (2014). Ocean Colour Remote Sensing of Harmful Algal Blooms in the Benguela System. In *Remote Sensing of the African Seas*, 185–203.

Bernard, S., Probyn, T., and Quirantes, A., (2009). Simulating the optical properties of phytoplankton cells using a two-layered spherical geometry. *Biogeosci*. Discuss. 6, 1497–1563.

Bishop, M. J., Mayer-Pinto, M., Airoldi, L., Firth, L. B., Morris, R. L., Loke, L. H. L., Hawkins, S. J., Naylor, L. A., Coleman, R. A., Chee, S. Y., & Dafforn, K. A. (2017). Effects of ocean sprawl on ecological connectivity: impacts and solutions. *Journal of Experimental Marine Biology and Ecology*, *492*, 7–30.

Blamey, L.K., Shannon, L.J., Bolton, J.J., Crawford, R.J.M., Dufois, F., Evers-King, H., Griffiths, C.L., *et al.,* (2015). Ecosystem Change in the Southern Benguela and the Underlying Processes. *Journal of Marine Systems* 144: 9–29.

Blanke, B., Sabrina Speich, S., Bentamy, A., Roy, C., and Sow, B., (2005). Modeling the Structure and Variability of the Southern Benguela Upwelling Using QuikSCAT Wind Forcing, 110 (February): 1–18.

Blondeau-Patissier, D., Gower, J. F., Dekker, A. G., Phinn, S. R., and Brando, V. E., (2014). A review of ocean color remote sensing methods and statistical techniques for the detection, mapping and analysis of phytoplankton blooms in coastal and open oceans. *Progress in Oceanography*. 123, 123– 144.

Borbor-Cordova, M.J., Torres, G., Mantilla-Saltos, G., Casierra-Tomala, A., Bermúdez, J.R., Renteria, W., and Bayot, B., (2019). Oceanography of Harmful Algal Blooms on the Ecuadorian Coast (1997–2017): Integrating Remote Sensing and Biological Data. *Frontiers in Marine Science* 6 (February).

Boyd, A.J., Shannon, L.J., Schulein, F.H., and Taunton-Clark, J., (1998). Food, Transport and Anchovy Recruitment in the Southern Benguela Upwelling System of South Africa. *From Local to Global Changes in Upwelling Systems*, 267–274.

Brewin, R.J.W., Hardman-Mountford, N.J., Lavender, S.J., Raitsos, D.E., Hirata, T., Uitz, J., Devred, E., Bricaud, A., Ciotti, A. & Gentili, B., (2011). An intercomparison of bio-optical techniques for detecting phytoplankton size class from satellite remote sensing. *Remote Sensing of Environment*, 115(2), 325-339.

Brown, A. R., Lilley, M., Shutler, J., Lowe, C., Artioli, Y., Torres, R., *et al.,* (2019). Assessing risks and mitigating impacts of harmful algal blooms on mariculture and marine fisheries. Rev. Aquacult.

Bryden L.H, Beal, L.M., and Duncan, L.M., (2005). Structure and Transport of the Agulhas Current and Its Temporal Variability. *Journal of Oceanography* 61: 479–492.

Cammen, L., Anderson, D.M., and Dortch, Q., (2001). Prevention, Control and Mitigation of Harmful Algal Blooms: A Research Plan. *Report for Congress, National Sea Grant*.

Cannizzaro, J.P., Carder, K.L., Chen, F.R., Heil, C.A., and G.A. Vargo., (2008). A novel technique for detection of the toxic dinoflagellate, Karenia brevis, in the Gulf of Mexico from remotely sensed ocean color data. *Continental Shelf Research*. 28:137-158.

Carder, K.L., Chen, F.R., Cannizzaro, J.P., Campbell, J.W., Mitchell, B.G., (2004) 'Performance of the MODIS semi-analytical ocean color algorithm for chlorophyll-a', *Advances in Space Research*, 33(7), pp. 1152–1159.

Carmichael, W., Backer, L.C., and Billing, L.M., (2013). Human Health Effects from Harmful Algal Blooms : A Synthesis. *International Joint Commission's Health Professionals Advisory Board* 1–53.

Chen, X., Li, Y.S., Liu, Z., Yin, K., Li, Z., Wai, O.W.H., King, B., (2004). Integration of multi-source data for water quality classification in the Pearl River estuary and its adjacent coastal waters of Hong Kong. *Continental Shelf Research* 24, 1827e1843.

Claustre, H., Babin, M., Merien, D., Ras, J., Prieur, L., (2005). Toward a taxon-specific parameterisation of bio-optical models of primary production: a case study in the North Atlantic. *Journal of Geophysical Research.*110, C07S12.

Cole, J., & Mcglade, J. (1998). Clupeoid population variability, the environ and satellite imagery in coastal upwelling systems. 471.

Cressey, D., (2009). Aquaculture: future fish. Nature, 458 (2009), pp. 398-400

Cusack, C., Dabrowski, T., Lyons, K., Berry, A., Westbrook, G., Salas, R., Duffy, C., Nolan, G., and Silke, J. (2016a). Harmful Algal Bloom Forecast System for SW Ireland. Part II: Are Operational Oceanographic Models Useful in a HAB Warning System. *Harmful Algae* 53: 86–101.

Dabrowski, T., Lyons, K., Cusack, C., Casal, G., Berry, A., & Nolan, G. D. (2015). Ocean modelling for aquaculture and fisheries in Irish waters. 1187–1217.

DAFF Annual Report. (2014). *Operation Phakisa*. *October*, 1–8.

DAFF (2017). *Aquaculture Yearbook 2016, South Africa*. Department of Agriculture, Forestry and Fisheries, Cape Town, South Africa.

Davidson, K., Anderson, D.M., Mateus, M., Reguera, B., Silke, B., Sourissueau, S., and Maguire, J., (2016). Forecasting the risk of harmful algal blooms: preface to the Asimuth special issue. *Harmful Algae* 53, 1–7.

Davidson, K., Gowen, R. J., Harrison, P. J., Fleming, L. E., Hoagland, P., and Moschonas, G., (2014). Anthropogenic nutrients and harmful algae in coastal waters. *Journal of Environmental Management*. 146, 206–216.

DEA. (2014). *South Africa's National Coastal Management Programme*. Department of Environmental Affairs South Africa.

Devlin, M. J., Breckels, M., Graves, C. A., Barry, J., Capuzzo, E., Huerta, F. P., Al Ajmi, F., Al-Hussain, M. M., LeQuesne, W. J. F., & Lyons, B. P. (2019). Seasonal and temporal drivers influencing phytoplankton community in Kuwait marine waters: Documenting a changing landscape in the Gulf. Frontiers in Marine Science, 6(APR), 1–22.

Esaias W.E., (1980). Remote Sensing of Oceanic Phytoplankton: Present Capabilities and Future Goals. In: Falkowski P.G. (*eds*) Primary Productivity in the Sea. *Environmental Science Research*, vol 19. Springer, Boston, MA.

Evers-King, H. (2014). *Phytoplankton community structure determined through remote sensing and in situ optical measurements* (Issue August).

FAO. (2014). *The State of World Fisheries and Aquaculture* 2014. Rome.

FAO. (2018). *The State of World Fisheries and Aquaculture 2018 - Meeting the sustainable development goals*. *Aq THE STATE OF THE WORLD series of the Food and Agriculture Organization of the United Nations.uaculture* **35**.

FAO. (2016). *The State of World Fisheries and Aquaculture*.

Fawcett, A, Bernard, S., Pitcher, G.C., Probyn, T.A., du Randt, A., and Randt, A., (2006). Real-Time Monitoring of Harmful Algal Blooms in the Southern Benguela. *African Journal of Marine Science* 28 (2): 257–260.

Fawcett, A., (2006). Multi-Sensor Mooring Development and Its Use to Characterise Physical Processes Relevant to Harmful Algal Bloom Dynamics in the St Helena Bay Area, South Africa. *Development*.

Fawcett, A., Pitcher, G.C., Bernard, S., Cembella, A.D., Kudela, R.M., 2007. Contrasting wind patterns and toxigenic phytoplankton in the southern Benguela upwelling system. Mar. Ecol. Prog. Ser. 348, 19–31.

Felemban, E., Shaikh, F. K., Qureshi, U. M., Sheikh, A. A., & Qaisar, S. Bin. (2015). Underwater Sensor Network Applications: A Comprehensive Survey. *International Journal of Distributed Sensor Networks*, *2015*.

Frolov, S., Kudela, R.M., and Bellingham, J.G., (2013). Monitoring of harmful algal blooms in the era of diminishing resources: a case study of the US west coast. *Harmful Algae*. 21 - 22:1–12.

Garrison, T (2005). Oceanography: An Invitation to Marine Science. Belmont CA.

Ghanea, M., Moradi, M., and Kabiri, K., (2016). A novel method for characterizing harmful algal blooms in the Persian Gulf using MODIS measurements. *Advanced in Space Research*. 58, 1348–1361.

Gilbert, P.M., Anderson, D.M., Gentien, P., Graneli, E., and Sellner, K.G., (2005). The global complex phenomena of harmful algal blooms. *Oceanography* 1818 (22), 136–147.

Gilerson, A., Gitelson, A., Zhou, J., Gurlin, D., Moses, W., Ioannou, I., Ahmed, S., (2010). Algorithms for remote estimation of chlorophyll-a in coastal and inland waters using red and near infrared bands. Opt. Express 18, 24109–24125.

Glibert, P., and Burford, M., (2017). Globally Changing Nutrient Loads and Harmful Algal Blooms: Recent Advances, New Paradigms, and Continuing Challenges. *Oceanography*, *30*(1), 58-69.

GlobalHAB. (2017). Global Harmful Algal Blooms. In *Science and Implementation Plan*.

Goschen, W.S., Bornman, T.G., Deyzel, S.H.P. and Schumann, E.H., (2015). Coastal Upwelling on the Far Eastern Agulhas Bank Associated with Large Meanders in the Agulhas Current. *Continental Shelf Research* 101: 34–46.

Goschen, W.S., and Schumann, E.H., (2011). The Physical Oceanographic Processes of Algoa Bay, with Emphasis on the Western Coastal Region. *South African Environmental Observation Network (SAEON), Internal Report*, no. April: 1–85.

Gower, J., and King, S., (2008). Satellite Images Show the Movement of Floating Sargassum in the Gulf of Mexico and Atlantic Ocean. Nature Proceedings

Gower, J., and King, S.A., (2011). Distribution of floating Sargassum in the Gulf of Mexico and the Atlantic Ocean mapped using MERIS. *International Journal of Remote Sensing* 32, 1917–1929.

Gower, J., King, S., and Goncalves, P., (2008). Global Monitoring of Plankton Blooms Using MERIS MCI. 1161.

Gower, J., King, S., Borstad, G., and Brown, G., (2005). Detection of intense plankton blooms using the 709 nm band of the MERIS imaging spectrometer. *International Journal of Remote Sensing*, 26(9), 2005–2012.

Gower, J.F.R., HU, C., Borstad, G.A. and King, S., (2006). Ocean color satellites show extensive lines of floating Sargassum in the Gulf of Mexico. *IEEE Transactions on Geoscience and Remote Sensing*, 44, pp. 3619–3625.

Grattan, L.M., Holobaugh, S., and Morris, J.G., (2016). Harmful algal blooms and public health. *Harmful Algae* 57, 2–8.

Hallegraeff, G.M., (2010). Ocean climate change, phytoplankton community responses, and harmful algal blooms: a formidable predictive challenge. *J. Phycol*. 46 (2), 220-235.

Hasle, G.R., (1978). The inverted-microscope method. In: Sournia, A. (Ed.), Phytoplankton manual, UNESCO, Paris, France, pp. 88–96.

Hill, A.E., Hickey, B.M., Shillington, F.A., Strub, P.T., Brink, K.H., Barton, E.D., Thomas, A.C., (1998) Eastern boundary currents: a pan-regional review. In: Robinson AR, Brink KF (*eds*) *The Sea*. John Wiley, New York, pp 29–68

Hu, C., and Feng, L., (2016). Modified MODIS Fluorescence Line Height Data Product to Improve Image Interpretation for Red Tide Monitoring in the Eastern Gulf of Mexico. *Journal of Applied Remote Sensing* 11 (1): 1–14

Hu, C., Lee, Z., Franz, B., (2012). Chlorophyll a algorithms for oligotrophic oceans: a novel approach based on three-band reflectance difference. *Journal of Geophysical Research*. 117, C01011.

Hu, C., Muller-Karger, F.E, Taylor, C., Carder, K.L., Kelble, C., Johns, E., and Heil, C.A., (2005). Red Tide Detection and Tracing Using MODIS Fluorescence Data: A Regional Example in SW Florida Coastal Waters. *Remote Sensing of Environment* 97 (3): 311–21.

Hutchings, L., Beckley, L.E., Griffiths, M.H., Roberts, M.J., Sundby, S., and van der Lingen, C.D., 2002. Spawning on the edge: spawning grounds and nursery areas around the southern African coast- line. *Marine and Freshwater Research*, 53: 307–318.

Jackson, J.M., Rainville, L., Roberts, M.J., McQuaid, C.D., Lutjeharms, J.R.E., (2012). "Mesoscale bio-physical interactions between the Agulhas Current and the Agulhas Bank, South Africa". *Cont. Shelf Res*. 49, 10–24.

Jarre, A., Hutchings, L., Crichton, M., Wieland, K., Lamont, T., Blamey, L. K., Illert, C., Hill, E., & Berg, M. V. A. N. D. E. N. (2015). Oxygen-depleted bottom waters along the west coast of South Africa , 1950 – 2011. 24, 56–73.

Joan, L., Marina, L., Jean-Baptiste, S., & Tagliabue, A. (2015). Onset, intensification, and decline of phytoplankton blooms in the Southern Ocean. *ICES Journal OfMarine Science*, *72*(6), 1971–1984.

Karaan, M., and Rossouw, S., (2004). The Microeconomic Strategy Project a baseline assessment of the fishing and aquaculture industry in the Western Cape. *Department of Agricultural Economics Stellenbosch University*.

Karki, S., Sultan, M., Elkadiri, R., and Elbayoumi, T., (2018). Mapping and Forecasting Onsets of Harmful Algal Blooms Using MODIS Data over Coastal waters Surrounding Charlotte County, Florida. *Remote Sensing* 10 (10).

Kirkman, S., Hutchings, L., Leslie, R. and Lamberth, S., (2011). Technical Report Volume 4 : Marine and Coastal Component Volume 4 : Marine and Coastal Component, 4.

Kudela, R.M., Berdalet, E., Bernard, S., Burford, M., Fernand, L., Lu, S. Roy, S., *et al.*, (2015). Harmful Algal Blooms: A Scientific Summary for Policy Makers. *Ioc/Unesco*, no. Paris IOC/INF-1320: 20.

Kudela, R.M., Howard, M.D.A., Jenkins, B.D., Miller, P.E., and Smith, G.J., (2010). Using the Molecular Toolbox to Compare Harmful Algal Blooms in Upwelling Systems. *Progress in Oceanography* 85 (1–2): 108–21.

Kudela, R.M., Seeyave, S., and Cochlan, W.P., (2010). The Role of Nutrients in Regulation and Promotion of Harmful Algal Blooms in Upwelling Systems. *Progress in Oceanography* 85 (1–2): 122–35.

Kyewalyanga, M.S., Naik, R., and Hegde, S., (2007). Phytoplankton biomass and primary production in Delagoa Bight Mozambique : *Application of remote sensing*. **74**.

Landsberg, J.H., (2002). The Effects of Harmful Algal Blooms on Aquatic Organisms. *Reviews in Fisheries Science* 10 (2): 113–390.

Lewandowska, A. M., Striebel, M., Feudel, U., Hillebrand, H., and Sommer, U. (2015). The importance of phytoplankton trait variability in spring bloom formation. *ICES Journal of Marine Science*, *72*(6), 1908–1915.

Lewitus, A.J., Horner, R.A., Caron, D.A., Garcia-Mendoza, E., Hickey, B.M., Hunter, M., Huppert, D.D., Kudela, R.M., Langlois, G.W., Largier, J.L., (2012). Harmful algal blooms along the North American west coast region: history, trends, causes, and impacts. *Harmful Algae*, 19 (9): 133-159.

Lips, I., & Lips, U. (2010). Phytoplankton dynamics affected by the coastal upwelling events in the Gulf of Finland in July-August 2006. Journal of Plankton Research, 32(9), 1269–1282.

Lutjeharms, J. R. E., Cooper, J., and Roberts, M., (2000). Upwelling at the inshore edge of the Agulhas Current. *Continental Shelf Research* 20: 1907–1939.

Lutjeharms, J.R.E., (2006). The Coastal Oceans of South-Eastern Africa. *The Sea* 14: 783–834.

Lutjeharms, J.R.E., and Ruijter, W.P.M., (1996). The influence of the Agulhas Current on the adjacent coastal ocean: possible impacts of climate change. Jo*urnal of Marine Systems* 7: 321-226.

Lutjeharms, J.R.E., Durgadoo, J.V., Schapira, M., and McQuaid, C.D., (2010). First Oceanographic Survey of the Entire Continental Shelf Adjacent to the Northern Agulhas Current. *South African Journal of Science* 106 (9–10): 9–11.

Marić, D., Ljubešić, Z., Godrijan, J., Viličić, D., Ujević, I., and Precali, R., (2011). Blooms of the Potentially Toxic Diatom *Pseudo-Nitzschia Calliantha* Lundholm, Moestrup & Hasle in Coastal Waters of the Northern Adriatic Sea (Croatia). *Estuarine, Coastal and Shelf Science* 92 (3): 323–31.

Matthews, M.W., and Bernard, S., (2015). Eutrophication and Cyanobacteria in South Africa's Standing Water Bodies: A View from Space. *South African Journal of Science* 111 (5–6): 1–8.

Matthews, S.G., and Pitcher, G.C., (1996). Worse recorded marine mortality on the South African coast.

McPartlin, D.A., Loftus, J.H., Crawley, A.S., Silke, J., Murphy, C.S., and O'Kennedy, R.J. (2017). Biosensors for the Monitoring of Harmful Algal Blooms, *Current Opinion in Biotechnology*, 45, 164–169.

Miller, D.C.M., Moloney, C.L., Van Der Lingen, C.D., Lett, C., Mullon, C., and Field, J.G., (2006). Modelling the Effects of Physical – Biological Interactions and Spatial Variability in Spawning and Nursery Areas on Transport and Retention of Sardine Sardinops Sagax Eggs and Larvae in the Southern Benguela Ecosystem, 61: 212–29.

Miller, P.I., Shutler, J.D., Moore, G.F. and Groom, S.B., (2006). SeaWiFS discrimination of harmful algal bloom evolution. *International Journal of Remote Sensing*. 27(11):2287- 2301.

Moradi, M, and Kabiri, K., (2012). Red Tide Detection in the Strait of Hormuz (East of the Persian Gulf) Using MODIS Fluorescence Data. *International Journal of Remote Sensing* 33 (4): 1015–1028.

Ndhlovu, A., Dhar, N., Garg, N., Xuma, T., Pitcher, G.C., Sym, S.D., and Durand, P.M., (2017). A Red Tide Forming Dinoflagellate *Prorocentrum Triestinum*: Identification, Phylogeny and Impacts on St Helena Bay, South Africa. *Phycologia* 56 (6): 649–665.

O'Reilly, J.E., Maritorena, S., Mitchell, B.G., Siegel, D.A., Carder, K.L., Garver, S.A., Kahru, M., Mcclain, C., (1998). Ocean color chlorophyll algorithms for SeaWiFS. *Journal of Geophysical Research*. 103, 24937–24953.

Oberholster, P.J., Botha, A.M., and Cloete, T.E., (2005). An overview of toxic freshwater cyanobacteria in South Africa with special reference to risk, impact and detection by molecular marker tools. *Biokemistri,* 17, 57−71.

Ocean, T. (2017). The Ocean Economy in 2030. *Water Intelligence Online*, *16*, 9781780408927.

Oseji, O. F., Fan, C., & Chigbu, P. (2019). Composition and dynamics of phytoplankton in the Coastal Bays of Maryland, USA, revealed by microscopic counts and diagnostic pigments analyses. Water (Switzerland), 11(2).

Page, T., Smith, P.J., Beven, K.J., Jones, I.D., Elliott, J.A, Maberly, S.C., Mackay, E.B., *et al.,* (2018). Adaptive Forecasting of Phytoplankton Communities. *Water Research* 134 (May): 74–85.

Palmer, S.C.J., Odermatt, D., Hunter, P.D., Brockmann, C., Présing, M., Balzter, H., *et al.*, (2015). Satellite remote sensing of phytoplankton phenology in Lake Balaton using 10 years of MERIS observations. *Remote Sensing of Environment*. 158, 441–452.

Pitcher, G. C., Cembella, A. D., Krock, B., Macey, B. M., & Mansfield, L. (2020). Do toxic Pseudo-nitzschia species pose a threat to aquaculture in the southern Benguela eastern boundary upwelling system? *Harmful Algae*, *99*(October), 101919.

Pitcher, G.C., and Calder, D., (2000). Harmful Algal Blooms of the Southern Benguela Current: A Review and Appraisal of Monitoring from 1989 to 1997. *South African Journal of Marine Science* 22 (1): 255–271.

Pitcher, G.C, and Pillar, S., (2010). Harmful Algal Blooms in Eastern Boundary Upwelling Systems. *Progress in Oceanography*.

Pitcher, G.C, Bernard, S., and Ntuli, J., (2008). Contrasting Bays and Red Tides in the Southern Benguela Upwelling System. *Oceanography* 21 (3): 82–91.

Pitcher, G.C., and Nelson, G., (2006). Characteristics of the Surface Boundary Layer Important to the Development of Red Tide on the Southern Namaqua Shelf of the Benguela Upwelling System. *Limnology and Oceanography* 51 (6): 2660–74.

Pitcher, G.C., Bernard, S., Ntuli, J., (2008). Contrasting Bays and red tides in the southern Benguela upwelling system. *Oceanography* 21 (3), 82–91.

Pitcher, G.C., Boyd, A.J., Horstman, D.A., and Mitchell-Innes, B.A., (1998). Subsurface dinoflagellate populations, frontal blooms, and the formation of red tide in the southern Benguela upwelling system. *Marine Ecology Progress Series*, 172, 243–264.

Pitcher, G.C., Figueiras, F.G., Hickey, B.M., and Moita, M.T., (2010). The Physical Oceanography of Upwelling Systems and the Development of Harmful Algal Blooms. *Progress in Oceanography* 85 (1–2): 5–32.

Pitcher, G.C., Foord, C.J., Macey, B.M., Mansfield, L., Mouton, A., Smith, M.E., *et al.*, (2019). Devastating farmed abalone mortalities attributed to yessotoxin-producing dinoflagellates. *Harmful Algae* 81, 30–41.

Pitcher, G.C., Jiménez, A.B., Kudela, R.M., and Reguera, B., (2017). Harmful algal blooms in eastern boundary upwelling systems: a GEOHAB core research project. *Oceanography* 30, 22–35.

Pitcher, G.C., Probyn, T.A., Du Randt, A., Lucas, A., Bernard, S., Evers-King, H., *et al.*, (2014). Dynamics of oxygen depletion in the nearshore of a coastal embayment of the southern Benguela upwelling system. *Journal of Geophysical Research*: Oceans 119: 2183–2200.

Probyn, T., Pitcher, G., Pienaar, R., & Nuzzi, R., (2001). Brown tides and mariculture in Saldanha Bay, South Africa. *Marine Pollution Bulletin*, 42(5), 405–408.

Probyn, T.A., Bernard, S., Pitcher, G.C., Pienaar, R.N., (2010). Ecophysiological studies on Aureococcus anophagefferens blooms in Saldanha Bay, South Africa. *Harmful Algae* 9: 123–133.

Probyn, T.A., Mitchellinnes, B.A., Brown, P.C., Hutchings, L. and Carter, R.A., (1994). REVIEW: Primary productivity across Agulhas bank. *South African Journal of Science* **90**, 166–173.

Quartly, G.D., and Srokosz, M.A., (2002). SST Observations of the Agulhas and East Madagascar Retroflections by the TRMM Microwave Imager, 1585–1592.

Radford, R., (2012). Scientific Analysis of the Harmful Algal Blooms and Hypoxia Research and Control Amendments Act of 2011.

Richardson, L.L., (1996). Remote Sensing of Algal Bloom Dynamics. *Bioscience* 46 (7): 492–501.

Reynolds, R. W., Zhang, H. M., Smith, T. M., Gentemann, C. L., & Wentz, F. (2005). Impacts of in situ and additional satellite data on the accuracy of a sea-surface temperature analysis for climate. International Journal of Climatology, 25(7), 857–864.

Rouault, M., Pohl, B., Penven, P., (2010). Coastal oceanic climate change and variability from 1982 to 2009 around South Africa. *African Journal of Marine Science* 32: 237–246.

Rubio, A., Blanke, B., Speich, S., Grima, N., and Roy, C., (2009). Mesoscale Eddy Activity in the Southern Benguela Upwelling System from Satellite Altimetry and Model Data. *Progress in Oceanography* 83 (1–4): 288–295.

SACN. 2016. State of South African Cities Report 2016. Johannesburg: SACN

Schumann, E.H., (1998). The coastal ocean off southeast Africa, including Madagascar. In: Robinson AR, Brink KH (eds), *The Sea, Vol. 11. The global coastal ocean: regional studies and syntheses*. New York: John Wiley & Sons. pp 557–582.

Schumann, E.H., Churchill, J.R.S., and Zaaymann, H.J., (2005). Oceanic variability in the western sector of Algoa Bay, South Africa. *African Journal of Marine Science* 27: 65-80.

Shannon, L., (2006). A plan comes together. *Benguela: Predicting a Large Marine Ecosystem*, 14:3–10.

Shannon, L.V., Nelson, G., (1996). The Benguela: large scale features and processes and system variability. In: Wefer G, Berger WH, Siedler G, Webb DJ (eds) *The South Atlantic: Present and Past Circulation*. Springer, Berlin, pp 163–210

Shen, L., Xu, H., and Guo, X., (2012). Satellite remote sensing of harmful algal blooms (HABs) and a potential synthesized framework. *Sensors* 12, 7778–7803.

Silva, A., & Palma, S. (2010). The Socio-Economical Impact of HABs : Portugal ' s Case Study (2005-2010). *Journal of Tourism and Sustainability*, *I*(1), 19–27.

Siswanto, E., Ishizaka, J., Tripathy, S.C., and Miyamura, K., (2013). Detection of Harmful Algal Blooms of Karenia Mikimotoi Using MODIS Measurements: A Case Study of Seto-Inland Sea, Japan. *Remote Sensing of Environment* 129: 185–96.

Smayda, T.J.J., (2000). Ecological Features of Harmful Algal Blooms in Coastal Upwelling Ecosystems. *South African Journal of Marine Science*. Vol. 22

Smith, M.E., (2016). The Use of Reflectance Classification for Chlorophyll Algorithm Application across Multiple Optical Water Types in South African Coastal Waters. PhD thesis, University of Cape Town.

Smith, M.E., and Bernard, S., (2020). Satellite Ocean Color Based Harmful Algal Bloom Indicators for Aquaculture Decision Support in the Southern Benguela. *Front. Mar. Sci.* **7**, 1–13.

Smith, M.E., and Pitcher, G.C., (2015). Saldanha Bay, South Africa I: The Use of Ocean Colour Remote Sensing to Assess Phytoplankton Biomass. *African Journal of Marine Science* 37 (4): 503–12.

Smith, M.E., Lain, L.R., and Bernard, S., (2018). An Optimized Chlorophyll a Switching Algorithm for MERIS and OLCI in Phytoplankton-Dominated Waters. *Remote Sensing of Environment* 215 (January): 217–227.

Srokosz, M.A., (2000). Biological Oceanography by Remote Sensing. In *Encyclopedia of Analytical Chemistry*, 8506–8533.

Stephen, V. C. and Hockey, P. A. R. (2007). Evidence for an increasing incidence and severity of Harmful Algal Blooms in the southern Benguela region, *South African Journal of Science*, 103(5-6), pp. 223–231.

Stickney, R.R., (2005). Aquaculture: an introductory text, CABI publishing, Cambridge (Mass.).

Stumpf, R.P., (2001). Applications of Satellite Ocean color sensors for monitoring and predicting harmful algal blooms. *Journal of Human Ecology*. Risk Assess. 7, 1363–1368.

Stumpf, R.P., and Tomlinson, M.C., (2005). Remote Sensing of Harmful Algal Blooms. *Remote Sensing of Coastal Aquatic …*, 277–296.

Tester, P.A., Steidinger, K.A., (1997). *Gymnodinium* breve red tide bloom: initiation, transport, and consequences of surface circulation. *Limnology of Oceanography*. 42, 1039–1051.

Trainer, V.L., Pitcher, G.C., Reguera, B., and Smayda, T.J., (2010). The Distribution and Impacts of Harmful Algal Bloom Species in Eastern Boundary Upwelling Systems, *Progress in Oceanography*, 85, 33–52

Trainer, V.L., Bates, S.S., Lundholm, N., Thessen, A.E., Cochlan, W.P., Adams, N.G., Trick, C.G., 2012. Pseudo-nitzschia physiological ecology, phylogeny, toxicity, monitoring and impacts on ecosystem health. Harmful Algae 14, 271–300.

Verheye, H.M., Lamont, T., Huggett, J.A., Kreiner, A., and Hampton, I., (2016). Plankton Productivity of the Benguela Current Large Marine Ecosystem (BCLME)." *Environmental Development* 17 (August): 75–92.

Waibel, A., Peter, H., & Sommaruga, R. (2019). Importance of mixotrophic flagellates during the ice-free season in lakes located along an elevational gradient. *Aquatic Sciences*, *81*(3), 1–10.

Walker, D.R., and Pitcher, G.C., (2010). The Dynamics of Phytoplankton Populations, Including a Red-Tide Bloom, during a Quiescent Period in St Helena Bay, South Africa. 7615.

Wells, M.L., Trainer, V.L., Smayda, T.J., Karlson, B.S.O., Trick, C.G., Kudela, R.M., Ishikawa, A., *et al*. (2015). Harmful Algal Blooms and Climate Change: Learning from the Past and Present to Forecast the Future. *Harmful Algae* 49: 68–93.

World Bank, & DESA. (2020). *The Potential of the Blue Economy: Increasing Long-term Benefits of the Sustainable Use of Marine Resources for Small Island Developing States and Coastal Least Developed Countries.* (Issue November, pp. 37–37).

World Wide Fund for Nature. (2016). Ocean's facts and futures: Valuing South Africa's ocean economy. WWF.

Zhao, J., Temimi, M., and Ghedira, H., (2015). Characterization of harmful algal blooms (HABs) in the Arabian Gulf and the Sea of Oman using MERIS fluorescence data. *ISPRS Journal of Photogrammetry and Remote Sensing*, 101, pp. 125-136.

Zingone, A., Siano, R., D'Alelio, D. & Sarno, D., (2006). Potentially toxic and harmful microalgae from coastal waters of the Campania region (Tyrrhenian Sea, Mediterranean Sea). *Harmful Algae* **5**, 321–337.

8. APPENDIX A

Resources used-

https://www.capenature.co.za/warning-red-tide-along-west-coast/

https://www.hermanusonline.mobi/hermanus-blog/what-is-the-red-tide-in-hermanus-is-it-harmful-to-swimmers

http://www.saeon.ac.za/enewsletter/archives/2014/february2014/doc04

Table 3: The list of recorded species along the south coast of South Africa and the number of frequent visits.

Recorded Yearly Frequence of species

2012		2013		2014		2015	
Alexandrium catenella	25	Alexandrium catenella	19	Ceratium dens	1	Alexandrium catenella	2
Asterionella glacialis	1	Asterionella glacialis	1	Ceratium furca	8	Asterionella glacialis	31
Biddulphia spp	45	Ceratium furca	29	Ceratium lineatum	2	Cerataulina spp	14
Ceratium dens	4	Chaetoceros convolutus	6	Chaetoceros convolutus	11	Ceratium dens	1
Ceratium furca	34	Coscinodiscus spp	5	Coscinodiscus spp	63	Ceratium furca	26
Ceratium fusus	1	Dictyocha octonaria	3	Dictyocha octonaria	11	Ceratium fusus	1
Ceratium lineatum	20	Dinophysis acuminata	27	Dinophysis acuminata	2	Ceratium lineatum	1
Chaetoceros convolutus	48	Dinophysis fortii	2	Dinophysis fortii	2	Chaetoceros convolutus	48
Coccolithophoriden spp	1	Dinophysis rotundata	4	Dinophysis rotundata	1	Coscinodiscus spp	152
Coscinodiscus spp	11	Dinophysis tripos	1	Ditylum spp	3	Dictyocha octonaria	28
Dinophysis acuminata	10	Ditylum spp	1	Gyrodinium spp	4	Dinophysis acuminata	11
Dinophysis fortii	18	Gonyaulax spinifera	8	Licmophora ehrenbergii	27	Dinophysis fortii	1
Dinophysis rotundata	3	Karenia cristata	16	Melosira sp	4	Dinophysis rotundata	2
Ditylum spp	3	Melosira sp	2	Nitzschia closterium	1	Ditylum spp	5
Eucampia spp	1	Noctiluca scintillans	1	Nitzschia spp	1	Gonyaulax polygramma	1
Eutreptiella spp	5	Peridinium	1	Peridinium	1	Gonyaulax spinifera	1
Gonyaulax grindeleyi	2	Prorocentrum micans	40	Pleurosigma spp	3	Gymnodinium sanguineum	3
Gonyaulax spinifera	12	Protoceratium reticulatum	16	Prorocentrum micans	23	Gymnodinium spp	6
Gymnodinium spp	2	Protoperidinium spp	3	Prorocentrum spp 1	1	Gyrodinium spp	10
Gyrodinium spp	5	Pseudonitzschia spp	17	Prorocentrum triestinum	1	Licmophora ehrenbergii	121
Licmophora ehrenbergii	3	Scrippsiella trochoideum	3	Protoceratium reticulatum	1	Noctiluca scintillans	1
Melosira sp	1	Skeletonema costatum	10	Protoperidinium excentricum	3	Peridinium	6
Peridinium	10	Thalassionema nitzschioides	6	Protoperidinium spp	13	Pleurosigma spp	3
Pleurosigma spp	5	Thalassiosira spp	4	Pseudonitzschia spp	18	Prorocentrum balticum	1
Prorocentrum balticum	1	Unidentified Dino. Spp	1	Rhizosolenia spp	6	Prorocentrum micans	23
Prorocentrum micans	107			Scrippsiella trochoideum	9	Prorocentrum spp 1	34
Prorocentrum rostratum	1			Skeletonema costatum	11	Prorocentrum triestinum	8
Protoceratium reticulatum	5			Thalassionema nitzschioides	6	Protoceratium reticulatum	1
Pseudonitzschia spp	73			Thalassiosira spp	33	Protoperidinium spp	20
Rhizosolenia spp	39					Pseudonitzschia spp	51
Scrippsiella trochoideum	6					Rhizosolenia spp	100
Skeletonema costatum	35					Scrippsiella trochoideum	21
Thalassionema nitzschioides	51					Skeletonema costatum	33
Thalassiosira spp	56					Thalassionema nitzschioides	52
						Thalassiosira spp	143

Continuation of table 3

Recorded Yearly Frequence of species

2016		2017		2018	
Alexandrium catenella	2	Asterionella glacialis	42	Asterionella glacialis	10
Alexandrium sp	2	Cerataulina spp	4	Cerataulina spp	3
Asterionella glacialis	55	Ceratium furca	56	Ceratium dens	7
Biddulphia spp	18	Ceratium fusus	7	Ceratium furca	37
Ceratium dens	4	Ceratium lineatum	18	Ceratium fusus	2
Ceratium furca	38	Chaetoceros convolutus	58	Chaetoceros convolutus	28
Ceratium fusus	2	Coscinodiscus spp	143	Coscinodiscus spp	75
Ceratium lineatum	5	Dictyocha octonaria	13	Dictyocha octonaria	18
Chaetoceros convolutus	61	Dinophysis acuminata	9	Dinophysis acuminata	7
Coscinodiscus spp	236	Dinophysis fortii	3	Dinophysis fortii	1
Dictyocha octonaria	66	Dinophysis hastata	1	Ditylum spp	7
Dinophysis acuminata	14	Dinophysis tripos	1	Eucampia spp	1
Dinophysis fortii	1	Ditylum spp	16	Gonyaulax grindeleyi	11
Dinophysis rotundata	1	Eucampia spp	2	Gonyaulax spinifera	1
Ditylum spp	42	Gonyaulax grindeleyi	7	Gymnodinium spp	5
Eucampia spp	3	Gonyaulax spinifera	8	Gyrodinium spp	11
Gonyaulax grindeleyi	13	Gymnodinium mikimotoi	3	Licmophora ehrenbergii	56
Gonyaulax polygramma	9	Gymnodinium spp	5	Lingulodinium polyedrum	2
Gyrodinium spp	14	Gyrodinium spp	13	Melosira sp	1
Licmophora ehrenbergii	153	Licmophora ehrenbergii	174	Pleurosigma spp	18
Melosira sp	22	Lingulodinium polyedrum	38	Prorocentrum balticum	16
Nitzschia spp	1	Melosira sp	14	Prorocentrum gracile	1
Noctiluca scintillans	1	Pleurosigma spp	5	Prorocentrum micans	11
Peridinium	1	Prorocentrum balticum	17	Prorocentrum spp 1	3
Pleurosigma spp	3	Prorocentrum gracile	1	Protoperidinium excentricum	1
Prorocentrum balticum	3	Prorocentrum micans	75	Protoperidinium spp	24
Prorocentrum micans	103	Prorocentrum spp 1	22	Protoperidinium steinii	1
Prorocentrum spp 1	18	Prorocentrum triestinum	1	Pseudonitzschia spp	14
Protoceratium reticulatum	1	Protoperidinium excentricum	4	Rhizosolenia spp	32
Protoperidinium excentricum	1	Protoperidinium spp	66	Scrippsiella trochoideum	17
Protoperidinium spp	42	Pseudonitzschia spp	32	Skeletonema costatum	20
Pseudonitzschia spp	104	Rhizosolenia spp	37	Thalassionema nitzschioides	30
Rhizosolenia spp	57	Scrippsiella trochoideum	46	Thalassiosira spp	76
Scrippsiella trochoideum	43	Skeletonema costatum	21		
Skeletonema costatum	23	Thalassionema nitzschioides	65		
Thalassionema nitzschioides	52	Thalassiosira spp	155		
Thalassiosira spp	122				